



بسم الله الرحمن الرحيم

**Sudan University of Science & Technology (SUST)**  
**Faculty of Graduate Studies**

تحديد مستويات النشاط الاشعاعي والمخاطر البيولوجية للعينات الصخرية من محاجر  
مصانع الاسمنت بولاية نهر النيل – السودان

**Determination of Radioactivity Levels and Biological Hazards of  
Rock Samples Quarries Cement factories in  
River Nile State-Sudan**

A thesis submitted for the degree of Ph.D Degree in Physics Science

**By:**

**Mohamed Abu baker Hussein Dahab**

M.Sc. in Radiation & Environmental Protection (2016) Sudan

Academy of Sciences (SAS)

**Supervisor**

**Dr. Ahmed Al Hassan Alfaki**

December 2021



## Approval Page

(To be completed after the college council approval)

Name of Candidate: Mohamed Abubaker Hussein Dahab

Thesis title: ...Determination of Radioactivity Levels....  
...and Biological Hazards of Rock Samples Quarries.  
...Cement Factories in River Nile State - Sudan.

Degree Examined for: .....

Approved by:

## 1. External Examiner

Name: Prof. Abdelmaseim M. Awadelfird

Signature: ..... Date: 29/12/2021

## 2. Internal Examiner

Name: Dr. Kout Elhaj Mohamed

Signature: Kout ..... Date: 27/12/2021

## 3. Supervisor

Name: Dr. Ahmed Elhassan Elfaki

Signature: ..... Date: 27/12/2021

## **Acknowledgments**

This thesis would not have been possible without the support of many people. First of all, I would like to express my gratitude to my supervisor, Dr. Ahmed Hassan Alfaki, whose encouragement, guidance and support from the initial to the final level enabled me to develop an understanding of the research. Thanks also for his kindness, patience and good motivation for me to achieve my PhD. Massive thanks to Dr. Ahmed Salih Alhag, my co-supervisor for his advice and supervision throughout my research.

I am grateful to all the members of the department of Physics at Education college Nile Valley University for their stimulating support. Especially, I would like to thank Dr. Mohamed Hashim for the helpful technical support.

I am deeply indebted to the Sudanese Civil Defense General Administration for their sponsorship. I am also grateful to the Institute of Radiation Safety of the Sudanese Atomic Energy Authority and the laboratory department at Al-Salam cement factory for providing the various facilities for doing my research.

Finally, I would like to show my gratitude and my love to my family for their support and love through the duration of my PhD life. One of the most important motivations to achieve my PhD has been to make you proud. Also, special thanks to all of my friends for their friendship and support, and I offer my regards and blessings to all of those who supported me in any respect during the completion of the research.

## Abstract

The aim of this study was to determine environmental radioactivity level and elemental concentrations of rock and soil samples from Quarries cement factories (River Nile State -Sudan). The activity concentrations of naturally occurring radioactive materials in the  $^{238}\text{U}$  and  $^{232}\text{Th}$  decay chains and from  $^{40}\text{K}$  were determined by means of a gamma-ray spectrometry system using a sodium iodide (Na I) detector in a low background configuration. The ranges of activity concentrations of  $^{238}\text{U}$ ,  $^{232}\text{Th}$  and  $^{40}\text{K}$  were found to be  $3.15 \leftrightarrow 39.14$ ,  $7.42 \leftrightarrow 60.59$  and  $38.29 \leftrightarrow 612.59 \text{ Bq.kg}^{-1}$ , respectively. The results of this current study have been compared with the world mean values of 35, 30 and 400  $\text{Bq.kg}^{-1}$ , respectively, specified by the UNSCEAR (2000). The artificial radionuclide,  $^{137}\text{Cs}$ , was not observed in statistically significant amounts above the background level in the current study.

Concerning radiological risk to human health, the absorbed gamma dose rate (D) in air at 1 meter above the ground surface was estimated to lie in the range 9.49 to 62.51  $\text{nGy.h}^{-1}$ ; the outdoor annual effective dose equivalent (AEDE) was evaluated to vary from 0.012 to 0.10  $\text{mSv.y}^{-1}$ , with the arithmetic mean value of 0.028  $\text{mSv.y}^{-1}$ , which is comparable to the worldwide effective dose of 0.070  $\text{mSv.y}^{-1}$ . Also, the values of the  $\text{Ra}_{\text{eq}}$  and the Hex for all rock and soil samples in the present work are lower than the accepted safety limit value of 370  $\text{Bq.kg}^{-1}$  and below the limit of unity, respectively. The results indicate that the radiation hazard from primordial radionuclides in all soil samples from the area studied in this current work is not significant.

Additionally hazards health of human exposure of radon-222 have been determined out of the statistical analysis didn't show any significant difference between the background concentrations of  $^{222}\text{Rn}$  of all cement quarries using portable device radon scout plus (SARAD). Based on the UNSCEAR guidelines for annual doses of ionizing radiation by source, the recommended upper threshold effective dose of total radon and their progenies is  $1\text{mSvy}^{-1}$ , with a typical range of observed doses up to  $0.66 \pm 0.11\text{mSv/y}$ . The mean risk of lung cancer in the cement quarries is  $11.7 \pm 1.98$  which is much lower than the standard ICRP (170-230 lung cancer).

## ملخص البحث

هدفت هذه الدراسة لتحديد مستوى النشاط الإشعاعي البيئي الطبيعي والتركيزات الأولية لعينات الصخور والتربة من مصانع الأسمنت بالمحاجر (ولاية نهر النيل - السودان) وتم أخذ عدد (64) عينة صخرية من مواقع المحجار لعدد ثلاثة مصانع للأسمنت الموجودة بالولاية وعدد (3) عينات ترابية من المواد الإضافية التي تدخل في صناعة الاسمنت. تمت دراستها وتحليلها بواسطة جهاز مطياف أشعة جاما باستخدام كاشف يودييد الصوديوم, وذلك لمعرفة تركيزات تلك العينات الصخرية والترابية وتم العثور على نطاقات من تركيزات النشاط لكل من نيودات البوتاسيوم - 40 واليورانيوم - 238 والثوريوم - 232 ووجد أن تركيز النشاط الإشعاعي ل  $^{238}\text{U}$  ما بين 3.15 الى 39.14 ( $\text{Bq.kg}^{-1}$ ) و تركيز  $^{232}\text{Th}$  بين 7.42 الي 60.59 ( $\text{Bq.kg}^{-1}$ ) و  $^{40}\text{K}$  من 38.29 الي 612.59 ( $\text{Bq.kg}^{-1}$ ).أنتضح أن جميعها تقع تحت حدود المستوي المسموح به لمستويات النشاط الإشعاعي العالمي البالغة 35 و 30 و 400 كيلوجرام بكريل ، وهى التي حددتها(UNSCEAR (2000) لم يتم ملاحظة النويدات المشعة الاصطناعية كالسيزيوم - 137 في الدراسة الحالية.

ايضاً تم تحديد المخاطر الإشعاعية على صحة الإنسان ، وقدر معدل جرعة جاما الممتصة (**D**) في الهواء على ارتفاع متر واحد فوق سطح الأرض في النطاق من 9.49 الي 62.51 ( $\text{nGy.h}^{-1}$ ) ؛ تم تقييم مكافئ الجرعة الفعالة السنوية الخارجية (**AEDE**) من 0.012 الي 0.10 ( $\text{mGy.h}^{-1}$ ) ،ويمكن مقارنته بالجرعة الفعالة في جميع أنحاء العالم والتي تبلغ 0.070 ملي سيفرت في السنة. أيضاً تم تقييم **Ra<sub>eq</sub>** و **H<sub>ex</sub>** لجميع عينات الصخور والتربة وظهرت النتائج بأنها أقل من قيمة حد الأمان المقبولة البالغة 370 ( $\text{Bq.kg}^{-1}$ ). إضافة لذلك تم تحديد المخاطر الصحية للتعرض البشري لغاز الرادون- 222 من خلال التحليل الإحصائي الذي لم يظهر أي فرق كبير بين تركيزات  $^{222}\text{Rn}$  في جميع محاجر الأسمنت وذلك وفقاً للإرشادات الصادرة من UNSCEAR وكان نطاق العينات المرصوده يصل إلى ( $0.11 \pm 0.66$ ) ملي سيفرت/سنة كما جاء متوسط خطر الإصابة بسرطان الرئة في مناطق المحاجر لكل المصانع  $11.7 \pm 1.98$  وهو أقل بكثير من توصيات الهيئة الدولية للوقاية من الإشعاع **ICRP** القياسي (170- 230) لسرطان الرئة.

## Table of Contents

No	Title	Page
1	Acknowledgments	I
3	Abstract	II
4	ملخص البحث	III
5	<b>CHAPTER ONE: Introduction</b>	
6	1.1 Introduction	1
7	1.2 Statement of the research problem	2
8	1.3 Hypotheses	2
9	1.4 Objectives of the Research	3
10	1.4.1 General Objective	3
11	1.4.2 Specific Objective	3
	<b>CHAPTER TWO: Literature review</b>	
12	2.1 General Background	4
13	2.2 NORM Background	5
14	2.3 NORM Review	7
15	2.4 Cement Composition	7
16	2.5 Rock Analysis	9
17	2.6 Rock Radioactivity	10
18	2.6.1 Potassium	10
19	2.6.2 Thorium	11
20	2.6.3 Uranium	11
21	2.7 Review of the cement Quarries in River Nile State	14
22	2.8 Radioactivity and Radioactivity Decay	15
23	2.8.1 General	15
24	2.8.2 Serial Radioactive Decay	17
25	2.8.3 Equations for Serial Radioactive Decay Chain	19
26	2.8.4 Radioactive Equilibrium	19
27	2.8.4.1 Secular Equilibrium	20
28	2.8.4.2 Transient Equilibrium	21
29	2.8.4.3 No Equilibrium	22
30	2.9 Nuclear Decays Types	23
31	2.9.1 Alpha Decay	23
32	2.9.2 Beta Decay	23
33	2.9.3 Gamma Decay	24
34	1.10 Interaction of gamma rays with matter	24
35	2.10.1 Photoelectric absorption	25
36	2.10.2 Compton scattering	26

37	2.10.3 Pair production	29
39	2.11 Radiation Dosimetry	29
40	2.11.1 Basic Radiation Quantity and Unit Exposure	30
42	2.11.1.1 Absorbed Dose	30
43	2.11.1.2 Equivalent and Effective Dose	31
44	2.11.2 Sources of Radiation Exposure	32
45	2.11.2.1 Natural Sources	33
46	2.11.2.2 Artificial Sources	33
47	2.11.3 Radiation Protection and Dose Limits	35
48	<b>CHAPTER THREE: Materials and methods</b>	
49	3.1 Gamma-ray spectroscopy	38
50	3.1.1 Introduction	38
51	3.1.2 Principles	38
52	3.1.3 Instrumentation	39
53	3.1.3.1 The detector	40
54	3.1.3.1.1 Sodium iodide – NaI (TI)	40
55	3.1.3.2 Low voltage power supply	41
56	3.1.3.3 Preamplifiers	41
57	3.1.3.4 High voltage power supply	41
58	3.1.3.5 Amplifier	42
59	3.1.3.6 Multi-Channel Analyzer (MCA)	42
60	3.1.3.7 Analog to Digital Conversion (ADC)	42
61	3.1.4 Detection limit of gamma spectroscopy	42
62	3.1.5 Advantage and disadvantage	42
63	3.1.5.1 Advantages	42
64	3.1.5.2 Disadvantage	42
65	3.2 Radon Scout Plus (SARAD GmbH)	43
66	3.3 Material and methods	43
67	3.3.1 Study area	43
68	3.3.2 Samples collection	44
69	3.3.3 Sample preparation	47
70	3.4 Samples measurement	49
71	3.4.1 Energy Calibration	49
72	3.4.2 Efficiency Calibration	50
73	3.4.3 Background measurement	51
74	3.4.4 Sample Measurement	52
75	3.5 Assessment of Dose	53
76	3.5.1 Absorbed Dose Rate (D)	53
77	3.5.2 Annual Effective Dose Equivalent (AEDE)	53

79	3.5.3 Radium Equivalent Activity ( $Ra_{eq}$ )	53
80	3.5.4 External Hazard Index ( $H_{ex}$ )	54
81	<b>CHAPTER FOUR : Results and Discussion</b>	
82	4.1 Spectrum Analysis and Nuclides Identification	55
83	4.1.1 Background Spectrum	55
84	4.1.2 Rock Spectrum	57
85	4.2 Measurement of Radioactivity	58
86	4.3 Assessment of Radiological Hazard	67
87	4.4 Determine of $^{222}Rn$ concentration and Assessment of Radiological Hazard	70
88	<b>CHAPTER FIVE: Conclusion and Recommendations</b>	
89	5.1 Conclusion	74
90	5.2 Recommendations	75
91	References	76
92	Appendix	85

## List of Tables

No	Title	Page
<b>Table 2.1</b>	Ranges and averages of the concentrations of $^{238}\text{U}$ , $^{232}\text{Th}$ , and $^{40}\text{K}$ in typical rocks and soils	6
<b>Table 2.2</b>	Approximate composition of the cement clinker	9
<b>Table 2.3</b>	Radiation weighting factors for different ionizing radiations	31
<b>Table 2.4</b>	Tissue weighting factors	32
<b>Table 2.5</b>	Annual average doses from all sources	34
<b>Table 2.6</b>	ICRP 60 recommended effective dose limits	37
<b>Table 3.1</b>	The locations of different sampling areas in River Nile state at this present work	45
<b>Table 3.2</b>	The result of Gamma Spectroscopy Analysis using Reference Source(MW652)	49
<b>Table 3.3</b>	The energies, their respective branching ratios and the corresponding efficiency of the radionuclides in the standard	51
<b>Table 4.1</b>	The results of the calculated activity concentrations of selected gamma-ray transitions from $^{238}\text{U}$ series , $^{232}\text{Th}$ series and $^{40}\text{K}$ with the weighted mean activity concentrations of $^{238}\text{U}$ , $^{232}\text{Th}$ and $^{40}\text{K}$ in each rock samples	60
<b>Table 4.2</b>	The results of the mean activity concentrations of $^{238}\text{U}$ , $^{232}\text{Th}$ and $^{40}\text{K}$ in all rock samples	62
<b>Table 4.3</b>	Comparison between the average mean activity concentrations of $^{238}\text{U}$ , $^{232}\text{Th}$ and $^{40}\text{K}$ in sampling areas from all factories and overall results with the mean value for the worldwide	65
<b>Table 4.4</b>	Comparison of mean and range values of the activity concentration of $^{238}\text{U}$ , $^{232}\text{Th}$ and $^{40}\text{K}$ in Bq.kg-1with some countries	67
<b>Table 4.5</b>	The results of the absorbed dose rate ( <b>D</b> ), the annual effective dose equivalent ( <b>AEDE</b> ), the radium equivalent activity ( <b>Ra<sub>eq</sub></b> ) and the external hazard index ( <b>H<sub>ex</sub></b> ) in all rock samples	68
<b>Table 4.6</b>	The calculated, combined absorbed dose rate ( <b>D</b> ), annual effective dose equivalent ( <b>AEDE</b> ), radium equivalent activity ( <b>Ra<sub>eq</sub></b> ) and external hazard index ( <b>H<sub>ex</sub></b> )	69
<b>Table 4.7</b>	$^{222}\text{Rn}$ concentrations ( <b>Mean<math>\pm</math>SD</b> ) Bq/m <sup>3</sup> of indoor air samples of quarries cement factories River Nile State, Sudan	72

## List of Figures

No	Title	Page
<b>Figure 2.1</b>	Average annual dose to the world population from various sources	5
<b>Figure 2.2</b>	Shows the decay scheme of three nuclear chains	13
<b>Figure 2.3</b>	Map of Sudan showing an area of the Quarries cement (River Nile State-Sudan)	14
<b>Figure 2.4</b>	The exponential radioactive decay curve of $^{228}\text{Ac}$ with half-life, $T_{1/2}$	16
<b>Figure 2.5</b>	Growth of a short lived daughter ( $^{222}\text{Rn}$ ) from a much longer lived parent ( $^{226}\text{Ra}$ ) until reaching Secular Equilibrium	20
<b>Figure 2.6</b>	Growth and decay of a short lived daughter ( $^{212}\text{Bi}$ ) from a slightly longer lived parent ( $^{212}\text{Pb}$ ) in Transient equilibrium	21
<b>Figure 2.7</b>	Growth and decay of a longer lived daughter ( $^{218}\text{Po}$ ) from a short lived parent ( $^{214}\text{Pb}$ ) in case of no equilibrium	22
<b>Figure 2.8</b>	Photon Probability interaction with mater	24
<b>Figure 2.9</b>	The transmission curve for alpha particles, mono energetic electrons and gamma rays, showing with their respective mean ranges	25
<b>Figure 2.10</b>	Schematic of the photoelectric absorption process	26
<b>Figure 2.11</b>	Schematic of the Compton scattering process	27
<b>Figure 2.12</b>	Schematic of the pair production process and annihilation	29
<b>Figure 2.13</b>	The three gamma-ray interaction processes and their regions of dominance	29
<b>Figure 2.14</b>	Possible, theoretical dose-response curves	35
<b>Figure 3.1</b>	Block diagram of a basic gamma spectrometry system	40
<b>Figure 3.2</b>	Electronic instrumentation used in the current study and A coaxial Sodium Iodide (NaI) detector	40
<b>Figure 3.3</b>	Schematic diagram of a scintillation detector	41
<b>Figure 3.4</b>	Map Quarries cement factories River Nile State, Sudan	44
<b>Figure 3.5</b>	The apparatus for sample preparation (a) a Jo crusher (b) a Vibratory mill	48
<b>Figure 3.6</b>	A prepared soil sample filling in a Marinelli beaker sealed with plastic tape to prevent the escape of airborne radionuclide	48
<b>Figure 3.7</b>	Energy Calibration Curve for NaI Detector	50
<b>Figure 3.8</b>	Efficiency Calibration Curve for NaI Detector	51
<b>Figure 3.9</b>	Instrumentation set -up of gamma-spectroscopy	52
<b>Figure 4.1</b>	Background spectrum measured counted for 10,900 seconds (3 hours)	57

<b>Figure 4.2</b>	Gamma-ray spectrum associated with decays from radionuclides detected from sample code TKM-12, obtained at location ALTakamul Cement Factory	58
<b>Figure 4.3</b>	The overall activity concentrations of $^{238}\text{U}$ , $^{232}\text{Th}$ and $^{40}\text{K}$ in rock samples studied from different sampling areas	64
<b>Figure 4.4</b>	The mean average values of $^{238}\text{U}$ , $^{232}\text{Th}$ and $^{40}\text{K}$ activity concentrations for each Quarries area measured in the current work	64
<b>Figure 4.5</b>	Comparison between the average mean activity concentrations of $^{238}\text{U}$ , $^{232}\text{Th}$ and $^{40}\text{K}$ in sampling areas from all factories	66
<b>Figure 4.6</b>	Comparison of $^{222}\text{Rn}$ indoor concentration in cement quarries, background and mean concentration	73

# **Chapter One**

## **Introduction**

# Chapter One

## Introduction

### 1.1 Introduction

Sudan is a country rich in raw materials and minerals and has seen in recent decades, a major development in the field of infrastructure, can be seen from the number of increasing in buildings with a modern style, which requires the use of some materials used in construction such as cement and other materials.

Is the cement industry of important industries in Sudan and concentrated the industry in the state of the Nile River, which is located north of Sudan, so that helped the existing earth's crust in that area on the presence of limestone which represent a large proportion of materials consisting of cement, which the reason to the existence of four factories specialized in the manufacture of Cement due to the ease of presence of the raw material used in the manufacture of cement. There can be a probability to contain that area high concentrations of radioactivity, especially that there were previous studies of commercial cement samples for some factories in that area.

The cement composed of raw materials that are usually found in the earth's crust, and they contain small but measurable amounts of naturally occurring radioactive materials [1]. Although building materials act as a source of radiation to the inhabitants in their dwellings, they also have the role of a shield against outdoor radiation [2]. All building raw materials and products derived from rock and soil contain various amounts of mainly natural radionuclides of the uranium ( $^{238}\text{U}$ ) and thorium ( $^{232}\text{Th}$ ) series, and the radioactive isotope of potassium ( $^{40}\text{K}$ ). In the  $^{238}\text{U}$  series, the decay chain segment starting from radium ( $^{226}\text{Ra}$ ) is radiologically the most important and, therefore, reference is often made to  $^{226}\text{Ra}$  instead of  $^{238}\text{U}$  [3]. It has long been known that some construction materials are naturally more radioactive than others. The level of natural radioactivity in construction materials, even of low-level activity, gives rise to external and internal indoor exposure [4]. The external radiation exposure is caused by gamma radiation originating from members of the uranium and thorium decay chains and from  $^{40}\text{K}$  and the internal radiation exposure, mainly affecting the respiratory tract, is due to the short-lived daughter products of radon which are released from construction

materials into room air [5]. Thus, the knowledge of radioactivity in building materials is important to estimate the radiological hazards to human health [6].

The most important naturally occurring radionuclides present in cements are  $^{226}\text{Ra}$ ,  $^{232}\text{Th}$  and  $^{40}\text{K}$ , as mentioned above. Knowledge of basic radiological parameters such as radioactive contents and attenuation coefficients in building materials is important in the assessment of possible radiation exposure of the population as most people spend about 80% of their life inside houses and offices. This knowledge is essential for the development of standards and guidelines for the use of these materials [7].

With the increased probability various nuclear incidents in many areas or Incorrect disposal of radioactive materials, the possibility of radioactive contamination or the presence of high concentrations of the natural occurring radioactive material may be high in these materials, which could affect human health and the environment. This risk can reduce by ensuring that the contaminated material is not up to the public, through the assessment of the quality of the raw material for manufacturing.

The International Commission on Radiological Protection (**ICRP**) has developed a series of guidelines and technical documents related to the safety and dose limits permitted from natural occurring radioactive materials. There are a lot of laws that govern importing of these materials.[8]

## **1.2 Statement of the research problem**

The health effects of chronic exposure to low background levels of radiation are poorly understood and there is need for further studies in this area. Such studies are not easily carried out in the laboratory settings because they require large populations of the subjects, e.g. human, environment, etc .

The Results of studies so far carried out in some cement samples from many Sudanese cement factories are generally inconclusive and sometimes contradictory. Sudan also has a number of high background radiation areas (e.g. Jibal alnoba, Aro, Krn and some areas in western Sudan etc). The present study is therefore proposed to exploit the rare opportunity presented by the presence of the results of studies so far carried out in some cement samples Sudanese cement factories this result was an indicator of study this study.

### **1.3 Hypotheses**

Most of population of Sudan are exposed to background radiation levels from components of buildings and dwellings and the cement is considered as an essential component, there is need therefore to investigate radiation levels in components of buildings and dwellings.

Most of population generally and worker especially at the cement factories quarries were exposed levels for radon gas, is recognized to cause lung cancer. However, The dangers of indoor radon exposure have led to guidelines by the World Health Organization (WHO) and public health legislation in many countries to require radon monitoring and mitigation.

### **1.4 Objectives of this study**

The objectives of this study are:

#### **1.4.1 General objective**

To determine environmental radioactivity level and elemental concentrations of rock and soil samples from Quarries cement factories (River Nile State-Sudan).

#### **1.4.2 Specific objectives**

1. To determine the absorbed gamma dose rates in air above soil containing uniform distribution of radio- nuclides ( $^{232}\text{Th}$ ,  $^{238}\text{U}$ ,  $^{226}\text{Ra}$  and  $^{40}\text{K}$ ) using Gamma-ray spectroscopy.
2. To determine radionuclide content and understanding of the nature of distribution (i.e. activity concentrations) of rock samples from Quarries cement factories.
3. Assessment of radiological hazard by calculate the annual effective dose from the activity concentrations.
4. To measure the Radon ( $^{222}\text{Rn}$ ) concentrations in indoor air guidelines at the Quarries cement factories using portable device radon scout plus (SARAD)..
5. Evaluate the radiological hazard from exposure of the Radon ( $^{222}\text{Rn}$ ) by calculate the probability of lung cancer cases per million people (CPPP).

# **ChapterTwo**

## **Literature review**

# Chapter Two

## Literature review

### 2.1 General background

After the discovery of radioactivity in 1896 by A. H. Becquerel [9], the science of radioactivity has been extensively studied. Radionuclides are the sources of radioactivity and emit nuclear radiations which have become a part of our daily lives. The most common forms of ionizing radiation are alpha particles, beta particles and gamma rays [10]. Radiation can arise not only from natural radionuclides but it can also be from man-made sources. The properties of radiations have been widely applied to various purposes such as medicine, biology, industry, agriculture, and electric power generation [11]. As a result of the applications of radiation, humans can be exposed to the radiation emitting from different radioactive sources depending upon their activities and surroundings [12]. However, not all of the population is subjected to all the various sources of radiation exposure. For instance, patients who are treated with medical irradiation or members of staff who work in the nuclear industries may receive higher radiation exposure levels than members of general public [13].

The most obvious radiation sources to which all individuals are exposed (both in working and public environments) are the ionizing radiation arising from radionuclides in the earth's surroundings and the interaction of cosmic rays on the earth's atmosphere [14].

According to the National Council on Radiation Protection and Measurements Report (NCRP) No.45, the most significant source of radiation exposure to humans is due to natural radiation in the environment [15]. This exposure to naturally occurring radiation also accounts for up to 85% of annual exposure dose received by the world population, as shown in Figure 2.1 [16]. The International Atomic Energy Agency (IAEA) reports that the exposure from natural radiation is, in most cases, of little or no concern to the public, except those working with mineral ores and naturally occurring radioactive material (NORM) [17]. Nevertheless, the World Nuclear Association (WNA) states that any dose of radiation involves a possible risk to human health [16], even though the level of individual exposure from naturally occurring radioactive elements is usually statistically insignificant on an individual basis, from a health physics point of view. In order to protect the general public health against the radiation risk

originating from naturally occurring radiation, the measurement of radioactivity in the environment needs to be considered to assess the biological effect on the human. This has also become the focus of greater attention by the IAEA in recent years [17].

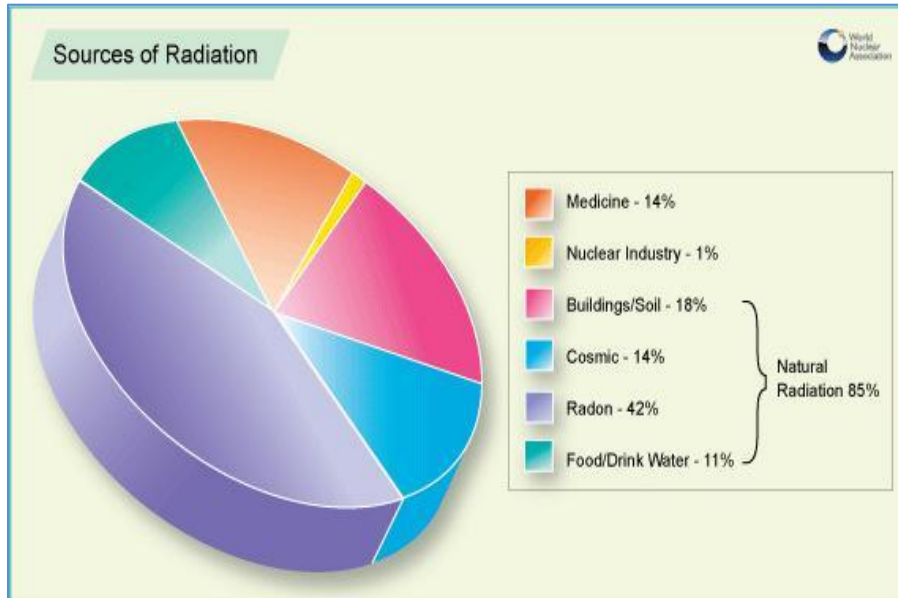


**Figure 2.1: Average annual dose to the world population from various sources.[16].**

## 2.2 NORM background

The exposure of human beings to naturally occurring radiation arises mainly from two different origins [14]. The first source comes directly from cosmic radiation from the outer space. The interactions of cosmic-ray particles in the atmosphere can create a number of radioactive nuclei such as  $^3\text{H}$ ,  $^7\text{Be}$ , and  $^{14}\text{C}$  [15]. The other main contributor is the terrestrial radioactive materials which originate from the formation of the earth and are present everywhere in the earth’s crust, and in the human body itself. Apart from the exposure from direct cosmic rays and cosmogenic radionuclides, natural exposures arise mainly from the primordial radio nuclides which are spread widely and are present in almost all geological materials in the earth’s environment [15, 18]. These radionuclides are known as Naturally Occurring Radioactive Material or by the acronym ‘NORM’ [16, 18]. Only very long lived nuclides, with decay half-lives comparable to the age of the earth, and their decay products, contribute to this natural radiation background in significant quantities [14]. The majority of naturally occurring radionuclides

belong to the radionuclides in the  $^{238}\text{U}$  and  $^{232}\text{Th}$  series, and the single decay radionuclide,  $^{40}\text{K}$  [19].

Those radionuclides which emit either alpha or beta particles may be taken into the body by ingestion or inhalation and can give rise to internal exposures. Additionally, some of these nuclear species may emit gamma rays following their radioactive decay; these represent the main sources of external (whole body) exposures to humans [13-14].

**Table 2.1: Ranges and averages of the concentrations of  $^{238}\text{U}$ ,  $^{232}\text{Th}$ , and  $^{40}\text{K}$  in typical rocks and soils. Data is taken from references [11, 19].**

Rock Type	Potssuim-40		Thorium -232		Uranium -238	
	Total K (%)	Bq.Kg <sup>-1</sup>	ppm	Bq.Kg <sup>-1</sup>	ppm	Bq.Kg <sup>-1</sup>
<b>Igneous rocks</b>						
Basalt						
Crustal average	0.8	300	3-4	10-15	0.5-1	7-10
Mafic	0.3-1.1	70-400	1.6, 2.7	7	0.5, 0.9	7
Salic	4.5	1100-1500	16, 20	60	3.9, 4.7	50
Granite (crustal aver.)	>4	>1000	17	70	3	40
<b>Sedimentary rocks</b>						
Shale, sandstones	2.7	800	12	50	3.7	40
Clean quartz	<1	<300	<2	<8	<1	<10
Dirty quartz	2	400	3-6	10-25	2-3	40
Arkose	2-3	600-900	2	<8	1-2	10-25
Beach sands (unconsolidated)	<1	<300	6	25	3	40
Carbonate rocks	0.3	70	2	8	2	25
All rock (range)	0.3-4.5	700-1500	1.6-20	7-80	0.5-4.7	7-60
Continental crust (ave.)	2.8	850	10.7	44	2.8	36
Soil (ave.)	1.5	400	9	37	1.8	22

Terrestrial radio nuclides present in all soils at different trace levels, give rise to external exposures due to gamma radiation [14]. The specific levels of the radioactivity of various soils are related to the nature of the parent rock from which the soils are derived and the process of soil formation [20]. For example, igneous rocks, such as granite, generally exhibit higher radioactivity than sedimentary rocks (excluding some shales and phosphate rocks which have relatively high content of radionuclides) [14]. Table 2.1 gives typical natural radioactivity concentrations in common rocks and soils.

### **2.3 NORM reviews**

There have been many studies concerning naturally occurring radioactive materials in soil media which provide information on the nature and levels of background radiation and to observe the change in radioactivity levels in that particular area. Most of these studies show that most soils contain  $^{40}\text{K}$  and nuclides of the uranium and thorium series, with a range of their concentrations which varies broadly. For example, Assessment of Natural Radioactivity Levels and Radiological Hazards of cement samples in Iraq by Zaki A., et.al) the results of the activity concentrations of  $^{226}\text{Ra}$  ranged from  $5.8 \leftrightarrow 43.17 \text{ Bq kg}^{-1}$ , with an average value  $24.25 \text{ Bq kg}^{-1}$  for  $^{226}\text{Ra}$  from  $0.99 \leftrightarrow 55.79 \text{ Bq kg}^{-1}$ , with an average value  $25.41 \text{ Bq kg}^{-1}$  for  $^{232}\text{Th}$  and from  $53.28 \leftrightarrow 185.34 \text{ Bq kg}^{-1}$ , with an average value  $93.17 \text{ Bq kg}^{-1}$  for  $^{40}\text{K}$  [21].

In 2004, Matiullah, et.al) reported the mean activity of  $^{226}\text{Ra}$ ,  $^{232}\text{Th}$ ,  $^{40}\text{K}$ , and  $^{137}\text{Cs}$  in soil samples of Bahawalpur, Pakistan being 32.9, 53.6, 647.4 and 1.5  $\text{Bq.kg}^{-1}$  [22]. In the same year, the activity concentration levels arising from radionuclides  $^{238}\text{U}$ ,  $^{232}\text{Th}$ , and  $^{40}\text{K}$  in surface soils in Cyprus were carried out by Tzortzis, et.al) ranging between  $0.01 \leftrightarrow 39.3$ ,  $0.01 \leftrightarrow 39.8$  and  $0.04 \leftrightarrow 565.8 \text{ Bq.kg}^{-1}$ , respectively [23]. Soil and sediments were used for measuring the natural radioactivity levels of Firtina Valley in Turkey by the team of Karadeniz Technical University, University of Rize, and Cekmece Nuclear Research and Training. The average concentrations of  $^{238}\text{U}$ ,  $^{232}\text{Th}$ ,  $^{40}\text{K}$ , and  $^{137}\text{Cs}$  in the area surveyed in that study were found to be 50, 42, 643, and 85  $\text{Bq.kg}^{-1}$  in soil samples, and 39, 38, 573 and 6  $\text{Bq.kg}^{-1}$  in sediment samples [24].

### **2.4 Cement composition**

Cement is a powdery substance made with calcined lime and clay as major ingredients. Clay used provides silica, alumina, and iron oxide, while calcined lime

basically provides calcium oxide[25]. In cement manufacturing, raw materials of cement are obtained by blasting rock quarries by boring the rock and setting off explosives [26]. These fragmented rocks are then transported to the plant and stored separately in soils. They are then delivered, separately, through chutes to crushers where they are then crushed or pounded to chunks of ~1/2 inch – sized particles [27]. Depending on the type of cement being produced, required proportions of the crushed clay, lime stones, and any other required materials are then mixed by a process known as prehomogenization and milled in a vertical steel mill by grinding the material with the pressure exerted through three conical rollers that roll over a turn in milling table. Additionally, horizontal mills inside which the material is pulverized by means of steel balls are also used. It is then homogenized again and calcined, at 1400°C, in rotary kilns for the raw material to be transformed to a clinker, which is a small, dark grey nodule 3-4 cm in diameter. The clinker is discharged from the lower end of the kiln while it is red hot, cooled by various steps, ground and mixed with small amounts of gypsum and limestone, and very finely ground to produce cement [28].

In the calcinations process, in the kiln, at high temperatures, the above oxides react forming more complex compounds[29]. For instance, reaction between  $\text{CaCO}_3$ ,  $\text{Al}_3(\text{SiO}_3)_2$ , and  $\text{Fe}_2\text{O}_3$  would give a complex mixture of alite,  $(\text{CaO})_3\text{SiO}_2$ ; belite,  $(\text{CaO})_2\text{SiO}_2$ ; tricalcium aluminate,  $\text{Ca}_3(\text{Al}_2\text{O}_3)$ ; and ferrite phasetetracalciumaluminoferrite,  $\text{Ca}_4\text{Al}_2\text{O}_3\text{Fe}_2\text{O}_3$  with the evolution of  $\text{CO}_2$  gas in the Portland cement clinker [30]. However, there can be many other minor components also since natural clay also contains Na, K, and so on. In the chemical analysis of cement, its elemental composition is analyzed (e.g., Ca, Si, Al, Mg, Fe, Na, K, and S). Then, the composition is calculated in terms of their oxides and is generally expressed as wt.% of oxides. For simplicity, if we assume that the clinker contains the above four main oxides, they can be simply represented by the Bogue formulae where CaO,  $\text{Al}_2\text{O}_3$ ,  $\text{Fe}_2\text{O}_3$ , and  $\text{SiO}_2$  are denoted as C, A, F, and S, respectively [31]. In this notation, alite (tricalcium silicate)  $[(\text{CaO})_3\text{SiO}_2]$ , belite (dicalciumsilicate)  $[(\text{CaO})_2\text{SiO}_2]$ , celite (tri calcium aluminate)  $[\text{Ca}_3\text{Al}_2\text{O}_6=3\text{CaO}\cdot\text{Al}_2\text{O}_3]$ , and brown millerite (tetra calcium aluminoferrite)  $[\text{Ca}_4\text{Al}_2\text{Fe}_2\text{O}_{10}=4\text{CaO}\cdot\text{Al}_2\text{O}_3\cdot\text{Fe}_2\text{O}_3]$  are represented by  $\text{C}_3\text{S}$ ,  $\text{C}_2\text{S}$ ,  $\text{C}_3\text{A}$ , and  $\text{C}_3\text{AF}$ , respectively. If we analyze the elemental composition of Ca, Al, Fe, and Si, usually from X-ray fluorescence spectroscopy, then we express them as wt.% of their respective oxides. However, cement contains water ( $\text{H}_2\text{O}$ ), sulphate ( $\text{SO}_3$ ), sodium

oxide ( $\text{Na}_2\text{O}$ ), potassium oxide ( $\text{K}_2\text{O}$ ), gypsum ( $\text{CaSO}_4 \cdot 2\text{H}_2\text{O}$ ), which are denoted as H, S, N, K, and CSH<sub>2</sub>, respectively. Note that gypsum (calcium sulphate dihydrate) is considered as  $\text{CaO} \cdot \text{SO}_3 \cdot 2\text{H}_2\text{O}$  and hence its notation is CSH<sub>2</sub> [32]. As such, approximate composition of the cement clinker is different from the above values and is depicted in Table 2.2[25].

**Table 2.2 Approximate composition of the cement clinker[25].**

Compound	Formula	Notation	Wt%
<b>Celite</b> (trickiumalmuminate)	$\text{Ca}_3\text{Al}_2\text{O}_6$ [3CaO.Al <sub>2</sub> O <sub>3</sub> ]	<b>C<sub>3</sub>A</b>	<b>10</b>
<b>Brownmillerite</b> (tetracalcium aluminoferrite)	$\text{Ca}_4\text{Al}_2\text{Fe}_2\text{O}_6$ [4CaO.Al <sub>2</sub> O <sub>3</sub> .Fe <sub>2</sub> O <sub>3</sub> ]	<b>C<sub>4</sub>AF</b>	<b>8</b>
<b>Belite</b> (dicalcium silicate)	$\text{Ca}_2\text{SiO}_4$ [2CaO.SiO <sub>2</sub> ]	<b>C<sub>2</sub>S</b>	<b>20</b>
<b>Alite</b> (tricalcium silicate)	$\text{Ca}_3\text{SiO}_5$ [3CaO.SiO <sub>2</sub> ]	<b>C<sub>3</sub>S</b>	<b>55</b>
<b>Sodium oxide</b>	$\text{Na}_2\text{O}$	<b>N</b>	<b>2</b>
<b>Potassium oxide</b>	$\text{K}_2\text{O}$	<b>K</b>	<b>≤2</b>
<b>Gypsum</b> (calcium sulphate dihydrate)	$\text{CaSO}_4 \cdot 2\text{H}_2\text{O}$ [CaO.SO <sub>4</sub> .2H <sub>2</sub> O]	<b>CSH<sub>2</sub></b>	<b>5</b>

## 2.5 Rock analysis

Environmental monitoring includes sampling and analyses of the rock extensive surveillance, monitoring, and research activities are required to assess the extent and severity of rock contamination, to evaluate the effects of contaminated rocks on freshwater and marine environment, and to prepare a plan for appropriate remedial action. In field studies, monitoring is carried out to determine the variation in the concentrations of different contaminants as a function of time and depth. In many reports on the investigations of rocks, a detailed description of sampling techniques is often overlooked. Sampling procedures often vary depending on the objectives of the monitoring, method of analysis and the need of the analyst. However, in order to compare the results of the studies carried out at sites with different environmental conditions and contaminants, harmonized sampling techniques must be used. Processing a non-

representative or incorrectly collected or stored sample may lead to erroneous conclusions and the waste of resources. Without adequate care QA/QC measures, sampling could become the weakest link in the entire process of rock analysis. Therefore, it is of paramount importance to harmonize guidelines for sampling and sample preparation that will meet the requirements of the various methods of analysis[33].

Analysis of rocks provides environmentally significant information. Their chemical characterization is needed to understand the naturally compounds. Sample preparation includes separation of coarse material, homogenization and drying, and it is the first crucial step of rock analysis. Nuclear and related analytical techniques such as gamma ray spectrometry is used for radionuclides determination while neutron activation analysis (NAA). Although these are non-destructive techniques, they require proper sample preparation prior to theanalysis[33].

## **2.6 Rock radioactivity**

Natural radionuclides have been the components of the earth since its existence. It is widely spread in earth's environment and exists in soil, rock, sediment, water, plants and air. There are many naturally occurring radionuclides in environment, containing uranium and thorium series radioisotopes and natural  $^{40}\text{K}$ . The natural radioactivity in soil comes from  $^{238}\text{U}$  and  $^{232}\text{Th}$  series and natural  $^{40}\text{K}$ . Natural environmental radioactivity and associated external exposure due to gamma radiation depend primarily on the geological conditions of soil and rock formations of each region in the world. The distribution of natural radionuclides in the field can be used as a tracer for both rocks and dredged soil dispersal and accumulation mechanisms. Usually, the activity concentration of radionuclides increases inversely with the grain size and, in proportion, with the density and types of the rocks . The  $^{238}\text{U}$  - $^{232}\text{Th}$  radionuclides are associated with heavy minerals, whereas  $^{40}\text{K}$  is concentrated within clay minerals. In addition, other parameters such as mineralogy, organic content, and geochemical composition could play an important role in the absorption of radioactive elements in the rock samples [34].

### **2.6.1Potassium ( $^{40}\text{K}$ )**

Potassium is a soft, silver-white metal. An important constituent of soil, it is widely distributed in nature and is present in all plant and animal tissues.

Potassium is one of the most reactive metals in nature, and it forms a number of compounds that have many commercial uses. Potassium-40 is a naturally occurring radioactive isotope of potassium. (An isotope is a different form of an element that has the same number of protons in the nucleus but a different number of neutrons.) Two stable (nonradioactive) isotopes of potassium exist, potassium-39 and potassium-41. Potassium-39 comprises most (about 93%) of naturally occurring potassium, and potassium-41 accounts for essentially all the rest. Radioactive potassium-40 comprises a very small fraction (about 0.012%) of naturally occurring potassium [35].

### **2.6.2 Thorium ( $^{232}\text{Th}$ )**

Thorium is a naturally occurring radioactive metal that is found at low levels in soil, rocks, water, plants and animals. Almost all naturally occurring thorium exists in the form of radioactive isotope thorium-232, thorium-230 and thorium-228. There are more than 10 other thorium isotopes that can be artificially produced. Smaller amounts of these isotopes are usually produced as decay products of other radionuclides and as unwanted products of nuclear reactions [36].

Thorium-232 is not a stable isotope. As thorium-232 decays, it releases radiation and forms decay products which include radium-228 and thorium-228. The decay process continues until a stable, nonradioactive decay product is formed. In addition to thorium-232, thorium-228 is present in background. Thorium-228 is a decay product of radium-228 and thorium-228 decays into radium-224. The radiation from the decay of thorium and its decay products is in the form of alpha and beta particles, and gamma radiation. Alpha particles can travel only short distances and cannot penetrate human skin. Beta particles are generally absorbed in the skin and do not pass through the entire body. Gamma radiation, however, can penetrate the body. The half-life of thorium-232 is very long at about 14 billion years.

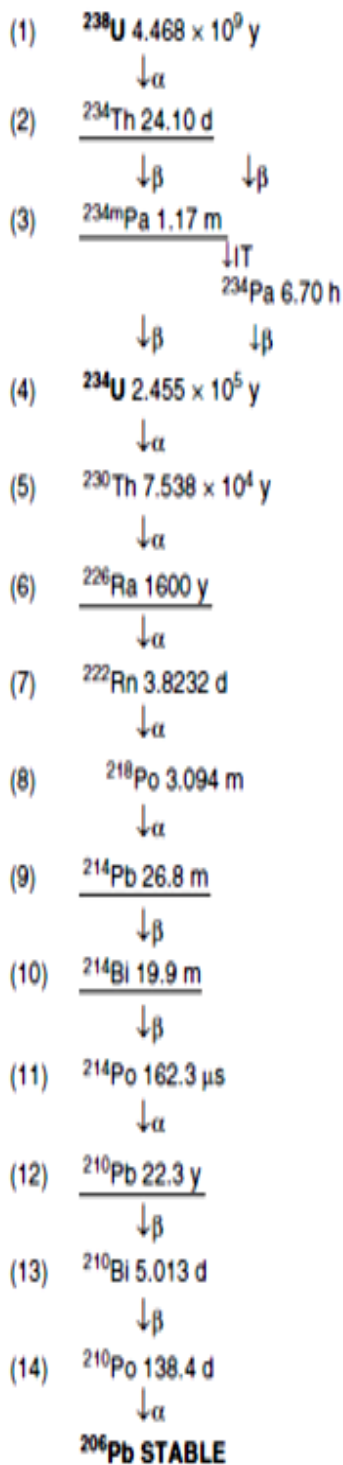
Due to the extremely slow rate of decay, the total amount of natural thorium in the earth remains fairly constant, but it can be moved from place to place by natural processes and human activities. Thorium is used to make ceramics, lantern mantles, welding rods, camera and telescope lenses, and metals used in the aerospace industry [36].

### **2.6.3 Uranium ( $^{238}\text{U}$ )**

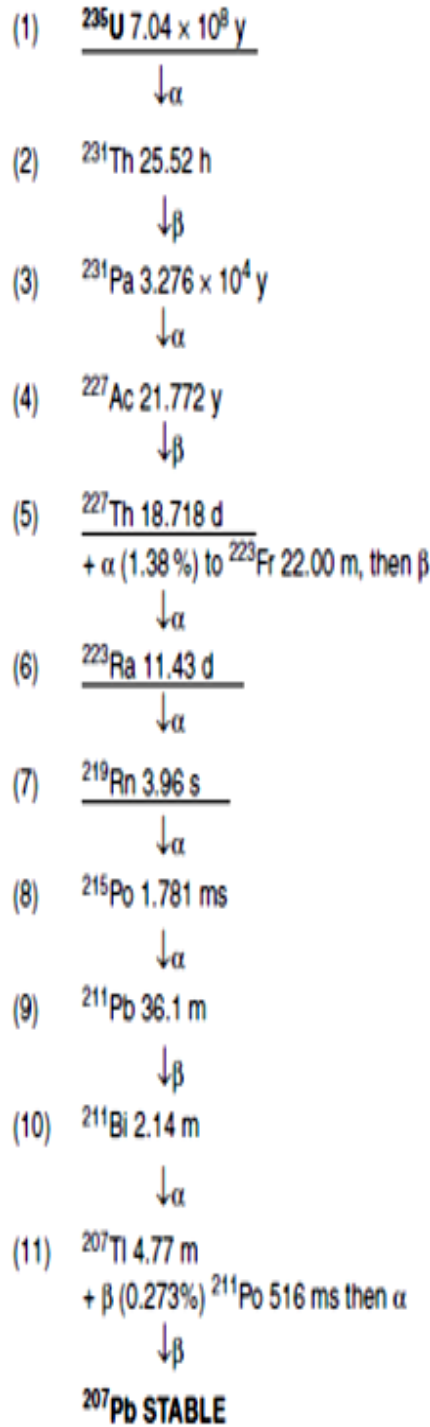
Is a silvery-white metallic chemical element in the actinide series of the periodic table, with atomic number 92. The uranium nucleus binds between 141 and 146 neutrons, establishing six isotopes ( $^{233}\text{U}$  through  $^{238}\text{U}$ ), the most common of which are uranium-238 (146 neutrons) and uranium-235 (143 neutrons). All isotopes are unstable and uranium is weakly radioactive. Uranium has the second highest atomic weight of the naturally occurring elements, lighter only than plutonium-244 [35].

Natural radionuclides occur in different types of rocks such as sedimentary, metamorphic and igneous rocks in the earth for example,  $^{235}\text{U}$ ,  $^{238}\text{U}$ , and  $^{232}\text{Th}$  and their radionuclide daughters which are called terrestrial radionuclides source. Such radionuclides have long half-lives about billions of years. Besides, their unstable daughter decay leads to a stable nuclide,  $^{206}\text{Pb}$ . Terrestrial radionuclides are classified in three main nuclear chains; The first is the  $^{238}\text{U}$  chain, which represents 99% of uranium in nature and contains 14 radionuclides.  $^{238}\text{U}$  decays to  $^{234}\text{Th}$  through alpha decay until it reaches the stable  $^{206}\text{Pb}$ . All  $^{238}\text{U}$  daughters have half-lives shorter than that of  $^{238}\text{U}$  which means the daughter and the parent are in secular equilibrium. The second nuclear chain is  $^{235}\text{U}$  decay chain, which represents 0.72% of uranium in nature. The chain is shorter compared to the  $^{238}\text{U}$  chain as it contains 12 radionuclides. The last nuclear chain is from  $^{232}\text{Th}$ . It represents 100% of thorium in nature. This series contains 10 radionuclides. Finally, it is important to know that not all radionuclides in the chains emit characteristic gamma rays, only those radionuclides underlined shown in figure 2.2 are measurable by gamma spectrometry [37].

### The uranium series U-238



### The actinium series U-235



### The thorium series Th-232

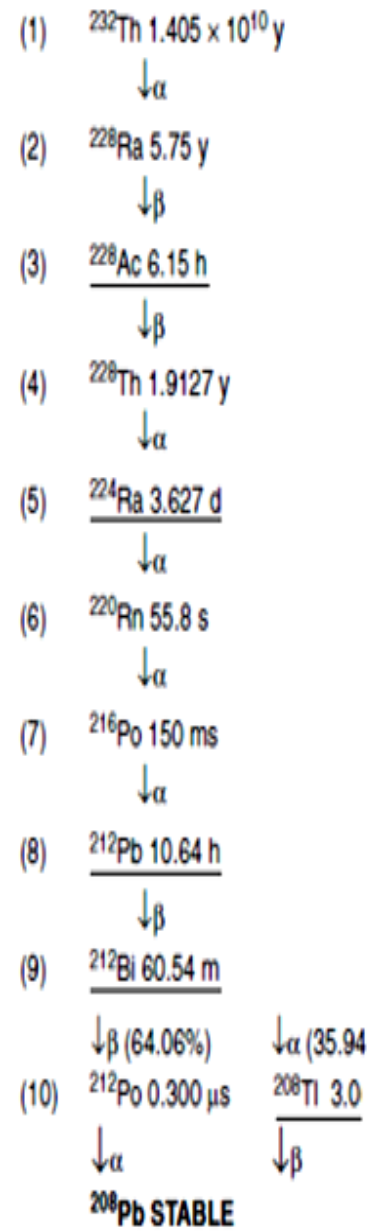
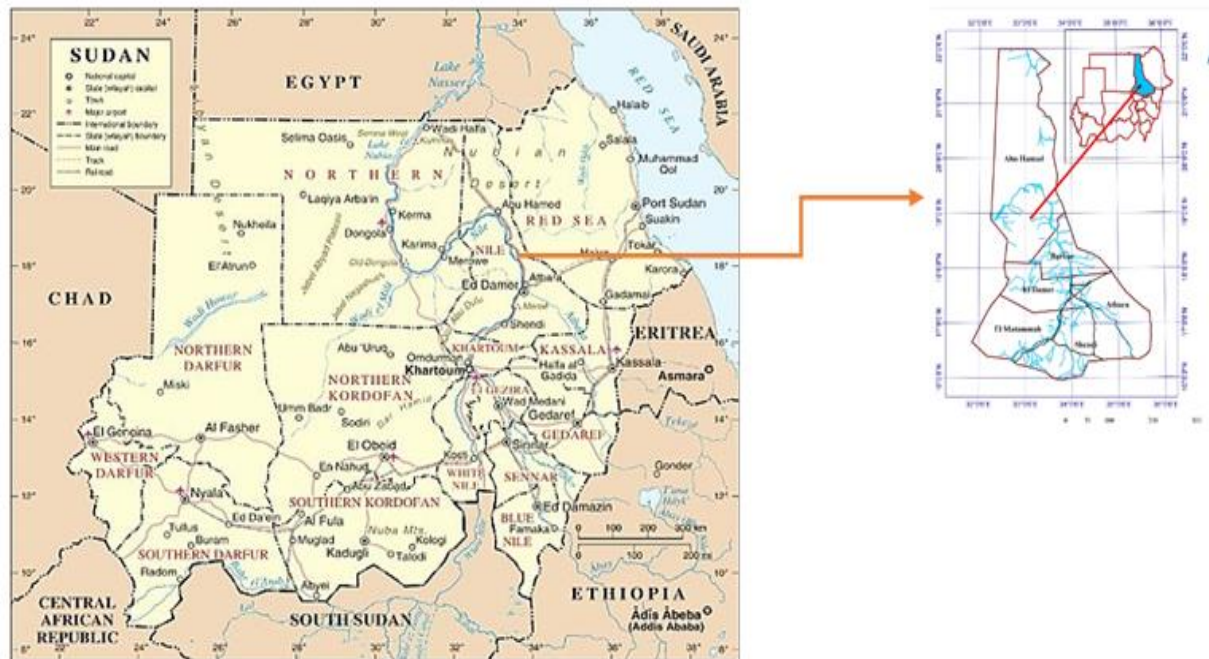


Figure 2.2: Shows the decay scheme of three nuclear chains [37].

## 2.7 Review of the cement quarries in the River Nile State Sudan:

Sudan is situated in northern Africa, with a 853 km (530 mi) coastline bordering the Red Sea.[38]. It has land borders with Egypt, Eritrea, Ethiopia, South Sudan, the Central African Republic, Chad, and Libya. With an area of 1,886,068 km<sup>2</sup> (728,215 sq. mi), it is the third-largest country on the continent (after Algeria and Democratic Republic of the Congo) and the sixteenth-largest in the world. Sudan lies between latitudes 8° and 23°N. The terrain is generally flat plains, broken by several mountain ranges . In the east are the Red Sea Hills.[39] shown in the figure 2.3.



**Figure 2.3: Map of Sudan showing an area of the Quarries cement (River Nile State-Sudan)**

The area can be divided into two main series: Abu Harrik (high-grade gneisses) and Kurmut (low-grade volcanoes dimentary) series overlain by Nubian Sandstone Formation, Tertiary volcanics and superficial sediments, respectively. The Abu Harrik area has been investigated for the purpose of determining the extent of the marble bands and their suitability for cement industry. Three deposits have been located, namely, Abu Harrik, Abu Haraz and Abu Khosus. Abu Harrik is about 12.5 km west of the Nile River near the Abu Haraz-Berber ferry. The marble bands strike NNESSW and extend for about 4.4 km with a width ranging between 70 to 200 meters. These results show that this marble is suitable for

cement industry. Depending on pre-determined blending proportions the marble in these three occurrences can be used for producing high quality cement. Clays, as necessary ingredients for a cement manufacture are found around Kadabas area close to the Nile. The average values of chemical analyses of samples taken from these clays gave 6.07% CaO; 2.07% MgO; 54.15% SiO<sub>2</sub>; 7.89% Al<sub>2</sub>O<sub>3</sub>; 5.31% Fe<sub>2</sub>O<sub>3</sub> and 11.81% , which is suitable for cement industry. The amount of clays, covering about 7 km<sup>2</sup> and 120- 170 m deep, is sufficient for such an industry[40].

## **2.8 Radioactivity and radioactive decay**

### **2.8.1 General**

Radioactivity is a statistical process describing the spontaneous transformation of unstable atomic nuclei (called ‘parent nuclei’) into a more stable configuration (called ‘daughter’ nuclei) [10, 41,42] without the effect of physical and chemical condition [43]. In case where the daughter product is also unstable, the decay process carries on until a daughter nucleus reaching stability[10]. Consequently, the energy of the transformation can be released by the emission of nuclear particles and/or in terms of electromagnetic radiations [41,44].

The strength or intensity of the radioactivity is called the activity and is defined as the rate of nuclei number decaying [41,45,46]. The probability per unit of time for the decay of a given nucleus is a constant which can be commonly named as the disintegration or decay constant ( $\lambda$ ) [10,47]. The rate of radioactive decay which is related to the activity can be expressed by the fundamental law of radioactive decay by [48,50].

$$A = -\frac{dN}{dt} = \lambda N \quad (\text{Eq.2.1})$$

As shown in equation 2.1, A is the activity of an isotopically pure source, which is equal to the number, dN, of radioactive nuclei disintegrating in a given time, dt, and is proportional to the number, N, of radioactive nuclei present at time, t [41,45].  $\lambda$  is the decay constant and the negative sign indicates that the number of radioactive nuclei decrease when the time increases [10, 47, 51]. Originally, the unit of activity is curie (Ci) which is based on the activity of 1 gram of Radium (<sup>226</sup>Ra), which is equivalent to 3.7 x 10<sup>10</sup> disintegrations per second [51,53]. Currently, the Becquerel (Bq) has become the standard unit of activity and is defined as one disintegration per second [10, 46, 49]. Thus, 1 Ci is equal to 3.7x10<sup>10</sup>Bq [38, 44, 49].

The solution to equation 2.1 leads to the exponential law of radioactive decay which may be written as [46, 54]

$$N = N_0 e^{-\lambda t} \text{ (Eq.2.2)}$$

where  $N_0$  is the original number of nuclei present at time  $t = 0$ . The number of nuclei decreases exponentially with time [54]. Figure 2.4 illustrates the number of nuclei decaying as a function of time.

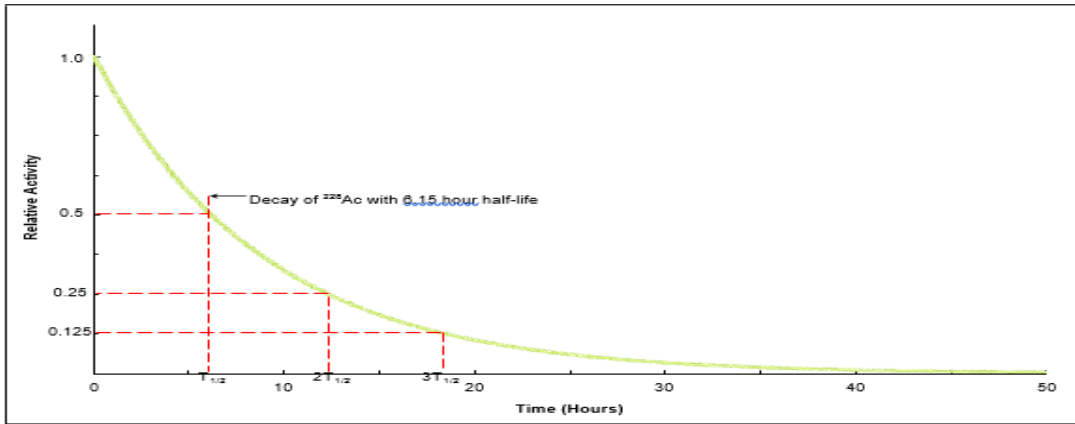


**Figure 2.4: The exponential radioactive decay curve of  $^{228}\text{Ac}$  with half-life,  $T_{1/2}$  [54].**

Usually, the rate of radioactive decay can be characterized in terms of a specific time frame known as the half-life [41, 46]. The half-life ( $T_{1/2}$ ) is the time required for one-half of a certain number of active nuclei to disintegrate [43] as shown in Figure 2.4 The decay constant correlates with the half-life by [47]

$$\lambda = \frac{0.693}{T_{1/2}} \text{ (Eq.2.3)}$$

The decay constant is also considered in terms of the **mean lifetime**,  $\tau$  which is described as the mathematical average time a radioactive nucleus is likely to survive before it decays. The relationship between the decay constant and the mean lifetime is [45, 47,48].

$$\tau = \frac{1}{\lambda} \text{ (Eq.1.4)}$$

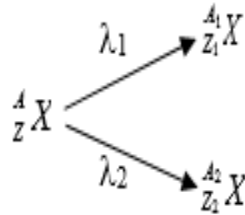
Thus, the mean lifetime can be expressed in terms of the half-life by using equation 2.3 and 2.4 as

$$\tau = \frac{T_{1/2}}{0.693} \text{ (Eq.2.5)}$$

The half-life and mean lifetime for radionuclides can range from fractions of seconds to billions of years [40]. For the decay constant, the units will be expressed in reciprocal time depending on the half-life of the radioactive nuclide

used in equation 2.3 [41,51]. In some cases, unstable nuclei may decay by several competing modes as shown by

This type of disintegration is named **a branching decay** [43, 47] and the relative probability of the competing modes can be specified by the **branching ratios** [47,55]. Each decay mode



has their own characteristic decay constant which can be assigned for each mode of decay by multiplying the total observed decay constant with the ratio of that branch [43]. The total observed decay constant is equal to the sum of the partial decay constants [43,54] as

$$\lambda_{tot} = \lambda_1 + \lambda_2 + \dots \quad (\text{Eq.2.6})$$

Similarly, the partial half-lives for each decay mode correlate with the partial decay constants for  $n$ -th mode of decay [54] as

$$T_{1/2}(n) = \frac{0.693}{\lambda_n} \quad (\text{Eq.2.7})$$

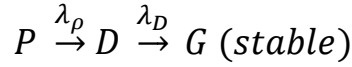
### 2.8.2 Serial radioactive decay

The simplest radioactive decay is that of a radioactive parent nuclide decaying with a unique decay constant leading to a stable daughter nuclide [41]. For example, the  $^{14}\text{C}$  nuclide decays to form the stable product of  $^{14}\text{N}$  as indicated by



There are several radioactive isotopes which decay by this simple parent-daughter decay mode such as  $^3\text{H}$ ,  $^{14}\text{C}$ ,  $^{32}\text{P}$ ,  $^{35}\text{S}$ ,  $^{36}\text{Cl}$ ,  $^{45}\text{Ca}$ , and  $^{131}\text{I}$  [41]. However, another common decay sequence can take place when the decay of parent radionuclide forms a daughter product which is also itself radioactive [10, 47]. There are many examples of decay series among the radioactive nuclides particularly in the natural radioactive series [45,48]. A more complicated radioactive decay chain begins with a radioactive parent nucleus  $P$  decaying with a decay constant  $\lambda_p$  into a daughter nucleus  $D$ , which in turn is radioactive and then

subsequently decays with a decay constant  $\lambda_D$  into a stable grand-daughter, G as described below [41,47].



To consider the numbers of nuclei of P, D, and G at any time, t, the radioactive series can be given by the following three equations [45].

$$\frac{dN_P}{dt} = -\lambda_P N_P \quad (\text{Eq.2.8})$$

$$\frac{dN_D}{dt} = \lambda_P N_P - \lambda_D N_D \quad (\text{Eq.2.9})$$

$$\frac{dN_G}{dt} = \lambda_D N_D \quad (\text{Eq.2.10})$$

From the above three equations, the rate of depletion of the number of radioactive parent nuclei  $dN_P$  follows as equation 2.1 [45]. The rate of change in the number of daughter nuclei,  $dN_D$ , equals the difference between the supply of the new daughter nuclei through decay of the parent nuclei and the loss of the daughter nuclei from the decay of itself to a stable product [43,47,56]. The production rate of the stable end product  $dN_G$  increases at the same rate as the decay rate of daughter nuclei [45].

According to equation 2.2, the number of parent nuclei can be written as [10,44,53]

$$N_P(t) = N_P(0)e^{-\lambda_P t} \quad (\text{Eq.2.11})$$

where  $N_P(0)$  is the initial number of parent nuclei at time  $t = 0$

From equation 2.1 and 2.11, the activity of the radioactive parent nuclei  $A_P(t)$  as a function of time can be derived as [47]

$$A_P(t) = \lambda_P N_P(t) = \lambda_P N_P(0)e^{-\lambda_P t} = A_P(0)e^{-\lambda_P t} \quad (\text{Eq.2.12})$$

The initial activity at  $t = 0$  is  $A_P(0) = \lambda_P N_P(0)$

Using the expression of  $N_P(t)$  in equation 2.11 inserted into equation 2.9, this gives

$$\frac{dN_D}{dt} = \lambda_P N_P(t) - \lambda_D N_D(t) = \lambda_P N_P(0)e^{-\lambda_P t} - \lambda_D N_D(t) \quad (\text{Eq.2.13})$$

The solution of this equation for the number of daughter nuclei presents as [10,48,53]

$$N_D(t) = N_P(0) \frac{\lambda_P}{\lambda_D - \lambda_P} (e^{-\lambda_P t} - e^{-\lambda_D t}) \quad (\text{Eq.2.14})$$

The activity of the daughter nuclei  $A_D(t)$  may then be expressed as [47]

$$A_D(t) = \lambda_D N_D(t) = N_P(0) \frac{\lambda_P \lambda_D}{\lambda_D - \lambda_P} (e^{-\lambda_P t} - e^{-\lambda_D t}) \text{ (Eq.2.15)}$$

In some situations, the grand-daughter of a radioactive decay is still unstable and continues with producing another radioactive product. Thus, it is possible to have series or chains of radioactive decays as called ‘**decay chain**’ or ‘**radioactive series**’ [10,47].

### 2.8.3 Equations for serial radioactive decay chain

A set of first-order differential equations, called the **Bateman equations** can be derived for the growth and the decay of the members of a sequential decay [51,54,57]. The differential equations for radioactive decays of n-nuclide series in the case that the parent nuclei is present alone at t = 0 are as follows [45, 47,57]

$$\frac{dN_1}{dt} = -\lambda_1 N_1 \quad \text{(Eq.2.16)}$$

$$\frac{dN_i}{dt} = -\lambda_{i-1} N_{i-1} - \lambda_i N_i \quad (i = 2, n)$$

The general solution for the number of nuclei of the *n*th member at time, *t*, can be given by [46,47,57]

$$N_n(t) = \frac{N_1(0)}{\lambda_n} \sum_{i=1}^n \lambda_i \alpha_i e^{-\lambda_i t} \text{ (Eq.2.17)}$$

Where

$$\alpha_i = \prod_{\substack{j=1 \\ j \neq i}}^n \frac{\lambda_j}{(\lambda_j - \lambda_i)} \text{ (Eq.2.18)}$$

Calculations using equation 2.16 can become rather tedious for the decay chains with several members [54] and it is apparent that the coefficients,  $\alpha_i$ , can be calculated only if all decay

constants are different [57].

For the decays of sequential radioactive decays, there are three main limiting conditions involving the term **equilibrium**, these being (i) secular equilibrium; (ii) transient equilibrium; and (iii) the state of no equilibrium [41]. Each of these cases is discussed in the next section.

### 2.8.4 Radioactive equilibrium

Radioactive equilibrium is the term usually used to explain the state when the members of the radioactive series decay at the same rate as they are produced [58].

The three predominant cases of the state of equilibrium can be explained as below.

### 2.8.4.1 Secular equilibrium

‘**Secular Equilibrium**’ is a steady- state condition that in which the half- life of the parent is very much greater than that of the daughter, therefore,  $\lambda_P \ll \lambda_D$  [46,48,52].

Since,  $\lambda_P \ll \lambda_D$  and  $\lambda_P \approx 0$ , then  $e^{-\lambda_P t} \approx 1$  and the number of the daughter nuclei in equation 2.13 be simplified to [41,47,51].

$$N_D(t) = N_P(0) \frac{\lambda_P}{\lambda_D} (1 - e^{-\lambda_D t}) \text{ (Eq.2.19)}$$

Consider equation 2.18, when time increases, the term  $e^{-\lambda_P t}$  can be neglected during the growth of the daughter and the number of the daughter nuclei will reach an equilibrium value after about seven half-life of the daughter [50, 52, 56]. At equilibrium, the parent and daughter activities are equal, i.e., [50,52]

$$\lambda_P N_P = \lambda_D N_D \text{ (Eq.2.20)}$$

When secular equilibrium is established, the activity of the daughter becomes equal to that of its parent with time [41,50,52]. In a decay chain, the numbers of nuclei of the various daughters present at equilibrium are inversely proportional to their decay constants and the formation rate and the decay rate of every radioactive daughter equals the decay rate of its parent,  $\lambda_P N_P$  [48,52, 54]. For instance, the sequence of  $^{226}\text{Ra}$  with half-life 1600 years to  $^{222}\text{Rn}$  with half-life 3.8235 days is of the interest for the state of secular equilibrium. Figure 2.5 shows the build-up and establishment of secular equilibrium of  $^{222}\text{Rn}$  from the extremely long-lived parent  $^{226}\text{Ra}$ .

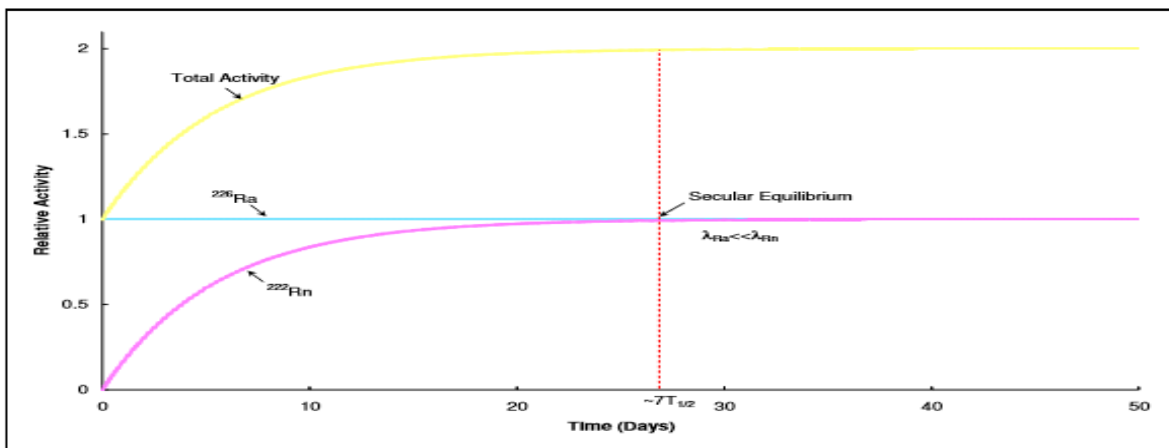


**Figure 2.5: Growth of a short lived daughter ( $^{222}\text{Rn}$ ) from a much longer lived parent ( $^{226}\text{Ra}$ ) until reaching Secular Equilibrium.**

### 2.8.4.2 Transient equilibrium

A different state of equilibrium, called ‘Transient Equilibrium’ can occur in which the parent half life is longer – lived than that of the daughter but not significantly longer [38, 40, 49], i.e., where ,  $\lambda_P < \lambda_D$  In exponential term of the daughter,  $e^{-\lambda_P t}$  becomes much smaller and can negligible compared with  $e^{-\lambda_D t}$  after a sufficiently long period of time [41,50,52]. Under this condition, equation 2.13 may be written as [41, 45, 51].

$$N_D(t) = N_P(0) \frac{\lambda_P}{\lambda_D - \lambda_P} e^{-\lambda_D t} \text{ (Eq.2.21)}$$

Using equation 1.2 as  $N_P(t) = N_P(0)e^{-\lambda_P t}$ , equation 2.21 can be rewritten as

$$\frac{N_D}{N_P} = \frac{\lambda_P}{\lambda_D - \lambda_P} \text{ (Eq.2. 22)}$$

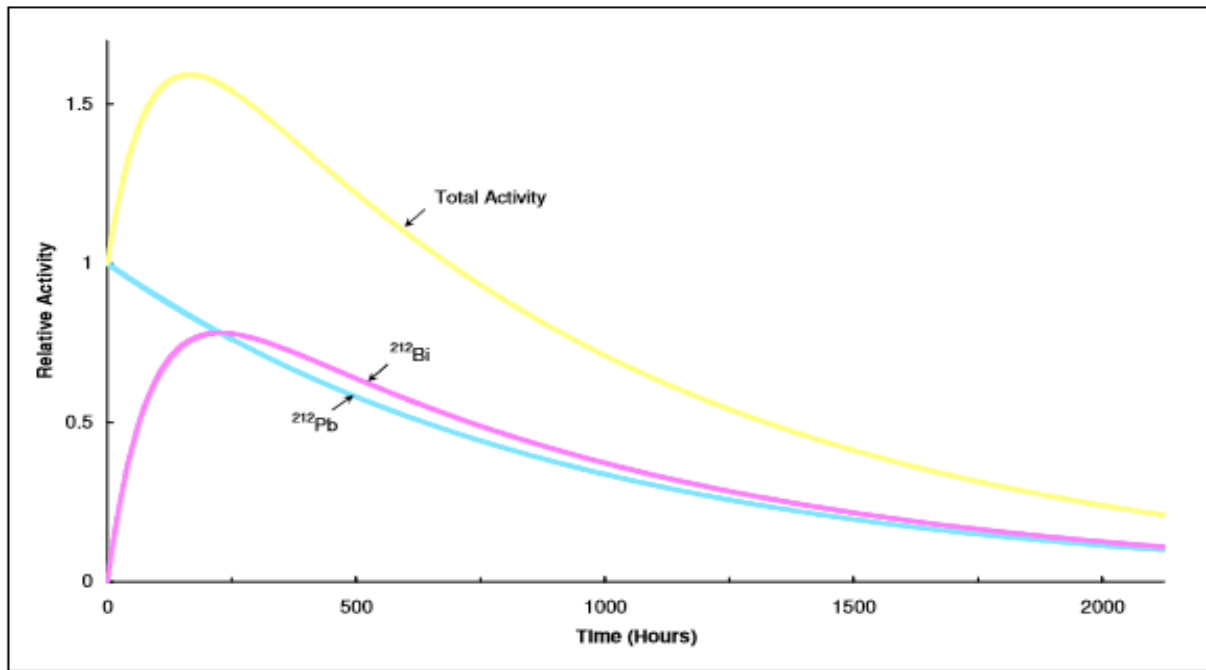


**Figure 2.6: Growth and decay of a short lived daughter ( $^{212}\text{Bi}$ ) from a slightly longer lived parent ( $^{212}\text{Pb}$ ) in Transient equilibrium.**

From equation 2.22, after a state of transient equilibrium exists, the ratio of the number of nuclei tends to the constant value [41, 45,51] and the parent and daughter nuclides will decay at the same rate, related to the decay of parent which is the characteristic of transient equilibrium [51,52,54]. An example of transient

equilibrium is the decay of  $^{212}\text{Pb}$  with half-life 10.64 hours to  $^{212}\text{Bi}$  with half-life 60.55 minutes shown in Figure 2.6.

The time at which equilibrium between the parent and daughter nuclides will be established depends on the magnitudes of their half-lives [51,52]. The shorter the half-life of the daughter compared with the parent, the faster the state of equilibrium will be reached [52].

### 2.8.4.3 No equilibrium

In case the half-life of the parent nuclide has shorter lived than that of the daughter product, the state of equilibrium will not be attained [47, 50,52].

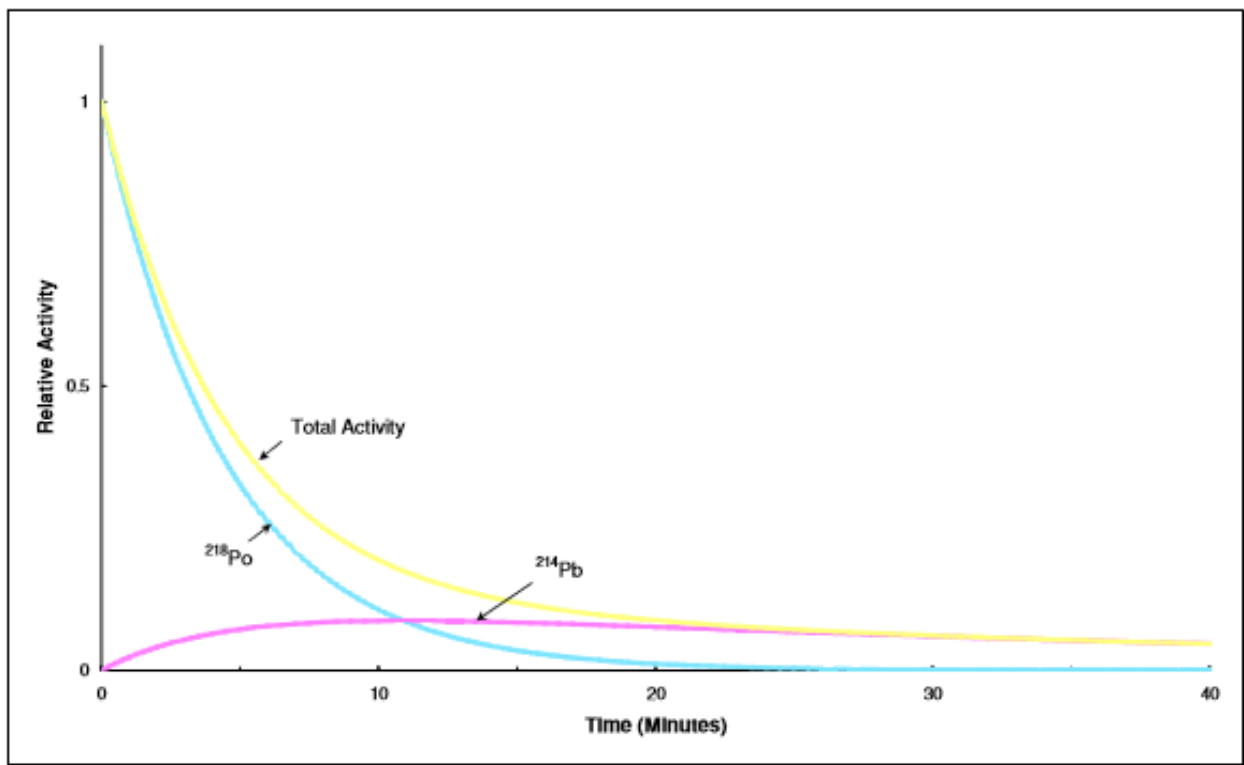


**Figure 2.7: Growth and decay of a longer lived daughter ( $^{218}\text{Po}$ ) from a short lived parent ( $^{214}\text{Pb}$ ) in case of no equilibrium**

The number of daughter nuclei can generally calculated from equation 2.13 For long times, the term  $e^{-\lambda_P t}$ , can be negligible and calculation of the daughter decay can be given by [47,51]

$$N_D(t) = N_P(0) \frac{\lambda_P}{\lambda_D - \lambda_P} e^{-\lambda_D t} \quad (\text{Eq.2. 23})$$

The parent, owing to its shorter half-life, will decay away while the number of daughter nuclei build up to a maximum and then decrease eventually with its own

characteristic half-life [43,50,52]. Figure 1.7 illustrates the decay of  $^{218}\text{Po}$  with half-life 3.1 minutes to  $^{214}\text{Pb}$  with half-life 26.8 minutes without the state of equilibrium.

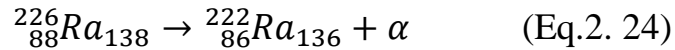
Note that the activity only describes the number of disintegrations per second and says nothing about the kind of radiations emitted or their energies [47]. The next section will describe types of radiations and their characteristic.

## 2.9 Nuclear decays types

The three major decay modes are alpha decay, beta decay and gamma decay. In alpha and beta decay an unstable nucleus emits alpha or beta particle to become stable. In case of gamma ray decay, a nucleus de-excites result by the emission of a photon.

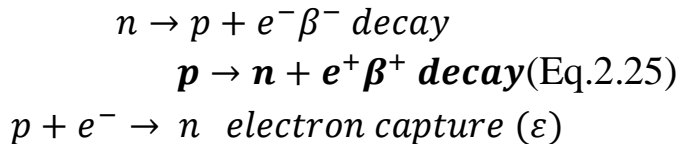
### 2.9.1 Alpha decay

Alpha decay is a nuclear decay leading to unstable nucleus to become stable. In this nuclear decay the atomic nucleus are divided into two protons even two neutrons (Helium atoms)[59]. Because of the loss of two protons in this decay, an element is changed to another one. For example, in the following decay:

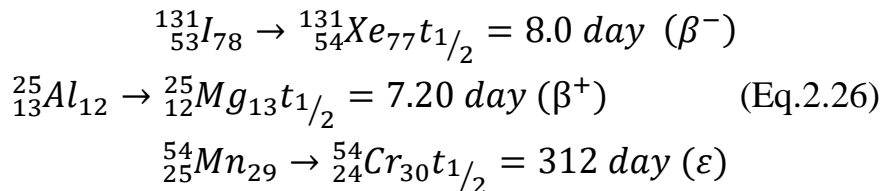


### 2.9.2 Beta decay

Beta decay is a nuclear decay leading to unstable nucleus to become more stable. In this decay a proton is converted to a neutron or a neutron is converted to a proton through the following process [48]:



The first type of beta decay is called negative where a neutron is converted to proton with an electron emission. The second type of beta decay is called positive beta decay where a proton is converted to a neutron and a positive electron emission results. In a third case, an electron is consumed by the nucleus. As a result, a proton is converted to a neutron. An example for this process follows:



The number of protons in the nucleus change by one unit, so an element changes to another one. The positron and the neutrino move away from the nucleus due to beta decay. The total mass number A, is still the same when this change occurs in the atoms.

### 2.9.3 Gamma decay

Electromagnetic radiation such as gamma ray interacts with matter through indirect forms which cause ionization by secondary processes. Gamma rays interact with matter through one of the three main mechanisms fig.(2.8), The first one is photoelectric effect, the second mechanism is Compton scattering and the last one is pair production. The photon interacts with the electron of an atom, loses the energy by ionization or excitation so it can be detected [60].

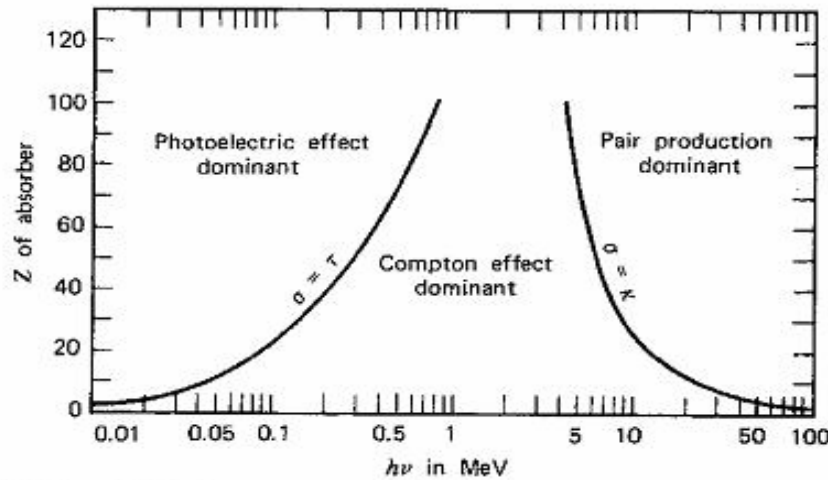
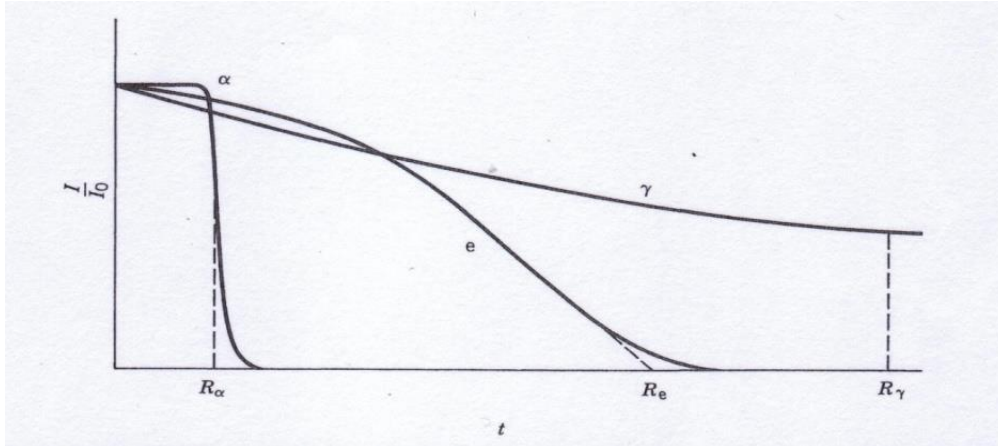


Figure 2.8: Photon Probability interaction with mater [60]

### 2.10 Interaction of gamma rays with matter:

Due to the properties of gamma radiation, the interaction of gamma rays with matter is different in that they have much greater penetration power and longer ranges than the charged, massive alpha and less-massive beta particles. The significant characteristic of gamma radiation absorption in matter is an exponential decay function with depth, without a well defined range, as is observed for charged particles [10, 49, 62].



**Figure 2.9: The transmission curve for alpha particles, mono energetic electrons and gamma rays, showing with their respective mean ranges [47].**

An uncharged gamma-ray photon can interact with electrons in the absorbing material and transfer all or part of its energy to electrons leading to indirect ionization. Interaction of gamma-ray photons with matter can occur by various mechanisms, but only three mechanisms play the most significant roles in radiation measurement [49,50,65]. The processes of photoelectric absorption, Compton scattering, and pair production all contribute to the observed response in gamma ray spectrometry [49].

Some fundamentals of the gamma ray interaction processes are introduced in the following subsection.

### **2.10.1 Photoelectric absorption:**

In the process of photoelectric absorption, a photon interacts with a bound electron in an absorber material in which the photon is completely absorbed. Then, an energetic electron called *photoelectron* is ejected from one of the electron shells with a kinetic energy given by the incident photon ( $h\nu$ ), minus the binding energy of the electron in its origin shell ( $E_b$ ). For typical gamma-ray energies, the emission of the photoelectron is likely to originate from the most tightly bound or, K-shell, of the atom. The binding energies of these K-shell electrons vary from a few Kev for low-Z materials to tens of Kev for material with higher atomic number[49]. The photoelectric absorption process is shown schematically in the diagram below.

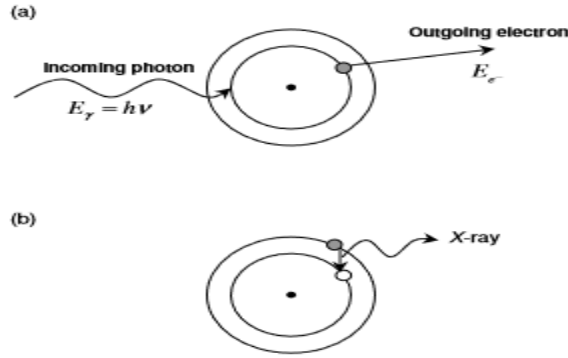


**Figure 2.10: Schematic of the photoelectric absorption process.**

As can be seen in Figure 2.10 (a), the outgoing electron is ejected with a kinetic energy given by the following equation [51,52-61,62].

$$(Eq.2.27) E_{e^-} \rightarrow h\nu - E_b$$

The photoelectron emission also creates a vacancy in a shell of the atom resulting in an excited state. The de-excitation of the atom can occur by the electron rearrangement from higher shells to fill in a vacancy leading to the emission of characteristic X-ray shown in Figure 2.10 (b). Alternatively, the excitation energy can be carried away by the release of other, less tightly bound electrons known as *Auger electrons*. The interaction cross section ( $\tau$ ) of the photoelectric process varies in a complex manner with  $E_\gamma$  and with the value of  $Z$  of the absorber.

A single analytic expression can not describe the probability of this process, but an approximation can be given by the following equation [10, 11,49]

$$(Eq.2.28) \tau \cong \text{const.} \frac{Z^n}{E_\gamma^m}$$

where the power indices  $n$  and  $m$  are numbers ranging from 3 to 5 over the gamma-ray energy region of interest. The photoelectric absorption probability strongly depends on photon energy and atomic number of an absorber material. The strong  $Z$  dependence indicates that a high- $Z$  material is very effective in the absorption of photons. The strong dependence on the photon energy is the reason why the photoelectric process is significant at low energy of photons, but becomes less dominant at higher energies.

### 2.10.2 Compton scattering:

The Compton scattering process describes a collision between the incident gamma-ray photon and weakly bound or free electron in the absorbing material. Instead of giving up its entire energy, only a portion of the photon energy is

transferred to the electron. The result of this interaction is that the incoming gamma-ray photon is degraded in energy and deflected from its original direction and an electron known as a recoil electron is created. From the laws of conservation of total mass-energy and linear momentum, the energies of the scattered photon and recoil electron are related to the angles at which they are emitted. Figure 2.11 shows a schematic of the Compton scattering process.

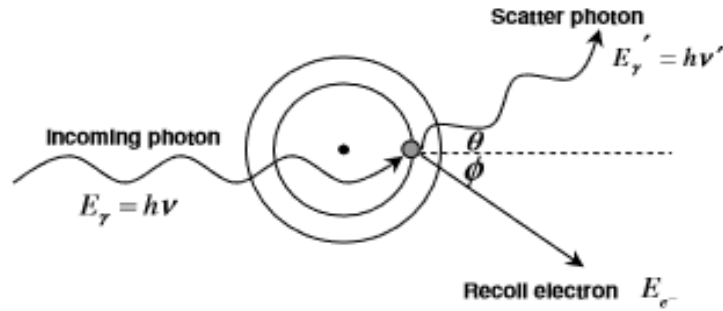


**Figure 2.11: Schematic of the Compton scattering process.**

The energy of the scattered gamma-ray  $h\nu'$  is related to its scattering angle  $\theta$  by the expression [41,45-61,62]

$$(Eq.2.29)h\nu' = \frac{h\nu}{1 + \left(\frac{h\nu}{m_0c^2}\right)(1 - \cos \theta)}$$

where  $m_0c^2 = 511$  KeV represents the rest mass energy of the electron. It then follows that the kinetic energy of the recoil electron is given by the following equation [44,51]

$$(Eq.2.30)E_e = h\nu - h\nu' = h\nu \left( \frac{\left(\frac{h\nu}{m_0c^2}\right)(1 - \cos \theta)}{1 + \left(\frac{h\nu}{m_0c^2}\right)(1 - \cos \theta)} \right)$$

The energy of the recoil electron can vary from zero ( $\theta = 0$ ) up to a maximum value ( $\theta = \pi$ )

depending upon the angle of scatter. The maximum energy of the recoil electron is given by the following equation:

$$(Eq.2.31)E_e = \frac{2h\nu}{2 + m_0c^2/h\nu}$$

The Compton cross section can( $\sigma$ ) be described by the Klein-Nishina formula for a differential solid angle  $d\Omega$  at an angle  $\theta$  as [46]

$$(Eq.2.32) \frac{d\sigma}{d\Omega} = Zr_o^2 \left( \frac{1}{1+\alpha(1-\cos\theta)} \right)^2 \left( \frac{(1+\cos^2\theta)}{2} \right) \left( 1 + \frac{\alpha^2(1-\cos\theta)^2}{(1+\cos^2\theta)[1+\alpha(1-\cos\theta)]} \right)$$

Where  $\alpha = h\nu/m_0c^2$ (photon energy in units of the electron rest energy) and  $r_o$  is the classical electron radius.

The probability of Compton scattering depends strongly on the number of electrons per unit mass of the interacting material. It also depends on the incoming gamma-ray energy as function of  $1/E_\gamma$  [10, 44].

Compton scattering is the dominant interaction process for gamma-ray energies ranging from 0.1 to 10 MeV [61]. At higher energy, another interaction mechanism, known as '*pair production*' becomes more significant.

### 2.10.3 Pair production:

The third significant interaction mechanism of gamma-rays with matter is pair production. This process becomes increasingly important when the incident gamma-ray photon has energy significantly greater than twice the rest mass energy of an electron ( $2m_0c^2 = 1.022 \text{ MeV}$ ). This interaction occurs within the Coulomb field of a nucleus in which the gamma-ray photon is absorbed into the vacuum and is converted into an electron-positron pair. Since an initial photon energy of at least  $2m_0c^2$  is required for the creation of the electron-positron pair, any excess energy ( $E_\gamma - 2m_0c^2$ ) carried in by the photon above  $1.022 \text{ MeV}$  is imparted to and shared equally by the positron and the electron as kinetic energy, given by the following equation [49,51].

$$(Eq.2.33) E_{e^-} + E_{e^+} = h\nu - 2m_0c^2$$

After electron and positron pair is created, they can traverse the medium, losing their kinetic energy by collisions with electrons in the surrounding material through ionization, excitation and/or *bremstrahlung*. Once, the positron slows down, it can combine with an atomic electron in the surrounding material and subsequently annihilate to form two photons, called *annihilation photons*, each with energies of about  $m_0c^2 = 0.511 \text{ MeV}$ . In order to conserve linear momentum these two photons must be emitted in opposite direction, i.e., back to back.

Figure 2.12 depicts the schematic diagram of the pair production process.

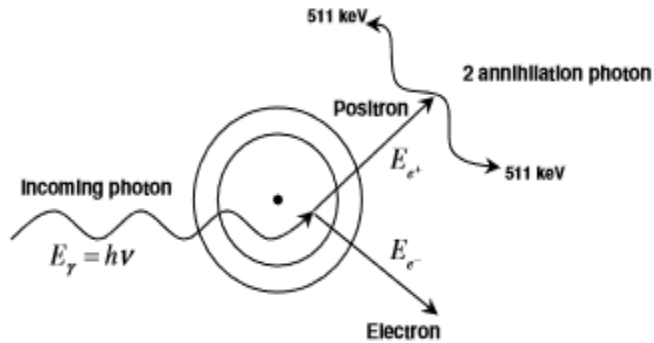


**Figure 2.12: Schematic of the pair production process and annihilation.**

The interaction cross section ( $\kappa$ ) for pair production is related to the atomic number of the material as approximately proportional to  $Z^2$  [44, 49-50]. The probability of pair production mechanism depends on the gamma-ray energy above the threshold (at  $1.022 \text{ MeV} = 2m_0c^2$ ) and becomes the dominant interaction process for gamma-ray energies greater than  $10 \text{ MeV}$  [49, 61].

Figure 3.5 represents the importance of the three principal gamma-ray interaction processes as a function of  $\gamma$ -ray energy and the value of  $Z$  of the absorber.

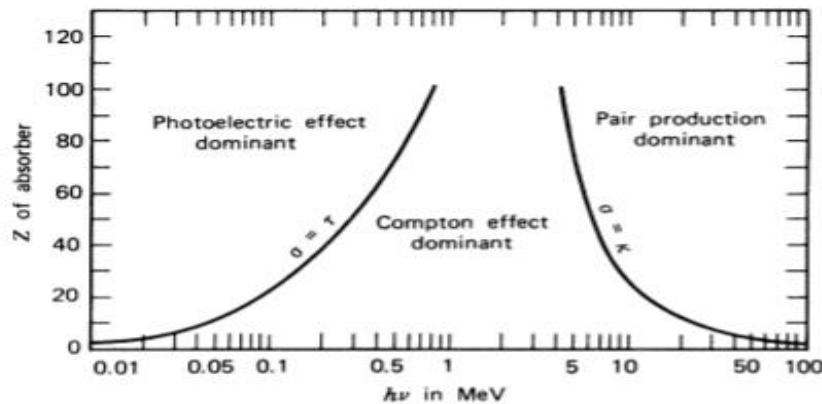


**Figure 2.13 The three gamma-ray interaction processes and their regions of dominance[49]**

## 2.11 Radiation dosimetry

### 2.11.1 Basic radiation quantity and unit exposure:

The 'roentgen' (R) is the unit to express the radiation exposure that can be defined as the amount of ionization that  $X$ - or  $\gamma$ radiation produces in air. This unit accounts for the production of 1 *esu* of electrical charge of either sign in 1  $\text{cm}^3$  or 0.001293 g of air at standard temperature and pressure [50,54]. Since 1 *esu* =  $3.34 \times 10^{-10}$  coulomb (C) [50], the exposure unit can be expressed in the SI system as follows [10, 50, 67]

$$1 R = 1 \frac{esu}{cm^3} = \frac{3.34 \times 10^{-10} C}{0.001293 g \times 10^{-3} Kg/g} = 2.58 \times 10^{-4} \frac{C}{Kg} \text{ (Eq.2.34)}$$

The exposure unit is designated only for limited energy range X- or  $\gamma$  radiation interacting with air [50, 67].

### Absorbed dose

One limitation of the exposure unit is that it does not reflect the biological significance of the radiation. A unit considering the quantity of energy absorption by any kind of ionizing radiation in any kind of material was introduced. The absorbed dose is measured in units of '**gray**' (Gy) where 1Gy equals to one joule of absorbed energy per one kilogram of irradiated target [10,52,67]. The absorbed dose can be expressed in another unit called the '**rad**'(radiation absorbed dose). The rad is the original unit and is defined as an absorbed energy of 100 erg per gram. It is related to the gray as follow [50,52,68]:

Since  $1 J = 10^7 ergs$ ,

$$1 Gy = 1 \frac{J}{Kg} = \frac{10^7 erg}{10^3 g} = 10^4 \frac{erg}{g} = 100 rad \quad \text{(Eq.2.35)}$$

$$1 rad = 0.01Gy = 1 centigray (cGy)$$

The total absorbed energy is not the only factor which determines the level of biological damage from the radiation. The type of radiation and its energy also have to be considered. In general, the biological effect of highly ionizing radiation in a tissue is more severe per unit absorbed dose than those of radiation which produce low ionization. For this reason, the term **relative biological effectiveness (RBE)** was introduced as a dimensionless quantity of the amount of absorbed dose of ionizing radiation relative to that of X- or  $\gamma$ radiation of a particular energy to provide the same biological response [10,52,67]. Due to the difficulty in applying such complicated functions of energy, RBE has been normalized to a factor known, as the radiation weighting factor ( $w_R$ ) by the ICRP and NCRP [52,67]. This factor is derived from the RBE over the range of energies for a particular type of radiation. A list of radiation weighting factors for various types of ionizing radiation is presented in Table 2.3

**Table 2.3 Radiation weighting factors for different ionizing radiations [49, 62, 64].\***

Type of Radiation	Energy range	Weighting factor, $w_R$
Photon, electrons, positrons and muons	All energies	1
Neutrons	< 10 keV	5
	> 10 keV to 100 keV	10
	> 100 keV to 2 MeV	20
	> 2 MeV to 20 MeV	10
	> 20 MeV	5
Protons	< 20 MeV	5
Alpha particles, fission fragments, non-relativistic heavy nuclei		20

\* Adapted from ICRP Publication 60

### Equivalent and effective dose

In order to determine the effect of the nature of the radiation by the weighting factor in Table 2.3, a unit called *the equivalent dose* ( $H_T$ ) is specified. This is the amount of the dose ( $D_{T,R}$ ) absorbed over a tissue or organ ( $T$ ) due to radiation ( $R$ ) and is given by [10,11-52,67]

$$H_T = \sum_R W_R D_{T,R} \quad (\text{Eq.2.36})$$

The ‘*sievert*’ ( $Sv$ ) is used to express the equivalent dose when the absorbed dose is in units of *gray* ( $Gy$ ); thus one sievert is also equal to one joule per kilogram. An older unit of the equivalent dose is the ‘*rem*’ (*radiation equivalent man*) with the absorbed dose expressed in units of *rad* [32], hence, 1 *Sv* equals to 100 *rem* [10,11,43-49,50].

$$E = \sum_T W_T H_T \quad (\text{Eq.2.37})$$

In addition to the radiation types and energy, the biological effect to radiation is concerned with the sensitivities of irradiated organs or tissues. The variation of radiation sensitivity of each organ is taken into account in the contribution of the equivalent dose in all tissues and organs of the body. The new

terms *the effective dose (E) and the tissue weighting factor (w<sub>T</sub>)* are introduced. The definition of the effective dose is the sum of the equivalent doses weighted by the tissue weighting factors for each tissue, as given in the following expression [52,67,68]. Considering equations 2.36 and 2.37

$$E = \sum_T W_T \sum_R W_R D_{T,R} \text{ (Eq.2.38)}$$

**Table 2.4: Tissue weighting factors [67,68].**

Tissue or Organ	Tissue weighting factors, $w_T$
Gonads	0.20
Colon	0.12
Lung	0.12
Red bone marrow	0.12
Stomach	0.12
Bladder	0.05
Breast	0.05
Oesophagus	0.05
Liver	0.05
Thyroid	0.05
Skin	0.01
Bone surfaces	0.01
Remainder	0.05

Table 2.4 lists the tissue weighting factors for tissues and organs of the human body. These factors were obtained from a reference population of equal numbers of men and women ranging in age. Because of the normalization of all tissue weighting factor values is unity, the effective dose equals a uniform equivalent dose over the whole body [67,68]. The SI unit of effective dose is also the *sievert (Sv)*.

### 2.11.2 Sources of radiation exposure:

Human beings are inevitably exposed to ionizing radiation either from external exposure arising from radioactive sources outside the body or internal exposure which comes from radioactive materials inside the body [14,68,70]. Both external and internal radiation exposure to humans mainly arises from the natural sources. In addition to the natural sources, the use of radiation and radioactive materials by human activities is another source of radiation exposure to individuals [14, 68,70].

### **2.11.2.1 Natural sources**

The sources of natural radiation exposure are cosmic radiation from the outer space and radioactive materials present in the earth's surroundings and wider environment, including the human body itself. About 85% of the average annual exposure dose of 2.4 mSv received by the world population is from the distribution of these natural radiation sources [10,16,70]. 15% of the total dose from natural sources is due to cosmic ray interactions at sea level; however, latitude and particularly altitude are the factors which give rise to dose rate variations from these environmental exposures [70]. Exposure dose from cosmic rays at the cruising altitude of commercial aircraft is significantly higher than those at the sea level [10,68,70]. In addition to cosmic-ray induced radiation, primordial radionuclides are a main contribution to the annual exposure dose due to natural sources. These naturally occurring radioactive materials include radionuclides which belong to the uranium and thorium decay chains and natural radioactive potassium ( $^{40}\text{K}$ ) are present in at least trace amounts in most geological materials in the earth's crust [15,18]. Gamma radiation arising from these radionuclides is the main source of natural, background, external exposure to human beings. The concentrations of such radionuclides at different places are a factor in the variation of external exposure due to gamma radiation from one place to another [14,70]. Inhalation and ingestion of primordial radionuclides can give rise to irradiation of organs inside the body. Airborne radionuclides, such as  $^{222}\text{Rn}$  from the  $^{238}\text{U}$  decay chain, can enter the human body by inhalation and represent a significant source of internal exposure [10,70]. Table 2.5 shows the annual exposure doses of individuals together with the typical ranges of exposure from such sources.

### **2.11.2.2 Artificial sources**

Human activity involving the application of radiation is another source of radiation exposure to human. Some of these activities can give rise to an enhanced level of exposure from natural sources such as the discharge of radioactive materials into the environment from nuclear power plants, the global dispersion of radionuclides from the nuclear weapon testing or the atmospheric fall-out from the nuclear reactor accidents at Chernobyl [10,68,70] and more recently Fukushima. However, the main artificial source of the annual dose received by the worldwide population is the use of radiation for medical purposes [10,71]. Some special groups of people who work in industry, medicine and research may be occupationally exposed to radiation used in their work.

The average dose from occupational exposure is relative small compared with the natural radiation exposure [10,71]. A summary of the annual average exposure dose of ionizing radiation and the range of artificial sources are also listed in Table 2.5.

**Table 2.5 Annual average doses from all sources (in mSv) [70].**

Source	Annual average dose (Worldwide)	Typical range of individuals doses	Comments
Natural sources of exposure			
Inhalation (radon gas)	1.26	0.2-10	The dose is much higher in some particular dwellings.
External terrestrial	0.48	0.3-1	The dose is higher in some geographical locations.
Ingestion	0.29	0.2-1	
Cosmic radiation	0.39	0.3-1	The dose increases with altitude.
Total of natural sources	2.4	1-13	
Artificial sources of exposure			
Medical diagnosis (not therapy)	0.6	0-several tens	Individual doses depend on specific examinations
Atmospheric nuclear testing	0.005	Some higher doses around test sites still occur.	The average has fallen from a peak of 0.11 mSv in 1963
Occupational exposure	0.005	~0-20	The average dose to all workers is 0.7 mSv. Most high exposures are due to natural radiation (specifically radon in mines)
Chernobyl accident	0.002 <sup>a</sup>	In 1986, the average dose to more than 300,000 recovery workers was nearly 150 mSv; and more than 350,000 other individuals received doses greater than 10 mSv.	The average in the northern hemisphere has decreased from a maximum of 0.04 mSv in 1986.
Nuclear fuel cycle (public exposure)	0.0002 <sup>a</sup>	Doses are up to 0.02 mSv for critical groups at 1 km from some nuclear reactor sites.	
Total of artificial sources	0.6	From essentially zero to several tens	Individual doses depend primarily on medical treatment

<sup>a</sup> Globally dispersed radionuclides. The value for the nuclear fuel cycle represents the maximum per capita annual dose to the public in the future, assuming the practice continues for 100 years, and derives mainly from globally

dispersed, long-lived radionuclides released during reprocessing of nuclear fuel and nuclear power plant operation.

### 2.11.3 Radiation protection and dose limits

Since ionizing radiation can damage biological organs in the human body, there have been many studies concerning the biological effects of radiation. The aims of these studies are to establish dose limits in order to protect radiation workers and members of the public from radiation exposure. Much of the knowledge of radiation effects on humans has been obtained from a group of people who survived from the atomic bombs in Hiroshima and Nagasaki and those individuals who received radiation exposure from routine work or accidents [10,11-52,67]. The relationship between biological effect and radiation exposure was studied by the Biological Effect of Ionizing Radiation (**BEIR**) in agreement with the United Nations Scientific Committee on the Effect of Atomic Radiation (**UNSCEAR**) and the International Commission on Radiological Protection (**ICRP**), as shown in Figure 2.14. Initial reports used a linear relationship between the effect and the amount of exposure (shown in curve A) as a ‘linear, no-threshold’ hypothesis. Further studies also allowed the possible hypothesis of a different trend (curve B) with the radiation exposure at very low levels not significant to cause harmful effects; this is referred to as the ‘threshold effect’. Curve C represents the hypothesis with the opposite effect, where absorbed doses of ionizing radiation at low levels are more dangerous [52,67].

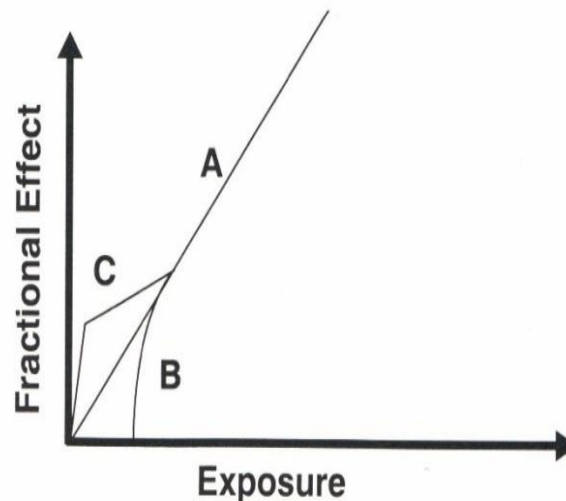


Figure 2.14: Possible, theoretical dose-response curves.

These curves show theoretical relationships between radiation exposure and the biological effect. Curve A shows the linear relationship that the effect and the exposure. The threshold effect represents the cut-off curve at the low levels of radiation exposure as shown in curve B. Curve C shows a possible increased effect at the low level of exposure [67].

The effect of radiation exposure can be classified into *deterministic effects and stochastic effects* [11,52- 67,68]. The effects which can be observed when organs of the body received a certain level of dose or threshold are called deterministic effects. Below this threshold, detrimental effects are not observed. The response of the effect is similar to curve B in Figure 2.14 The severity of the effect increases with the size of the dose [52,68]. Stochastic effects occur randomly and the probability of occurrence is dependent of the size of dose [52,68]. Cancer induction and genetic effects in future generation are thought to possibly result from these types of the effect. The expected relationship between the probability of the stochastic effect and the size of dose is along the lines of curve A in Figure 1.14.

To avoid unnecessary exposure causing the biological effects of radiation to radiation workers and the general public, all doses must be kept as low as reasonably achievable (**ALARA**) with the dose limits recommended by the ICRP [52,67]. The recommendations of the ICRP for radiation protection standards are based on three general principles as follows [52,68]:

1. Justification – any practice which does not produce a sufficient benefit to the exposed individuals should not be adopted.
2. Optimization – all exposures within a practice shall be kept as low as reasonably achievable (**ALARA**) considered with economic and social factors.
3. Dose limitation – individuals should receive exposure dose within the recommended limits.

In **ICRP** Publication 60, the recommended dose limits were set and estimated from the detrimental effect of the radiation which the prevention of deterministic effects and the limitation of stochastic effects were considered [68]. Dose limits recommended by **ICRP** are shown in Table 2.6

**Table 2.6 ICRP 60 recommended effective dose limits [52,67,69].**

Application	Dose limit	
	Occupational	Public
Whole body	20 mSv <sup>a</sup> per year, averaged over a defined period of 5 years <sup>b</sup>	1 mSv <sup>a</sup> in a year
Annual equivalent dose in Lens of the eye	150 mSv	15 mSv
Skin	500 mSv	50 mSv
Hand and feet	500 mSv	

<sup>a</sup>To find the recommended limit in rem, 1mSv = 0.1rem

<sup>b</sup> Maximum dose in any single year do not exceed 50mSv

For occupational exposure, the annual effective dose that the whole body is uniformly irradiated is limited to 20mSv averaged over a defined period of 5 years to limit the probability of stochastic effects. The dose can be allowed to be over 20mSv but cannot exceed 50mSv in any single year. The dose limit of a member of the general public is set to be lower than a group of radiation workers, at 1mSv per year. To prevent deterministic effects, occupational equivalent dose limits of 500, 500 and 150mSv per year are recommended for the skin, the hands and the feet, and the lens of the eye, respectively. The annual equivalent doses for individual members of the public are limited to be 15mSv for the lens of the eye and 50mSv for the skin [52,67,68]. For non-uniform irradiation of the body, the tissue weighting factors of various organs as shown in Table 2.4 are used for determining the detrimental effects that contribute to each individual organ due to their different radiation sensitivities. The weighting factors of the several tissues and organs are relative to the whole body which has a value of unity [67,68]. The total weighted dose of all tissues and organs is equal to the effective dose as described by equation 2.37.

# **Chapter Three**

## **Materials and methods**

# Chapter Three

## Materials and methods

### 3.1 Gamma-ray spectroscopy

#### 3.1.1 Introduction

Gamma-ray ( $\gamma$ -ray) spectroscopy is a quick and nondestructive analytical technique that can be used to identify various radioactive isotopes in a sample. In gamma-ray spectroscopy, the energy of incident gamma-rays is measured by a detector. By comparing the measured energy to the known energy of gamma-rays produced by radioisotopes, the identity of the emitter can be determined. This technique has many applications, particularly in situations where rapid nondestructive analysis is required.

Gamma rays are electromagnetic radiation and are part of photon radiation. They are produced when transitions between excited nuclear levels of a nucleus occur. Delayed gamma rays are emitted during the decay of the parent nucleus and often follow a Beta decay. There can be many transitions between energy levels of a nucleus, resulting in many gamma-ray lines. The typical wavelength is  $10^{-7}$  to  $10^{-13}$  m, corresponding to an energy range of 0.01–10 MeV. Gamma rays can be detected through their interaction with matter. There are three main processes: photoelectric absorption, Compton scattering and pair production. The photoelectric effect occurs when a gamma ray interacts with an electron of an inner shell of an atom and a photoelectron is emitted. This is the most important effect for the detection of gamma rays with semiconductor detectors. The effect of Compton scattering describes the interaction of a gamma ray with matter when some of its energy is transferred to the recoil electron. The energy transmitted is a function of the scattering angle. Therefore, the Compton effect results in a broad range of gamma-ray energies, which gives a continuous background in the gamma spectrum. Pair production is the third effect when a gamma ray is absorbed by matter and loses energy to produce an electron/positron pair. This effect only occurs when gamma rays have more than 1.02 MeV energy, twice the rest mass energy of an electron (0.551 MeV) [104].

#### 3.1.2 Principles

A gamma spectroscopy system consists of a detector, electronics to collect and process the signals produced by the detector, and a computer with processing

software to generate, display, and store the spectrum. Other components, such as rate meters and peak position stabilizers, may also be included.

Gamma spectroscopy detectors are passive materials that wait for a gamma interaction to occur in the detector volume. The most important interaction mechanisms are the photoelectric effect, the Compton effect, and pair production. The photoelectric effect is preferred, as it absorbs all of the energy of the incident gamma ray. Full energy absorption is also possible when a series of these interaction mechanisms take place within the detector volume. When a gamma ray undergoes a Compton interaction or pair production, and a portion of the energy escapes from the detector volume without being absorbed, the background rate in the spectrum is increased by one count. This count will appear in a channel below the channel that corresponds to the full energy of the gamma ray. Larger detector volumes reduce this effect[74,75].

The voltage pulse produced by the detector (or by the photomultiplier in a scintillation detector) is shaped by a multichannel analyzer (MCA). The multichannel analyzer takes the very small voltage signal produced by the detector, reshapes it into a Gaussian or trapezoidal shape, and converts that signal into a digital signal. In some systems, the analog-to-digital conversion is performed before the peak is reshaped. The analog-to-digital converter (ADC) also sorts the pulses by their height. ADCs have specific numbers of "bins" into which the pulses can be sorted; these bins represent the channels in the spectrum. The number of channels can be changed in most modern gamma spectroscopy systems by modifying software or hardware settings. The number of channels is typically a power of two; common values include 512, 1024, 2048, 4096, 8192, or 16384 channels. The choice of number of channels depends on the resolution of the system and the energy range being studied.

The multichannel analyzer output is sent to a computer, which stores, displays, and analyzes the data. A variety of software packages are available from several manufacturers, and generally include spectrum analysis tools such as energy calibration, peak area and net area calculation, and resolution calculation[75].

### **3.1.3 Instrumentation**

The analog system components are available in several different types, allowing the system to be tailored to the precise needs of the application and the available budget shown in figure 3.1.

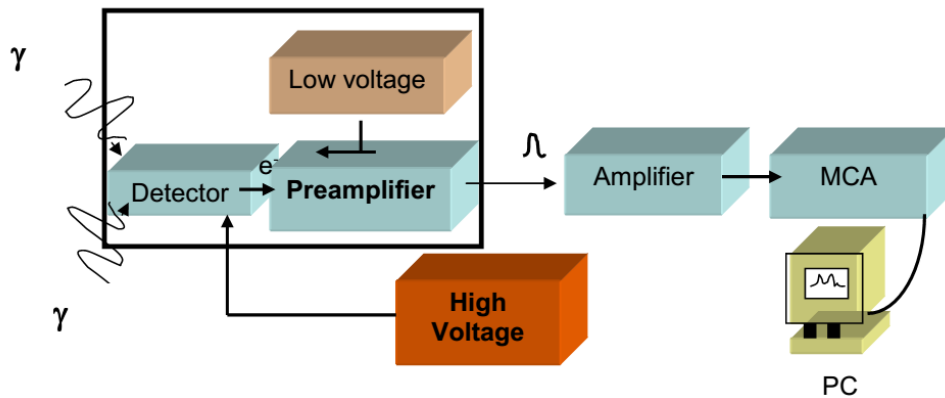


**Figure 3.1: Block diagram of a basic gamma spectrometry system**



**Figure 3.2: Electronic instrumentation used in the current study and A coaxial Sodium Iodide (NaI) detector**

### 3.1.3.1 The detector

The detector is the center piece of the gamma spectroscopy system. The gamma photons interact with the detection material and transfer their energies to electrons or to positrons in the case of annihilation. These produced particles lose their energy within the detector, creating ionized atoms and ion pairs. These secondary entities form the basis of the detector signal[72].

#### 3.1.3.1.1 Sodium iodide – NaI (TI)

This is the most commonly used scintillateor material. It is cheap and readily available. Detectors up to 0.75 m diameter have been produced. More typically, the 76 mm diameter by 76 mm high cylindrical sodium iodide detector was for many years the standard gamma-ray spectrometer detector. (At the time, this was referred to as a ‘3-by-3 detector’–3in.×3 in) shown in figure (3.3).

The iodide atom of the NaI (TI) provides a high gamma-ray absorption coefficient and, therefore, high intrinsic efficiency. At low energy, there is a high probability of complete absorption. Because NaI (TI) provides the greatest light output of all of the traditional inorganic scintillates using standard photomultipliers, it also has the best energy resolution[73].

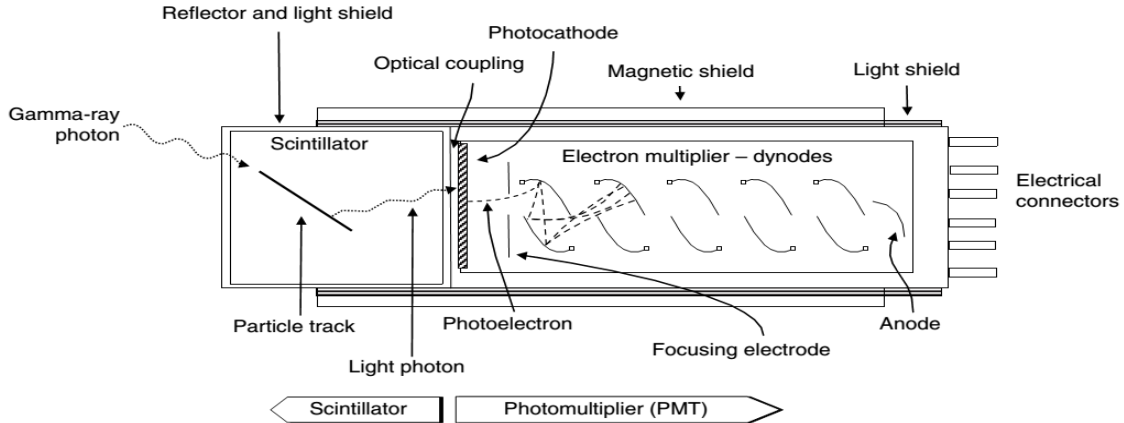


**Figure 3.3: Schematic diagram of a scintillation detector**

### 3.1.3.2 Low voltage power supply

The nuclear electronics industry has standardized the signal definitions, power supply voltages and physical dimensions of basic nuclear instrumentation modules using the Nuclear Instrumentation Methods (NIM) standard initiated in the 1960s. This standardization provides users with the ability to interchange modules, and the flexibility to reconfigure or expand nuclear counting systems, as their counting applications change or grow[72].

### 3.1.3.3 Preamplifiers

The charge created within the detector after the photon interaction with the detector crystal, is collected by the preamplifier. Additionally, the preamplifier also serves to provide a match between the high impedance of the detector and the low impedance of coaxial cables to the amplifier, which may be located at great distances from the preamplifier. Most Germanium detectors in use today are equipped with RC-feedback, charge sensitive preamplifiers.

These can have various modes of operation: current sensitive, voltage-sensitive and charge sensitive. Charge-sensitive preamplifiers are commonly used for most solid state detectors. In charge-sensitive preamplifiers, an output voltage pulse is produced that is proportional to the input charge. To maximize performance, the preamplifier should be located at the detector [72,73].

### **3.1.3.4 High voltage power supply**

The High Voltage Power Supply unit supplies the necessary high voltage to the detector and the necessary voltages to the rest of the system components. These units are usually able to supply up to 5000 V.

### **3.1.3.5 Amplifier**

The amplifier serves to shape the pulse as well as further amplify it. In this module the size (height) of the pulses are increased, and their form carefully manipulated to eliminate problems with electronic noise, shifts in the baseline, and pulses "riding" on the tails of those preceding them[72].

### **3.1.3.6 Multi-channel analyzer (MCA)**

The multichannel analyzer (MCA) is the heart of most experimental measurements. It performs the essential functions of collecting the data, providing a visual monitor, and producing output, either in the form of final results or data for later analysis the multichannel analyzer (MCA) consists basically of an analog-to-digital converter (ADC), control logic, memory and display. The multichannel analyzer collects pulses in all voltage ranges at once and displays this information in real time[72,73].

### **3.1.3.7 Analog to digital conversion (ADC)**

The analog-to-digital conversion module (ADC) forms the heart of the gamma spectrometer. It converts the analog information from the pulse train into a digital format that can be stored and processed by a computer. For each analog pulse received by the ADC, a number is generated that is proportional to the height of that pulse[73].

### **3.1.4 Detection limit of gamma spectroscopy**

There are many instances when it is very important to define a detection limit for certain radio nuclides. This limit known also as the minimum detectable emission rate or minimum detectable activity (MDA), will depend upon the sample composition, the energy of the radiation, the source to detector distance, the detector efficiency, the background and the counting time available. To quote MDAs it is necessary to define all these criteria[74].

### **3.1.5 Advantage and disadvantage**

#### **3.1.5.1 Advantages**

1. High light yield.
2. High density.

3. Good energy resolution.

### **3.1.5.2 Disadvantage**

1. Complicated crystal growth.
2. Large temperature dependence.
3. Very expensive.

## **3.2 Radon Scout Plus (SARAD GmbH)**

In addition to the Gamma-ray spectroscopy, radon monitors were used in this study Radon Scout Plus (SARAD GmbH), hereinafter Scout named RSB, was used as well. Operation mode and features for device are described below. The device used in this study have been calibrated. The device is based on pulsed ionization-chamber technology and alpha spectrometry to detect radon concentration. It has a measurement range 0 -10 MBq.m<sup>-3</sup> and its sampling method is a pump with 1 min<sup>-1</sup> airflow. The Sensitivity of device is 1.8 cpm @ 1000 Bq/m<sup>3</sup> (independent on the humidity) , 200 Bq/m<sup>3</sup> with 20% statistical error (1σ) at 1 hour interval , 1000 Bq/m<sup>3</sup> with an statistical error (1σ) < 10 % at 1 hour interval and 100 Bq/m<sup>3</sup> with 17% statistical error (1σ) at 3 h interval The uncertainty associated with the measurement performed by this device varies within the whole range or smaller in the concentration range[98].

The one used for this study was calibrated at the Sudanese Radiation Safety Institute. The detection system of the Radon Scout consists of a silicon detector in a chamber with high voltage collection. Radon gas enters a chamber and decays, high voltage is applied and radon daughters ionize and move towards the silicon detector surface that creates a pulse.

Then, the Radon Scout Plus is an instrument designed for general purpose long-term indoor measurements of the radon concentration and its principle of operation for radon measurements is a silicon detector and alpha spectroscopy. The measurement range of this monitor is 0 -10 MBq m<sup>-3</sup> and the preset integration time is 3 h with a 20% uncertainty after 7 days of measurements at 200 Bq m<sup>-3</sup> [105].

## **3.3 Material and methods**

### **3.3.1 Study area**

River Nile State locate in Northern Sudan with a population of over 1.4 million. The study's area of study located at a distance of 310 km from Khartoum city the capital of Sudan. River Nile State is rich in raw materials that can be used

for cement industry, so many cement factories have been established there. The area locates at the geographic coordinates  $33^{\circ}77'88''$  E and  $17^{\circ} 70'6''$  N as shown by the red area in Figure 3.4 [38].

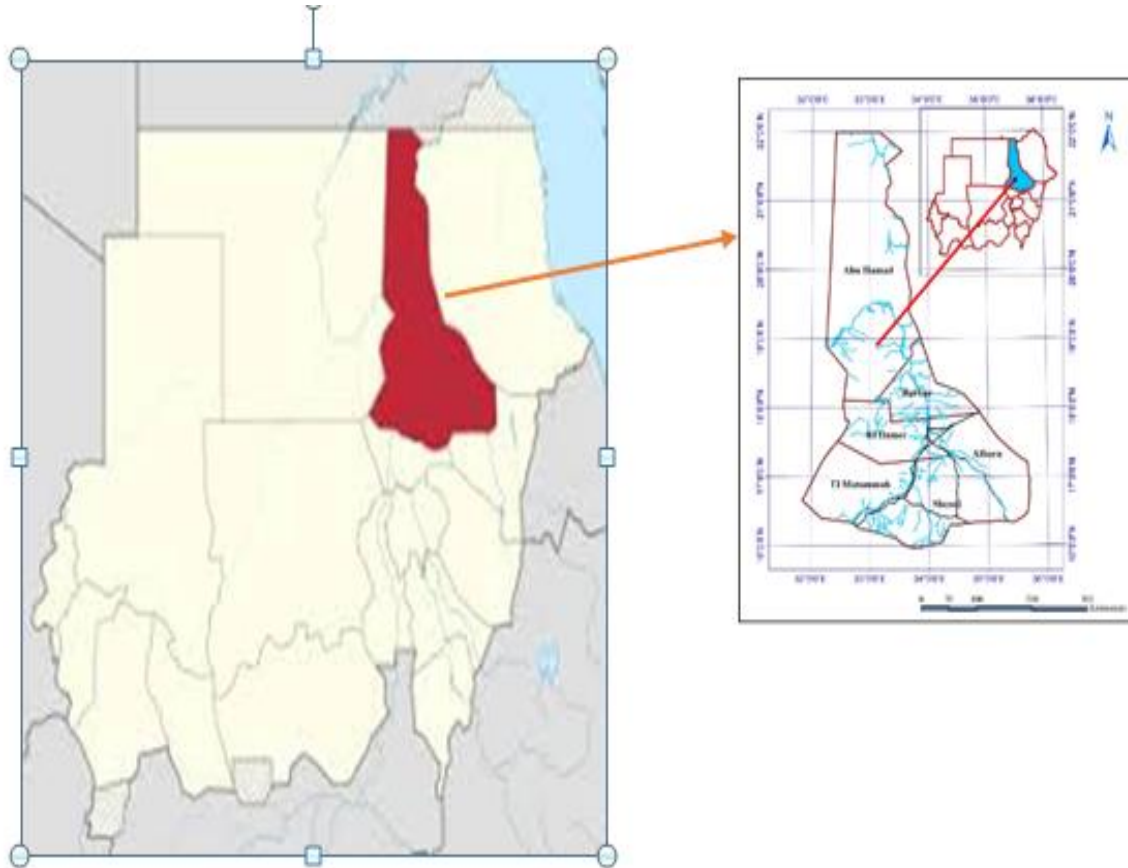


**Figure 3.4: Map quarries cement factories River Nile State, Sudan[38]**

### 3.3.2 Samples collection

In order to evaluate the levels of natural radioactivity in quarries cement factories, sixty seven (67) samples of cement's rock were collected randomly from different locations in the River Nile state include several points of cement factories quarries, Al-Salam cement, Atbara cement and Al-Takamul cement factories and three (3) samples were taken from the additional materials used to manufacture cement shown below table 3.1.

Matter, each rock sample was packed shipped to the laboratory at the Alsalam cement factory, Sudan for crushing and grinding. Table 2.1 listed the details of the sampling locations of rock samples from the quarries cement factories River Nile State studied in this current work.

**Table 3.1: The locations of different sampling areas in River Nile state at this present work.**

Samples Locations	Sample No.	Position		Sample code	Group name
		Latitude (°N)	Longitude (°E)		
<b>Al Salam Cement Factory</b>	1	17°41.792	033°47.959	SAL-1	GS-1
	2	17°41.762	033°47.968	SAL -2	
	3	17°41.781	033°47.948	SAL -3	
	4	17°41.751	033°47.931	SAL -4	
	5	17°47.438	033°47.771	SAL -5	
	6	17°47.405	033°47.758	SAL -6	GS-2
	7	17°47.451	033°47.782	SAL -7	
	8	17°47.473	033°47.748	SAL -8	
	9	17°44.224	033°46.900	SAL -9	
	10	17°44.201	033°46.881	SAL -10	
	11	17°44.192	033°46.872	SAL -11	GS-3
	12	17°44.239	033°46.858	SAL -12	
	13	17°44.248	033°46.823	SAL -13	
	14	17°44.258	033°46.739	SAL -14	
	15	17°44.213	033°46.998	SAL -15	
	16	17°44.268	033°46.778	SAL -16	GS-4
	17	17°44.179	033°46.724	SAL -17	
	18	17°44.159	033°46.748	SAL -18	
	19	17°44.244	033°46.837	SAL -19	
	20	17°44.258	033°46.803	SAL -20	
	21	17°45.527	033°47.485	SAL -21	GS-5
	22	17°45.503	033°47.498	SAL -22	
	23	17°45.541	033°47.471	SAL -23	
	24	17°45.558	033°47.403	SAL -24	

(continue) Table 2.1.

Samples Locations	Sample No.	Position		Sample code	Group name
		Latitude (°N)	Longitude (°E)		
<b>Atbara Cement Factory</b>	25	17°42.398	033°48.217	ATB -1	GA-1
	26	17°42.299	033°48.307	ATB -2	
	27	17°42.341	033°48.333	ATB -3	
	28	17°42.324	033°48.290	ATB -4	
	29	17°42.305	033°48.281	ATB -5	
	30	17°42.410	033°48.267	ATB -6	GA-2
	31	17°42.433	033°48.251	ATB -7	
	32	17°42.281	033°48.223	ATB -8	
	33	17°42.271	033°48.191	ATB -9	
	34	17°42.269	033°48.178	ATB -10	
	35	17°42.237	033°48.162	ATB -11	GA-3
	36	17°42.214	033°48.148	ATB -12	
	37	17°42.198	033°48.129	ATB -13	
	38	17°42.177	033°48.108	ATB -14	
	39	17°42.169	033°48.069	ATB -15	
	40	17°42.144	033°48.041	ATB -16	GA-4
	41	17°42.277	033°48.021	ATB -17	
	42	17°42.326	033°47.419	ATB -18	
	43	17°42.287	033°47.416	ATB -19	
	44	17°42.159	033°47.230	ATB -20	
	45	17°42.649	033°47.415	ATB -21	GA-5
	46	17°42.503	033°47.219	ATB -22	
	47	17°42.713	033°46.498	ATB -23	
	48	17°42.391	033°46.305	ATB -24	

(continue) Table 2.1.

Samples Locations	Sample No.	Position		Sample code	Group name
		Latitude (°N)	Longitude (°E)		
ALTakamul Cement Factory	49	17°49.292	033°48.800	TKM-1	GT-1
	50	17°49.310	033°48.811	TKM -2	
	51	17°49.305	033°48.789	TKM -3	
	52	17°49.280	033°48.802	TKM -4	
	53	17°49.967	033°48.969	TKM -5	GT-2
	54	17°49.951	033°48.939	TKM -6	
	55	17°49.942	033°48.924	TKM -7	
	56	17°49.923	033°48.915	TKM -8	
	57	17°50.602	033°49.215	TKM -9	GT-3
	58	17°50.571	033°49.198	TKM -10	
	59	17°50.502	033°49.181	TKM -11	
	60	17°50.621	033°49.170	TKM -12	
	61	17°51.120	033°49.348	TKM -13	GT-4
	62	17°51.215	033°49.305	TKM -14	
	63	17°51.178	033°49.333	TKM -15	
	64	17°51.230	033°49.299	TKM -16	

(continue) Table 2.1.

Samples Locations	Sample No.	Position		Sample code
		Latitude (°N)	Longitude (°E)	
River clay	65	17°66.108	033°97.385	RCL
Desert clay	66	17°75.704	034°20.285	DCL
kaolin	67	17°49.305	033°48.789	SIL

### 3.3.3 Sample preparation:

After collected all samples and return to the laboratory at Al-Salam cement factory, Rock samples were broken into small pieces easily crushed by milling machine and then the samples were placed in a custom plastic bags to collect samples after the transfer of designation.

After that, it was transferred to the laboratory of the Institute of Radiation Safety of the Sudanese Atomic Energy Authority and there it was packed in Marinelli cups of 500 grams which were sealed tightly with adhesive tape to prevent the escape of the  $^{222}\text{Rn}$  and  $^{220}\text{Rn}$  airborne in the samples and for fear of breaking the natural chain.

All samples were weighed and stored for three weeks prior to measurement with a gamma spectroscopy in order to attain radioactive secular equilibrium between  $^{226}\text{Ra}$  and  $^{228}\text{Ac}$  and their short-lived progeny ( $>7$  half-lives of  $^{222}\text{Rn}$  and  $^{220}\text{Rn}$ ). Figure 3.5 shows the apparatus for sample preparation. Figure 3.6 illustrates a Marinelli beaker filled with prepared rock sample and sealed with plastic tape.



(a)



(b)

**Figure 3.5: The apparatus for sample preparation (a) a Jo crusher (b) a Vibratory mill**



**Figure 3.6: A prepared soil sample filling in a Marinelli beaker sealed with plastic tape to prevent the escape of airborne radionuclide**

### 3.4 Samples measurement

#### 3.4.1 Energy calibration

If a gamma spectrometer is used for identifying samples of unknown composition, its energy scale must be calibrated first. For the present study, calibration is performed by using the peaks of a known source, such as cesium-137 or cobalt-60. Because the channel number is proportional to energy, the channel scale can then be converted to an energy scale. If the size of the detector crystal is known, one can also perform an intensity calibration, so that not only the energies but also the intensities of an unknown source or the amount of a certain isotope in the source can be determined as shown in Figure (3.7) and table(3.2) below.

$$A = A_0 * e^{-\lambda t} \text{ (Eq.3.1)}$$

Where:

A ≡ activity

A<sub>0</sub> ≡ initial activity

$$\lambda = \frac{\ln 2}{t_{\frac{1}{2}}} \text{ (Eq.3.2)}$$

λ ≡ Decay constant.

t<sub>1/2</sub> ≡ Half Life.

**Table 3.2 The result of gamma spectroscopy analysis using reference source (MW652)**

Radionuclide	Energy (Kev)	Activity (i) {Bq}	Half Life (Y)	ln2/Half Life (Y)	Time	Activity
Cs - 137	662	2720	30.17	0.022969838	16.0986301	1879.205274
Co - 60	1173	3120	5.271	0.131474104	16.0986301	375.791818
Co - 60	1333	3120	5.271	0.131474104	16.0986301	375.791818

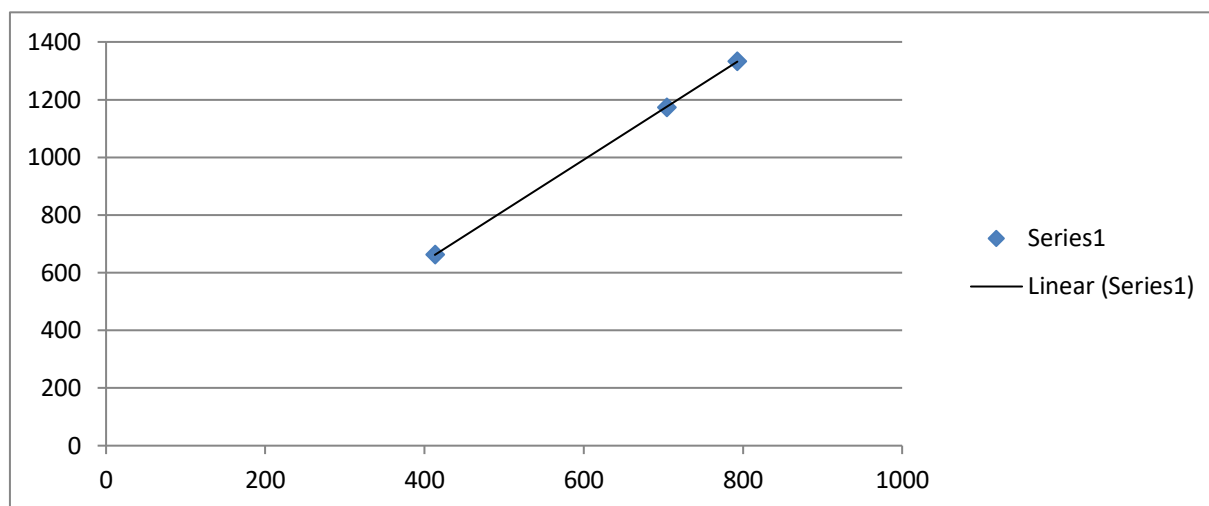


**Figure 3.7 Energy calibration curve for NaI detector**

### 3.4.2 Efficiency calibration

In general, the analysis of a sample by gamma spectroscopy is considered to be non-destructive, certain sample-source preparation steps are essential for precise measurements. For example, it is necessary that the sample to be completely homogenized and measurement are carried out in the same geometry on used in the efficiency calibration. Ideally, the calibration source and the samples to be measured should have the same chemical composition and density. If this is not the case, correction must be made for differences in the degree of self-attenuation. Corrections may also have to be made for coincidence summing, which occurs with radionuclide which emit gamma ray cascade and which is particularly important for low source detector distances. To suppress background radiation and this improve sensitivity, a passive shield made from ‘aged’ lead must surround all gamma detectors.

In this the detector efficiency was calibrated using a mixed radionuclide sources (MW625) in 500 ml Marinelli beaker geometry shown in fig 3.6 and table 3.2. The container was placed on the detector and counted. The spectrum was stored in the computer, and analyzed using the software “winTMCA32”. The following equation was used to obtain the efficiency curve of the detector for different energies:

$$\eta = \frac{\text{counts (cps)}}{I_{\gamma} \times A(\text{Bq/Kg})} \quad (\text{Eq 3.3})$$

Where:

$\eta$  ≡ the efficiency of the detector at specific energy.

$I_{\gamma}$  ≡ gamma intensity

$A$  ≡ the activity of the standard.

**Table3.3: The energies, their respective branching ratios and the corresponding efficiency of the radionuclides in the standard**

Radionuclide	Energy (Kev)	CPS	Activity	I <sub>γ</sub>	Eff-
<b>Cs - 137</b>	662	30.33	1879.205	0.851	0.011299
<b>Co - 60</b>	1173	6.71	375.7918	0.9997	0.004951
<b>Co – 60</b>	1333	6.00	375.7918	0.9998	0.004605

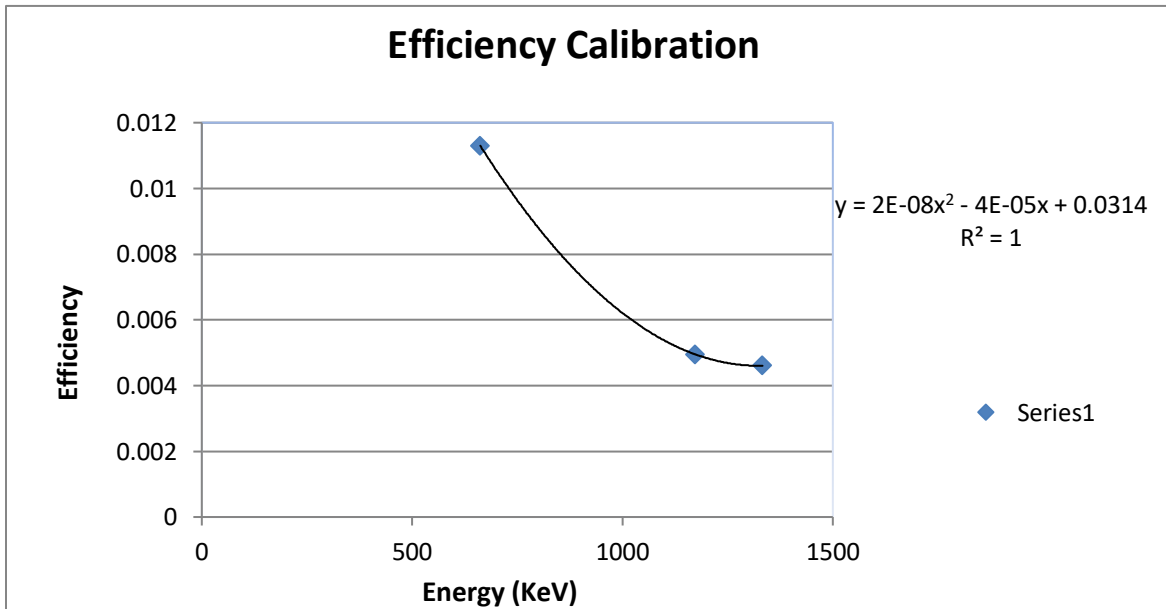


**Figure 3.8: Efficiency calibration curve for NaI detector**

### 3.4.3 Background measurement

The baseline, background-level measurement is significant and used to determine the minimum detectable activity. This is particularly important in the case low-level activity sources [38]. Background radiation can arise from various sources of radionuclides which are the constituent materials of the detector assembly and its shielding; exist in the earth’s surroundings including the air; and generated by the interaction of cosmic radiation with the detector and its surroundings [44,49]. A typical detector background is made up of 10% from radioactivity originating within the detector and unidentified sources, 10% from radon in the air surrounding the detector, 40% from the immediate

vicinity of the detector including radioactive contamination of shielding materials and the last 40% from the interactions of cosmic rays [44,49].

In order to determine the background level of germanium detector, a background measurement was counted for 3 hours with no radiation source present around the sodium iodide detector. A ‘standard’ background spectrum was taken with a 550 ml Marinelli beaker placed on the detector to remain the same geometrical conditions. The beaker was filled with inactive de-ionized water.

### 3.4.4 Sample measurements

Each sample was placed onto NaI detector and measured for three hours. The  $^{232}\text{Th}$  concentration was determined from the concentrations of  $^{212}\text{Pb}$  (238 Kev) and  $^{228}\text{Ac}$  (911Kev) in the samples, and that of  $^{238}\text{U}$  was determined from the average concentrations of the  $^{214}\text{Pb}$  (352 Kev) and  $^{214}\text{Bi}$  (609 Kev) decay products. Whereas  $^{40}\text{K}$  concentration was measured directly using its (1460 Kev) gamma-line. A gamma spectroscopy system consists of a detector, electronics to collect and process the signals produced by the detector, and a computer with processing software to generate, display, and store the spectrum shown in figure 3.9.

Other components, such as rate meters and peak position stabilizers, may also be included, (winTMCA32 scinti SPEC) software program for gamma spectroscopy.

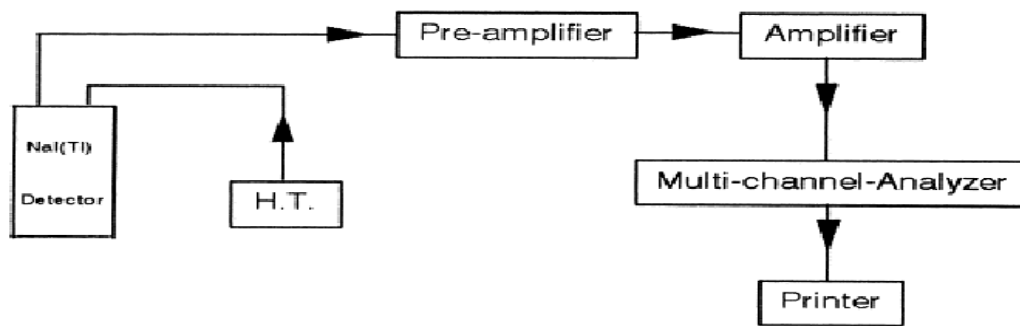


**Figure 3.9 : Instrumentation set -up of gamma-spectroscopy**

The determination of the activity amount in each sample done by the following equation:

$$A[\text{Bq}] = \frac{N(\text{cps})}{I\gamma \cdot \eta} \text{ (Eq.3.4)}$$

Where:

$\eta$  Is the efficiency of the detector at specific energy.

N Is the net area of the peak (count per second).

$I\gamma$  Is gamma intensity.

A Is activity of the element(which is required to find).

To determine concentration activity per mass (specific activity) can be divided activity obtained by mass of the sample and the unit that Becquerel per Kilogram (Bq/Kg).

### 3.5 Assessment of dose

#### 3.5.1 Absorbed dose rate in air(D)

In order to assess any radiological hazard, the exposure to radiation arising from radionuclides present in soil can be determined in terms of many parameters. A direct connection between radioactivity concentrations of natural radionuclides and their exposure is known as the absorbed dose rate in the air at 1 meter above the ground surface. The mean activity concentrations of  $^{226}\text{Ra}$  ( $^{238}\text{U}$ ),  $^{232}\text{Th}$ , and  $^{40}\text{K}$  ( $\text{Bq}\cdot\text{kg}^{-1}$ ) in the soil samples are used to calculate the absorbed dose rate given by the following formula [79,80 - 82,86]:

$$D_R(\text{nGy}\cdot\text{h}^{-1}) = 0.461 A_U + 0.623 A_{Th} + 0.0414 A_K \quad (\text{Eq.3.5})$$

where D is the absorbed dose rate in  $\text{nGy}\cdot\text{h}^{-1}$ ,  $A_{Ra}$ ,  $A_{Th}$  and  $A_K$  are the activity concentration of  $^{226}\text{Ra}$  ( $^{238}\text{U}$ ),  $^{232}\text{Th}$  and  $^{40}\text{K}$ , respectively. The dose coefficients in units of  $\text{nGy}\cdot\text{h}^{-1}$  per  $\text{Bq}\cdot\text{kg}^{-1}$  were taken from the UNSCEAR (2000) report [14].

#### 3.5.2 Annual effective dose equivalent(AEDE)

The absorbed dose rate in air at 1 meter above the ground surface does not directly provide the radiological risk to which an individual is exposed [76]. The absorbed dose can be considered in terms of the annual effective dose equivalent from outdoor terrestrial gamma radiation which is converted from the absorbed dose by taking into account two factors, namely the conversion coefficient from absorbed dose in air to effective dose and the outdoor occupancy factor. The annual effective dose equivalent can be estimated using the following formula [14,82,86]:

$$AEDE(\text{mSv}\cdot\text{y}^{-1}) = D_R(\text{nGy}\cdot\text{h}^{-1}) * 8760 \text{ h}\cdot\text{y}^{-1} * 0.7 * \frac{10^3 \text{ mSv}}{10^9 \text{ nGy}} * 0.2 \quad (\text{Eq.3.6})$$

The values of those parameters used in the UNSCEAR report(2000)are  $0.7 \text{ Sv}\cdot\text{Gy}^{-1}$  for the conversion coefficient from absorbed dose in air to effective dose received by adults and 0.2 for the outdoor occupancy factor [14].

#### 3.5.3 Radium equivalent activity ( $\text{Ra}_{\text{eq}}$ )

Due to a non uniform distribution of natural radionuclides in the soil samples, the actual activity level of  $^{226}\text{Ra}$ ,  $^{232}\text{Th}$  and  $^{40}\text{K}$  in the samples can be evaluated by means of a common radiological index named the radium equivalent

activity ( $Ra_{eq}$ ) [81]. It is the most widely used index to assess the radiation hazards and can be calculated using Equation 3.7 given by Beretka and Mathew [81].

This estimates that 370 Bq.kg<sup>-1</sup> of <sup>226</sup>Ra, 259 Bq.kg<sup>-1</sup> of <sup>232</sup>Th and 4810 Bq.kg<sup>-1</sup> of <sup>40</sup>K produce the same gamma-ray dose rate [24,76,77- 83,86].

$$Ra_{eq}(Bq.Kg^{-1}) = A_U + 1.43A_{Th} + 0.077A_K \text{ (Eq.3.7)}$$

where  $A_{Ra}$ ,  $A_{Th}$  and  $A_K$  are the activity concentration of <sup>226</sup>Ra, <sup>232</sup>Th and <sup>40</sup>K in Bq.kg<sup>-1</sup>, respectively. The permissible maximum value of the radium equivalent activity is 370 Bq.kg<sup>-1</sup> [14,87] which corresponds to an effective dose of 1mSv for the general public [85].

### 3.5.4 Annual external hazard index ( $H_{ex}$ )

To limit the radiation exposure attributable to natural radionuclides in the samples to the permissible dose equivalent limit of 1 mSv.y<sup>-1</sup>, the external hazard index based on a criterion have been introduced using a model proposed by Krieger (1981) [88] which is given by [24,76 - 84,86]:

$$H_{ex} = \frac{A_U}{370Bqkg^{-1}} + \frac{A_{Th}}{259Bqkg^{-1}} + \frac{A_K}{4810Bqkg^{-1}} \leq 1 \quad \text{(Eq.3.8)}$$

In order to keep the radiation hazard insignificant, the value of external hazard index must not exceed the limit of unity. The maximum value of  $H_{ex}$  equal to unity corresponds to the upper limit of radium equivalent activity 370 Bq.kg<sup>-1</sup> [24,84,89].

# **Chapter Four**

## **Results and Discussion**

# **Chapter Four**

## **Results and Discussion**

The aim of this study is To determine environmental radioactivity level and elemental concentrations of rock and soil samples from Quarries cement factories (River Nile State-Sudan) collected from different locations in several points of cement factories Quarries, Al-Salam cement, Atbara cement and Al-Takamul cement factories. The samples were prepared and stored prior to measurement. The radioactivity measurement was performed by means of high-resolution gamma-ray spectrometry in a low background configuration at the laboratory of the Institute of Radiation Safety of the Sudanese Atomic Energy Authority. The analysis of radionuclide contents and the determination of their activity concentration in samples are presented in this chapter.

### **4.1 Spectrum Analysis and Nuclides Identification**

The spectra observed from background and sample measurement were acquired via the winTMCA32 program. The regions and centroid energies for all of gamma-ray peaks in each spectrum were analyzed using this program. Considering the peak centroid energy, the radionuclides which were the sources of the measured gamma radiation which contributed to the peaks could be unambiguously identified.

#### **4.1.1 Background Spectrum**

The observed background spectrum is shown in Fig.4.1. Due to the provision of a large detector shield, the effect of the component continuously produced by the cosmic radiation and gamma ray sources in the vicinity of the detector It is significantly reduced compared to an unprotected reagent. On the other hand, the radioactive contaminants within the reagent group materials and their shielding become major sources of the background radiation level of the detector. Observable Most of the gamma-ray energy peaks shown in the spectrum arise from the decay of primordial radionuclides, namely the  $^{238}\text{U}$ ,  $^{232}\text{Th}$  and  $^{40}\text{K}$  decay chains; These are present in both the reagent material and the wider environment. These radionuclides may be present at trace levels in the materials used to manufacture and block the detector. For example, according to Gilmore (2008) aluminum, which is the structural structure The material of the end cap of

the detector and the other part inside the reagent jacket contain some of the daughter nuclides of uranium, thorium and potassium [44].

The external background radiation can be attenuated before reaching the detector by using a shielding material with a high density and large atomic number. The most widely used shielding material is lead [49]. The direct cosmic-ray interactions can be practically isolated from the detector by lead shielding, but the interaction of cosmic rays within the lead shielding itself can give rise to some secondary background counts. Although the detector shielding can reduce the levels of radioactivity arising from terrestrial gamma ray or cosmic radiation, it can also be the source of background radiation itself, due to the impurities from natural radioactive elements in common lead. Most of radioactive contaminants in lead can be removed by special refining processes but there is usually still some remaining radioactive  $^{210}\text{Pb}$  present. This is a daughter product in  $^{238}\text{U}$  decay chain [44]. The amount and activity from any  $^{210}\text{Pb}$  in the lead shield will reduce over time due to the  $^{210}\text{Pb}$  half life of 22.2 years [90]. Therefore, the use of aged lead (more than hundred years old) is preferred to modern lead for the selection of the passive shielding material.

In addition to the peaks of gamma-ray energy originating from the primordial radionuclides in the detector and surrounding areas, the interaction of high-energy gamma rays arising from those primordial radionuclides within the surrounding detector Substances can produce pair production processes, followed by annihilation radiation. These events contribute to the counts at the background peak at 511 keV.

Airborne radionuclides including radon ( $^{222}\text{Rn}$ ) and thoron ( $^{220}\text{Rn}$ ), which are short-lived radioactive daughter products in  $^{238}\text{U}$  and  $^{232}\text{Th}$  decay series, are also sources of background radiation in the detector. Dust particles can absorb these airborne radionuclides and deposit them onto the detector holding surfaces, leading ultimately to the observation of gamma-ray energy peaks associated with decays from of  $^{214}\text{Pb}$ ,  $^{214}\text{Bi}$  (from the  $^{238}\text{U}$  decay chain) and  $^{212}\text{Pb}$ ,  $^{212}\text{Bi}$  and  $^{208}\text{Tl}$  (from the  $^{232}\text{Th}$  decay chain) in the background spectrum. Furthermore, the interactions of cosmic radiation with the earth's atmosphere give rise to the production of  $^7\text{Be}$  which can contribute to a peak at 447.6 keV, although this

particular line was not observed above the critical limits in the background spectrum in the current study.

Fluctuations of the concentration of the radioactive gases and the cosmic ray intensity in the atmosphere depending on the time of day and meteorological conditions [49]. The effect of this variation in background level can be minimized by measuring the background level as close as possible to the time of the sample measurement [49]. Variations in the background also depend upon the size and the type of detector, and the extent of shielding that may be placed around the detector [49].

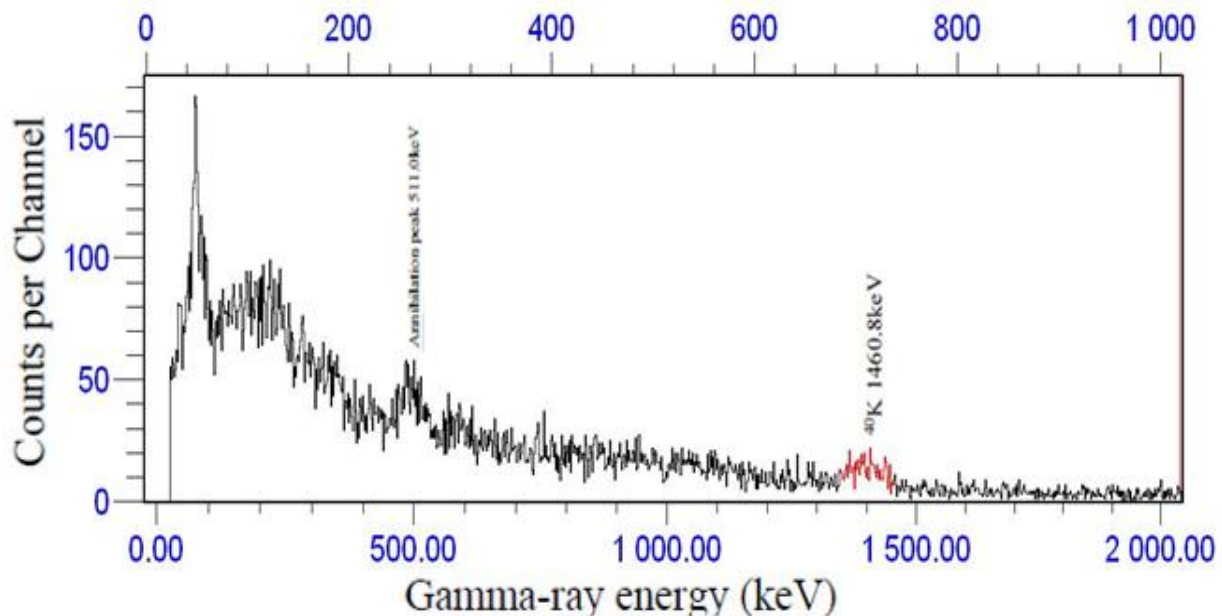


**Figure 4.1:Background spectrum measured counted for 10,900 seconds (3 hours)**  
**4.1.2 Rock Spectrum**

A range of gamma-ray transitions present in the observed spectra of all rock samples were identified and analyzed. These were used to identify unambiguously those radionuclide's which were contained in each sample. The observed shape of the gamma ray spectrum associated with decays from the radionuclides detected from sample code TKM-12, obtained at location AL-Takamul Cement Factory, is illustrated in Figure 4.2. As can be seen in Figure 4.2, most of identified radionuclides which are present in the spectrum belong to the  $^{238}\text{U}$  and  $^{232}\text{Th}$  decay chains and are similar to those observed in the background spectrum.

However, there are some gamma-ray energy peaks that were not detected in the background spectrum but can be observed clearly in the spectra of rock samples.

The significant radionuclides detected in the samples are  $^{214}\text{Pb}$  and  $^{214}\text{Bi}$  from  $^{238}\text{U}$  decay series and  $^{228}\text{Ac}$ ,  $^{212}\text{Pb}$  and  $^{212}\text{Bi}$  from  $^{232}\text{Th}$  decay series. Table 4.1 lists the identified nuclides and their signature gamma-ray energies which were observed from the spectra of all the rock samples used in the current study.

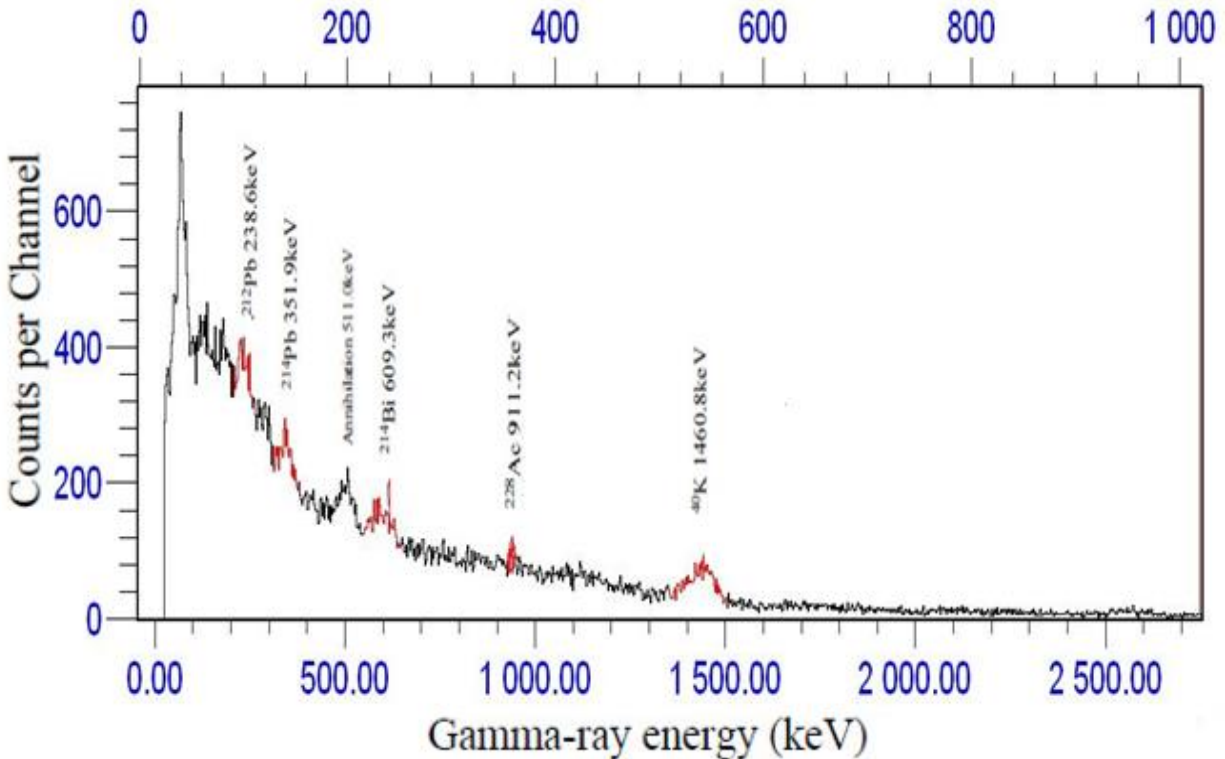


**Figure 4.2:Gamma-ray spectrum associated with decays from radionuclides detected from sample code TKM-12, obtained at location AL Takamul Cement Factory**

## 4.2 Measurement of Radioactivity

In addition to the identification of radionuclides in rock samples the most common aim in gamma-ray spectrometry with sodium iodide (NaI) detectors is the determination of the activity concentration of each gamma-emitting radionuclide species which is contained in the samples.

A wide range of relatively intense gamma-ray transitions were used and these could be combined to estimate the activity concentrations of  $^{238}\text{U}$  and  $^{232}\text{Th}$  in the samples. The activity concentration of  $^{238}\text{U}$  was determined using the gamma-ray transitions associated with decays of  $^{226}\text{Ra}$  (186.2keV),  $^{214}\text{Pb}$  (295.2 and 351.9keV) and  $^{214}\text{Bi}$  (609.3, 1120.2,1238.1, 1764.4 and 2204.2keV). The gamma-ray energy peaks associated with decays of  $^{228}\text{Ac}$  (338.3, 911.2 and 968.9keV),  $^{212}\text{Pb}$  (238.6

and 300.0keV),  $^{212}\text{Bi}$  (727.3 and 1620.5keV) and  $^{208}\text{Tl}$  (583.1 and 2614.5keV) were used to determine the activity concentration of  $^{232}\text{Th}$ . the measured gamma-ray lines were each used to determine the activity concentration for that particular radioisotope. The activity concentrations of  $^{40}\text{K}$  were derived directly from the measured intensity of the single 1460.8KeV gamma-ray transitions.

The net number of counts under each photo peak of interest were then background subtracted using the time corrected background spectrum taken. The absolute full energy peak efficiency and the relative gamma ray intensity were used to calculate the final activity concentrations of a particular nuclide as given by equation 3.4.

From the results, it can be seen that the highest activity concentrations of  $^{238}\text{U}$  and  $^{232}\text{Th}$  were found to be 39.14 and 60.59 respectively, for soil sample no.66 which was obtained from the additional materials brought from outside the manufacturing area but the highest activity concentration of  $^{40}\text{K}$  was found to be 612.59  $\text{Bq.kg}^{-1}$  measured from rock sample no.59 obtained at the location of AL-Takamul Cement Factory Quarries. Conversely, the lowest activity concentrations of  $^{238}\text{U}$ ,  $^{232}\text{Th}$  and  $^{40}\text{K}$  were found to be 3.15 ,7.42 and 38.29  $\text{Bq.kg}^{-1}$  respectively, measured from rock sample no.22 obtained at the location AL-Salam Cement Factory Quarries. The average mean activity concentrations of  $^{238}\text{U}$ ,  $^{232}\text{Th}$  and  $^{40}\text{K}$  for all rock and soil samples in this current study are 8.32, 13.76 and 172.63  $\text{Bq.kg}^{-1}$ , respectively. The standard deviation of  $^{238}\text{U}$ ,  $^{232}\text{Th}$  and  $^{40}\text{K}$  for all rock samples in this current study are 5.64, 8.31 and 99.24 , respectively. implying that no artificial radionuclide was observed in statistically significant amounts above the background level in the current study. From Figure 4.3 below, it is apparent is that  $^{40}\text{K}$  exhibited the highest activity concentrations for all measured radionuclides in all of the rock and soil samples measured in the current study shown below at table (4.1).

**Table 4.1. The results of the calculated activity concentrations of selected gamma-ray transitions from  $^{238}\text{U}$  series ,  $^{232}\text{Th}$  series and  $^{40}\text{K}$  with the weighted mean activity concentrations of  $^{238}\text{U}$  ,  $^{232}\text{Th}$  and  $^{40}\text{K}$  in each rock samples**

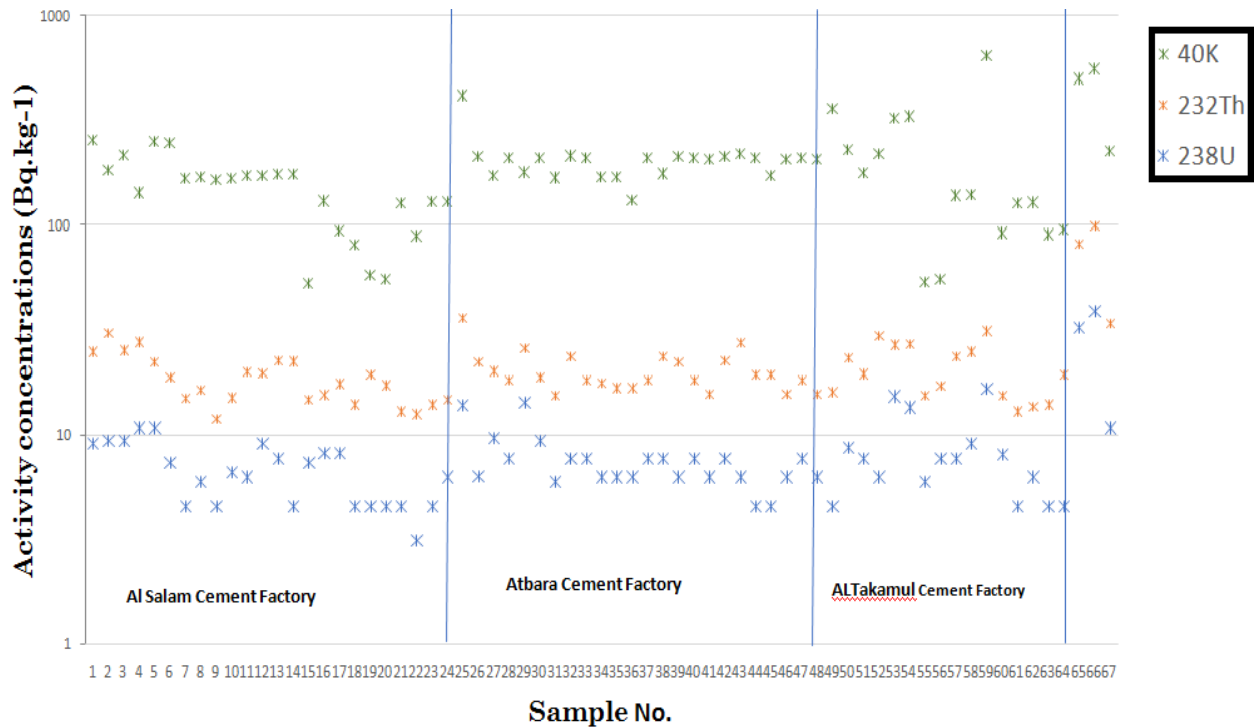
No.	Sample code	Activity Concentration (Bq.kg <sup>-1</sup> ) $^{238}\text{U}$ chain		Activity Concentration (Bq.kg <sup>-1</sup> ) $^{232}\text{Th}$ chain		Activity Concentration (Bq.kg <sup>-1</sup> )
		$^{214}\text{Pb}$	$^{214}\text{Bi}$	$^{212}\text{Pb}$	$^{228}\text{Ac}$	$^{40}\text{K}$
		352 Kev	609 Kev	238 Kev	911 Kev	1460 Kev
1.	SAL-1	11.18	6.99	10.25	21.52	229.72
2.	SAL -2	8.38	10.49	10.25	32.28	153.15
3.	SAL -3	8.38	10.49	10.25	21.52	191.44
4.	SAL -4	11.18	10.49	12.25	21.52	114.86
5.	SAL -5	11.18	10.49	12.25	10.76	229.72
6.	SAL -6	11.18	3.5	12.25	10.76	229.72
7.	SAL -7	5.59	3.5	10.25	10.76	153.15
8.	SAL -8	8.38	3.5	10.25	10.76	153.15
9.	SAL -9	5.59	3.5	4.08	10.76	153.15
10.	SAL -10	2.79	10.49	6.13	10.76	153.15
11.	SAL -11	5.59	6.99	6.13	21.52	153.15
12.	SAL -12	11.18	6.99	10.25	10.76	153.15
13.	SAL -13	8.38	6.99	8.17	21.52	153.15
14.	SAL -14	5.59	3.5	14.29	21.52	153.15
15.	SAL -15	11.18	3.5	4.08	10.76	38.29
16.	SAL -16	12.79	3.5	4.08	10.76	11486
17.	SAL -17	12.79	3.5	8.17	10.76	76.57
18.	SAL -18	5.59	3.5	8.17	10.76	66.57
19.	SAL -19	5.59	3.5	8.17	21.52	3829
20.	SAL -20	5.59	3.5	4.08	21.52	38.29
21.	SAL -21	5.59	3.5	6.13	10.76	11486
22.	SAL -22	2.79	3.5	8.17	10.76	76.57
23.	SAL -23	5.59	3.5	8.17	10.76	114.86
24.	SAL -24	5.59	6.99	6.13	10.76	114.86
25.	ATB -1	13.97	13.98	22.46	21.52	382.87
26.	ATB -2	5.59	7.00	10.21	21.52	191.44
27.	ATB -3	8.38	10.89	10.21	10.76	153.15
28.	ATB -4	8.38	6.99	10.21	10.76	191.43
29.	ATB -5	18.38	10.49	12.25	10.76	153.15
30.	ATB -6	8.38	10.48	8.17	10.76	191.43
31.	ATB -7	8.38	3.5	8.17	10.76	153.15
32.	ATB -8	8.38	6.99	10.21	21.52	191.44
33.	ATB -9	8.38	6.99	10.21	10.76	191.44
34.	ATB -10	5.59	6.99	12.25	10.76	153.15
35.	ATB -11	5.59	6.99	10.21	10.76	153.15

(continue) Table 4.1.

No.	Sample code	Activity Concentration (Bq.kg <sup>-1</sup> ) <sup>238</sup> U chain		Activity Concentration (Bq.kg <sup>-1</sup> ) <sup>232</sup> Th chain		Activity Concentration (Bq.kg <sup>-1</sup> ) <sup>40</sup> K
		<sup>214</sup> Pb	<sup>214</sup> Bi	<sup>212</sup> Pb	<sup>228</sup> Ac	
		352 Kev	609 Kev	238 Kev	911 Kev	
36.	ATB -12	5.59	6.99	10.21	10.76	114.86
37.	ATB -13	8.38	6.99	10.21	10.76	191.44
38.	ATB -14	8.38	6.99	10.21	21.52	153.15
39.	ATB -15	5.59	6.99	10.21	21.52	191.44
40.	ATB -16	8.38	6.99	10.21	10.76	191.44
41.	ATB -17	5.59	6.99	8.17	10.76	191.44
42.	ATB -18	8.38	6.99	8.17	21.52	191.44
43.	ATB -19	5.59	6.99	10.21	32.28	191.44
44.	ATB -20	5.59	3.5	8.17	21.52	191.44
45.	ATB -21	5.59	3.5	8.17	21.52	153.15
46.	ATB -22	5.59	6.99	8.17	10.76	191.44
47.	ATB -23	8.38	6.99	10.21	10.76	191.44
48.	ATB -24	5.59	6.99	8.17	10.76	191.44
49.	TKM-1	5.59	3.49	12.25	10.76	344.853
50.	TKM -2	13.97	3.49	18.38	10.76	206.296
51.	TKM -3	8.38	6.99	2.25	21.52	158.15
52.	TKM -4	5.59	6.99	14.29	32.28	191.45
53.	TKM -5	16.76	13.98	12.25	10.76	299.722
54.	TKM -6	16.76	10.49	16.33	10.76	306.3
55.	TKM -7	8.38	3.5	8.17	10.76	38.29
56.	TKM -8	8.38	6.99	8.17	10.76	38.29
57.	TKM -9	8.38	6.99	10.21	21.52	114.86
58.	TKM -10	11.18	6.99	10.21	21.52	114.86
59.	TKM -11	19.56	13.98	18.38	10.76	612.59
60.	TKM -12	5.59	10.49	4.08	10.76	76.57
61.	TKM -13	5.59	3.5	6.13	10.76	114.86
62.	TKM -14	5.59	6.99	4.08	10.76	114.86
63.	TKM -15	5.59	3.5	8.17	10.76	76.57
64.	TKM -16	5.59	3.5	8.17	21.52	76.57
65.	DCL	30.73	34.96	55.12	43.042	421.16
66.	RCL	36.32	41.95	67.37	53.80	459.44
67.	SIL	11.18	10.49	14.29	32.28	191.44

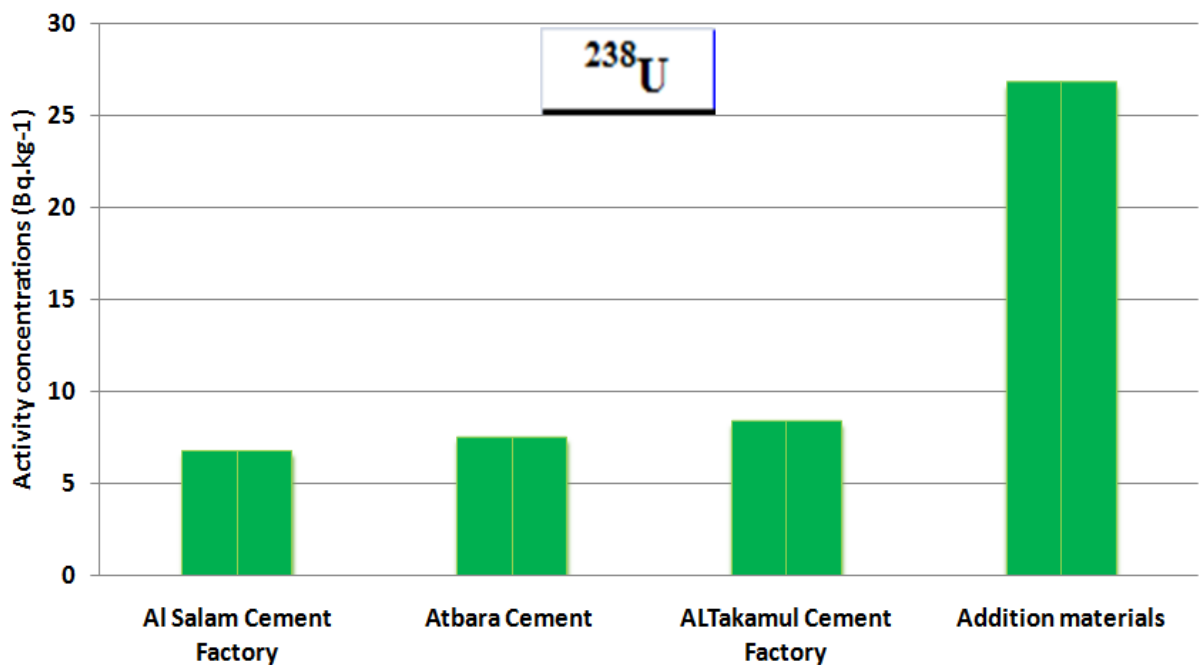
**Table 4.2. The results of the mean activity concentrations of  $^{238}\text{U}$ ,  $^{232}\text{Th}$  and  $^{40}\text{K}$  in all rock samples**

No	Sample code	Activity concentrations (Bq.kg <sup>-1</sup> )			No	Sample code	Activity concentrations (Bq.kg <sup>-1</sup> )		
		$^{238}\text{U}$	$^{232}\text{Th}$	$^{40}\text{K}$			$^{238}\text{U}$	$^{232}\text{Th}$	$^{40}\text{K}$
1	SAL-1	9.09	15.89	229.72	37	ATB -13	7.69	10.49	191.44
2	SAL -2	9.44	21.27	153.15	38	ATB -14	7.69	15.87	153.15
3	SAL -3	9.44	15.89	191.44	39	ATB -15	6.29	15.87	191.44
4	SAL -4	10.84	16.89	114.86	40	ATB -16	7.69	10.49	191.44
5	SAL -5	10.84	11.51	229.72	41	ATB -17	6.29	9.47	191.44
6	SAL -6	7.34	11.51	229.72	42	ATB -18	7.69	14.85	191.44
7	SAL -7	4.55	10.51	153.15	43	ATB -19	6.29	21.25	191.44
8	SAL -8	5.94	10.51	153.15	44	ATB -20	4.55	14.85	191.44
9	SAL -9	4.55	7.42	153.15	45	ATB -21	4.55	14.85	153.15
10	SAL -10	6.64	8.45	153.15	46	ATB -22	6.29	9.47	191.44
11	SAL -11	6.29	13.83	153.15	47	ATB -23	7.69	10.49	191.44
12	SAL -12	9.09	10.51	153.15	48	ATB -24	6.29	9.47	191.44
13	SAL -13	7.69	14.85	153.15	<b>Mean</b>		<b>7.55</b>	<b>12.84</b>	<b>182.61</b>
14	SAL -14	4.55	17.91	153.15	49	TKM-1	4.54	11.51	344.85
15	SAL -15	7.34	7.42	38.29	50	TKM -2	8.73	14.57	206.29
16	SAL -16	8.15	9.47	114.86	51	TKM -3	7.69	11.89	158.15
17	SAL -17	8.15	9.47	76.57	52	TKM -4	6.29	23.29	191.45
18	SAL -18	4.55	9.47	66.57	53	TKM -5	15.37	11.51	299.72
19	SAL -19	4.55	14.85	38.29	54	TKM -6	13.63	13.55	306.3
20	SAL -20	4.55	12.8	76.57	55	TKM -7	5.94	9.47	38.29
21	SAL -21	4.55	8.45	114.86	56	TKM -8	7.69	9.47	38.29
22	SAL -22	3.15	7.42	38.29	57	TKM -9	7.69	15.87	114.86
23	SAL -23	4.55	9.47	114.86	58	TKM -10	9.09	15.87	114.86
24	SAL -24	6.29	8.45	114.86	59	TKM -11	16.77	14.57	612.59
<b>Mean</b>		<b>6.78</b>	<b>11.99</b>	<b>132.74</b>	60	TKM -12	8.04	7.42	76.57
25	ATB -1	13.98	21.99	382.87	61	TKM -13	4.55	8.45	114.86
26	ATB -2	6.30	15.87	191.44	62	TKM -14	6.29	7.42	114.86
27	ATB -3	9.64	10.49	153.15	63	TKM -15	4.55	9.47	76.57
28	ATB -4	7.69	10.49	191.43	64	TKM -16	4.55	14.85	76.57
29	ATB -5	14.44	11.51	153.15	<b>Mean</b>		<b>8.40</b>	<b>12.32</b>	<b>186.95</b>
30	ATB -6	9.43	9.47	191.43	65	RCL	32.85	49.08	421.16
31	ATB -7	5.94	9.47	153.15	66	DCL	39.14	60.59	459.44
32	ATB -8	7.69	15.87	191.44	67	SIL	10.84	23.29	191.44
33	ATB -9	7.69	10.49	191.44	<b>Mean</b>		<b>27.61</b>	<b>44.32</b>	<b>357.35</b>
34	ATB -10	6.29	11.51	153.15	<b>Min</b>		<b>3.15</b>	<b>7.42</b>	<b>38.29</b>
35	ATB -11	6.29	10.49	153.15	<b>Max</b>		<b>39.14</b>	<b>60.59</b>	<b>612.59</b>
36	ATB -12	6.29	10.49	114.86	<b>Mean ± S.D.</b>		<b>8.32±5.64</b>	<b>13.76±8.3</b>	<b>172.63±99.24</b>



**Figure 4.3: The overall activity concentrations of  $^{238}\text{U}$ ,  $^{232}\text{Th}$  and  $^{40}\text{K}$  in rock samples studied from different sampling areas.**

The mean average value concentrations of  $^{238}\text{U}$ ,  $^{232}\text{Th}$  and  $^{40}\text{K}$  in each Quarries area from which the rock samples were collected are shown in Figure 4.4 with the weighted mean concentration for all rock samples in the current study.



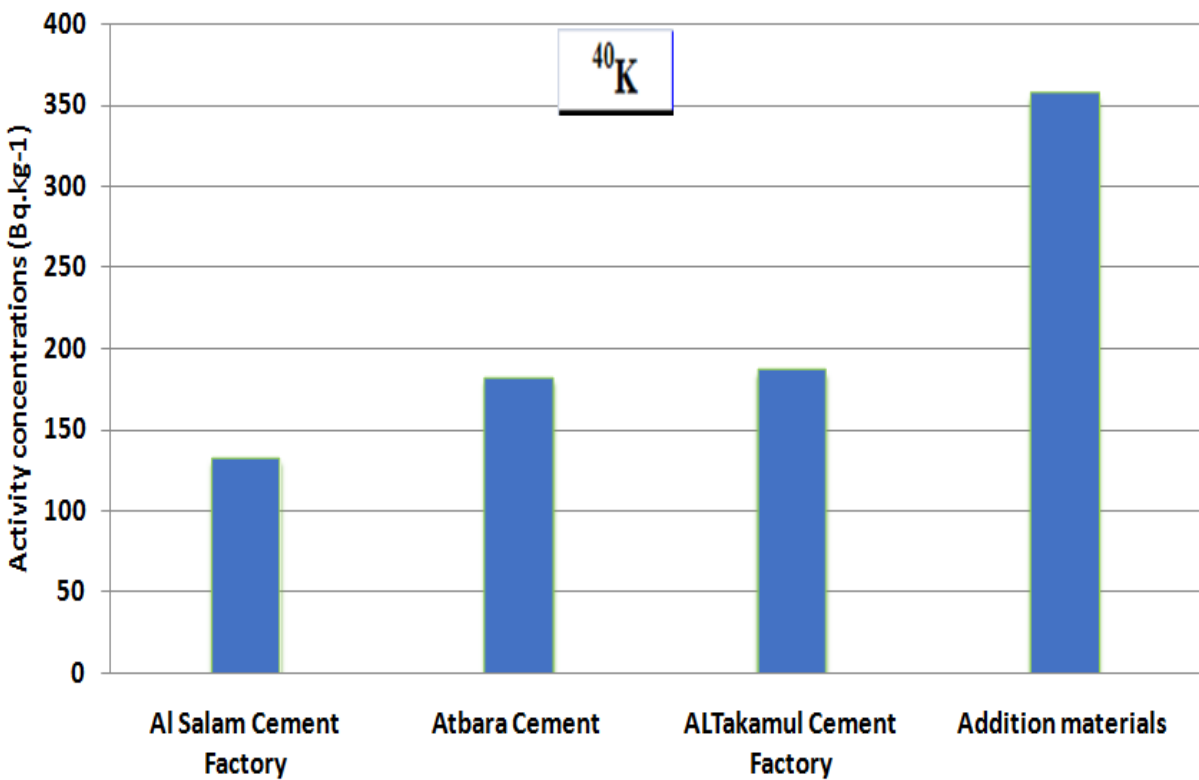
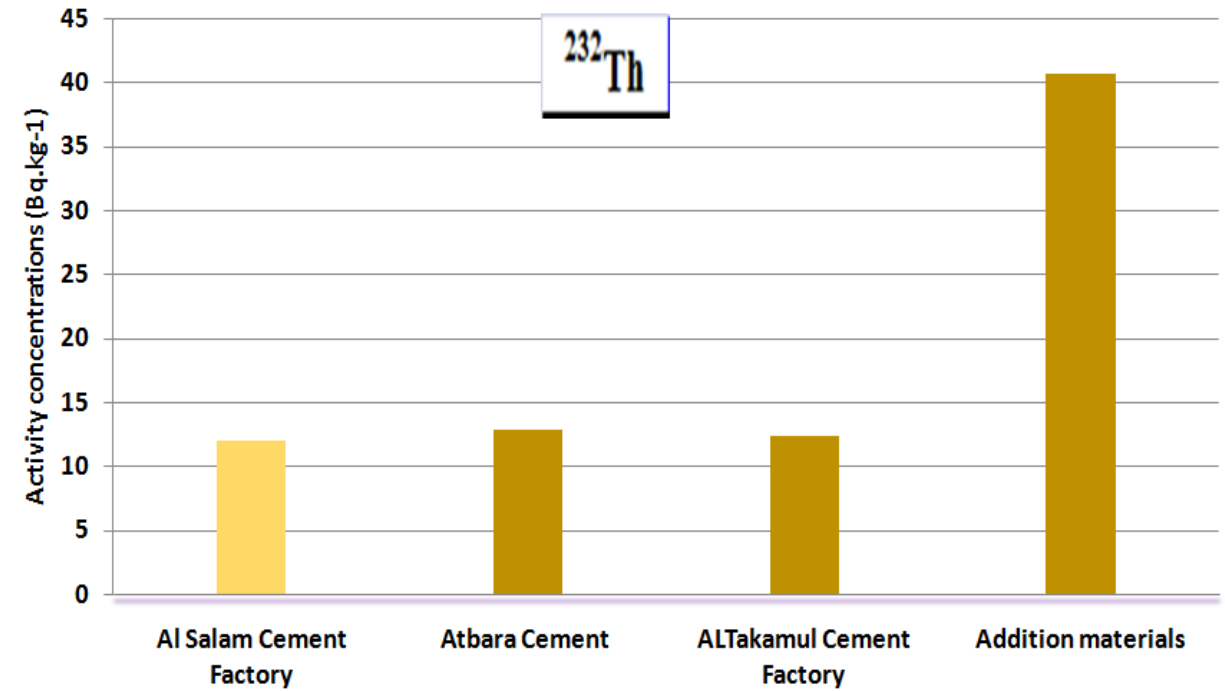


**Figure 4.4:**The mean average values of  $^{238}\text{U}$ ,  $^{232}\text{Th}$  and  $^{40}\text{K}$  activity concentrations for each Quarries area measured in the current work

The comparison between the observed activity concentrations of  $^{238}\text{U}$ ,  $^{232}\text{Th}$  and  $^{40}\text{K}$  in all rock samples and that of the worldwide mean values is also shown in Table 4.1 and Figure 4.5.

**Table 4.3: Comparison between the average mean activity concentrations of  $^{238}\text{U}$ ,  $^{232}\text{Th}$  and  $^{40}\text{K}$  in sampling areas from all factories and overall results with the mean value for the worldwide.**

Sampling area	Activity Concentration (Bq.kg <sup>-1</sup> )		
	$^{238}\text{U}$	$^{232}\text{Th}$	$^{40}\text{K}$
Al Salam Cement Factory	6.78	11.99	132.74
Atbara Cement Factory	7.55	12.84	182.61
AL Takamul Cement Factory	8.40	12.32	186.95
Addition Materials	27.61	44.32	357.35
<b>Worldwide Range</b>	17- 60	11- 64	140 - 850
<b>Mean</b>	35	30	400

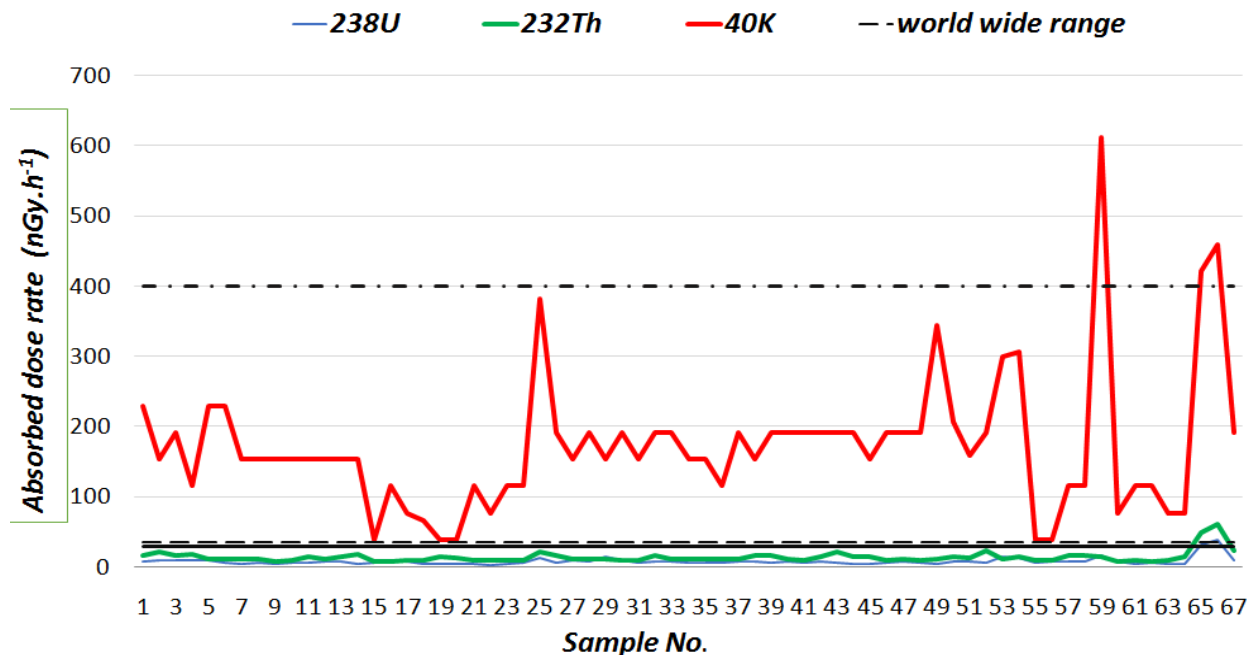


**Figure 4.5: Comparison between the average mean activity concentrations of <sup>238</sup>U, <sup>232</sup>Th and <sup>40</sup>K in sampling areas and overall results with the mean value for the worldwide.**

The results of the current study have been compared with the world mean activity concentrations in soil, as shown in Figure 4.5 and Table 4.1. According to the UNSCEAR report 2000 [14], the worldwide activity concentrations of <sup>238</sup>U, <sup>232</sup>Th and <sup>40</sup>K were reported to be 17↔60, 11↔64 and 140↔850 Bq.kg<sup>-1</sup> with the mean concentrations of 35, 30 and 400 Bq.kg<sup>-1</sup>, respectively. The obtained results show that the ranges of the activity concentrations of <sup>238</sup>U and <sup>232</sup>Th vary from 6.78 to 26.80 and 11.99 to 40.66 Bq.kg<sup>-1</sup>, respectively. The activity concentrations of <sup>238</sup>U and <sup>232</sup>Th are above the upper range of the worldwide values due to the high concentration values found in some soil samples from the Addition materials areas. However, the overall mean activity concentrations of <sup>238</sup>U and <sup>232</sup>Th are comparable to the mean activity worldwide concentrations. The activity concentrations of <sup>40</sup>K in all rock samples range from 132.74 to 357.3 Bq.kg<sup>-1</sup> and fall within the worldwide range, with a weighted mean value for the activity concentration of 214.89 Bq.kg<sup>-1</sup>, which is lower than the worldwide average value. The results shown in Figure 4.1 reveal that soil samples from the Addition materials contain the highest activity concentrations of <sup>40</sup>K. The higher concentrations of <sup>238</sup>U, <sup>232</sup>Th and <sup>40</sup>K in some rock and soil samples may be influenced in part by a result of variation in geological structure [24,91].

**Table 4.4: Comparison of mean and range values of the activity concentration of  $^{238}\text{U}$ ,  $^{232}\text{Th}$ , and  $^{40}\text{K}$  in  $\text{Bq.kg}^{-1}$  with some countries as listed in table:**

Country	Activity concentration Country ( $\text{Bq/kg-1}$ )						Ref.
	$^{238}\text{U}$		$^{232}\text{Th}$		$^{40}\text{K}$		
	Mean	Range	Mean	Range	Mean	Range	
Kuwait (north region)	66.57	46-115	11.27	3.3-17	384.47	78-492	[93]
Oman	29.7	-	15.9	-	225	-	[94]
Syria	23	10-64	20	10-32	270	87-780	[96]
Jordan	49	-	27	-	291	-	[95]
Iran	28	8-55	22	5-42	640	250-980	[96]
Egypt	37	6-120	18	2-96	320	29-650	[96]
Algeria	30	2-110	25	2-140	370	66-1 150	[96]
India	29	7-81	64	14-160	400	38-760	[96]
Japan	29	2-59	28	2-88	310	15-990	[96]
US	35	4-140	35	4-130	370	100-700	[96]
Sudan	15	-	33	-	230	-	[105]
<b>World-wide value</b>	<b>35</b>	<b>17 - 60</b>	<b>30</b>	<b>11 - 64</b>	<b>400</b>	<b>140 -850</b>	[96]
<b>Current study</b>	<b>8.32</b>	<b>3.15 - 39.14</b>	<b>13.76</b>	<b>7.42 - 60.59</b>	<b>172.63</b>	<b>38.29-612.59</b>	

As seen from Table 4.4 , the range of activity concentration of and the mean of the activity concentration of  $^{238}\text{U}$  ,  $^{232}\text{Th}$  and  $^{40}\text{k}$  is lower than that for all countries listed in the table

### 4.3 Assessment of Radiological Hazard

One of the main objectives of the radioactivity measurement in environmental sample is not simply to determine the activity concentrations of  $^{238}\text{U}$ ,  $^{232}\text{Th}$  and  $^{40}\text{K}$  but also to estimate the radiation exposure dose and to assess the biological effects on humans. The assessment of radiological risk can be considered in various terms. In the current study four related quantities were deduced, these being: (i) the absorbed dose rate ( $D$ ) in air at 1 meter above the ground surface; (ii) the annual effective dose equivalent ( $AEDE$ ) from outdoor terrestrial gamma radiation; (iii) the radium equivalent activity ( $Ra_{eq}$ ); and (iv) the external hazard index ( $H_{ex}$ ). These radiological parameters can be calculated from the measured activity concentrations of three main primordial radionuclides in rock and soil samples, using the relations described in Section 3.5. The values of these radiological hazard parameters as deduced in the current work are listed in Table(4.5) and Table (4.6).

**Table 4.5. The results of the absorbed dose rate (D), the annual effective dose equivalent (AEDE), the radium equivalent activity (Ra<sub>eq</sub>) and the external hazard index (H<sub>ex</sub>) in all rock samples.**

Sample No.	D (nGyh <sup>-1</sup> )	AEDE (mSv.y <sup>-1</sup> )	Ra <sub>eq</sub> (Bq.kg <sup>-1</sup> )	H <sub>ex</sub>	Sample No.	D (nGyh <sup>-1</sup> )	AEDE (mSv.y <sup>-1</sup> )	Ra <sub>eq</sub> (Bq.kg <sup>-1</sup> )	H <sub>ex</sub>
1	23.45	0.029	49.502	0.134	37	17.93	0.03	37.432	0.11
2	23.65	0.03	51.649	0.14	38	19.58	0.03	42.177	0.12
3	22	0.028	46.904	0.127	39	20.54	0.03	43.725	0.12
4	20.04	0.025	43.837	0.119	40	17.93	0.03	37.432	0.11
5	21.61	0.027	44.988	0.122	41	16.67	0.03	34.573	0.1
6	20.00	0.025	41.488	0.113	42	20.57	0.03	43.667	0.12
7	14.89	0.019	31.372	0.085	43	23.79	0.03	51.419	0.14
8	15.53	0.02	32.762	0.089	44	19.12	0.03	40.527	0.11
9	13.02	0.017	26.954	0.073	45	17.51	0.03	37.579	0.11
10	14.61	0.018	30.517	0.083	46	16.67	0.03	34.573	0.1
11	17.70	0.022	37.86	0.103	47	17.93	0.03	37.432	0.11
12	16.98	0.021	35.912	0.097	48	16.67	0.03	34.573	0.1
13	18.96	0.024	40.719	0.11	<b>Mean</b>	<b>18.95</b>	<b>0.028</b>	<b>39.984</b>	<b>0.113</b>
14	19.36	0.024	41.954	0.114	49	23.54	0.03	47.553	0.13
15	9.49	0.012	20.899	0.057	50	21.5	0.03	45.45	0.13
16	13.08	0.017	27.604	0.075	51	17.38	0.03	36.871	0.1
17	12.71	0.016	27.588	0.075	52	25.02	0.04	54.337	0.15
18	10.62	0.014	23.218	0.063	53	26.65	0.04	54.908	0.15
19	11.45	0.015	28.734	0.07	54	27.35	0.04	56.592	0.16
20	11.45	0.015	25.803	0.07	55	10.08	0.02	22.431	0.07
21	12.04	0.015	25.478	0.069	56	10.89	0.02	24.181	0.07
22	10.40	0.013	22.588	0.061	57	17.97	0.03	39.229	0.11
23	12.65	0.016	26.937	0.073	58	18.61	0.03	40.629	0.11
24	12.84	0.016	27.218	0.074	59	42.28	0.06	84.775	0.23
<b>Mean</b>	<b>15.772</b>	<b>0.0199</b>	<b>33.854</b>	<b>0.092</b>	60	11.42	0.02	24.547	0.07
25	35.83	0.045	74.907	0.203	61	12.04	0.02	25.478	0.07
26	20.54	0.026	43.735	0.119	62	12.22	0.02	25.745	0.07
27	17.23	0.022	36.434	0.099	63	11.04	0.02	23.988	0.07
28	17.93	0.023	37.431	0.102	64	14.29	0.02	31.682	0.09
29	20.06	0.025	42.692	0.116	<b>Mean</b>	<b>18.89</b>	<b>0.029</b>	<b>39.900</b>	<b>0.111</b>
30	18.12	0.03	37.713	0.11	65	62.51	0.08	135.464	0.37
31	14.90	0.02	31.275	0.09	66	73.98	0.10	161.161	0.44
32	21.18	0.03	45.125	0.13	67	27.12	0.04	58.886	0.16
33	17.93	0.03	37.432	0.11	<b>Mean</b>	<b>54.54</b>	<b>0.073</b>	<b>118.50</b>	<b>0.32</b>
34	16.30	0.03	34.542	0.10	<b>Min</b>	<b>9.49</b>	<b>0.012</b>	<b>20.899</b>	<b>0.057</b>
35	15.68	0.02	33.084	0.09	<b>Max</b>	<b>42.28</b>	<b>0.10</b>	<b>161.161</b>	<b>0.44</b>
36	14.07	0.02	30.135	0.09	<b>Mean ±S.D</b>	<b>19.41±10.35</b>	<b>0.028±0.014</b>	<b>41.28±22.38</b>	<b>0.114±0.061</b>

**Table 4.6. The calculated, combined absorbed dose rate (D), annual effective dose equivalent (AEDE), radium equivalent activity (Ra<sub>eq</sub>) and external hazard index (H<sub>ex</sub>) obtained from all the samples measured in the current study:**

<b>Sample Name.</b>	<b><i>D</i> (nGy.h<sup>-1</sup>)</b>	<b><i>AEDE</i> (mSv.y<sup>-1</sup>)</b>	<b><i>Ra<sub>eq</sub></i> (Bq.kg<sup>-1</sup>)</b>	<b><i>H<sub>ex</sub></i></b>
<b>Mean of Al Salam factory</b>	15.772	0.0199	33.854	0.09
<b>Mean of Al Takamol factory</b>	18.95	0.028	39.984	0.113
<b>Mean of Atbara factory</b>	18.89	0.029	39.900	0.111
<b>Mean of Addition Materials</b>	54.54	0.073	118.50	0.32
<b>Min</b>	9.49	0.012	20.899	0.057
<b>Max</b>	62.51	0.10	161.161	0.44
<b>(Mean ± S.D) of all samples</b>	<b>19.41±10.35</b>	<b>0.028±0.014</b>	<b>41.28±22.38</b>	<b>0.114±0.061</b>
<b>World Wide Range</b>	<b>57</b>	<b>0.070</b>	<b>&lt; 370</b>	<b>&lt; 1</b>

From Table 3.4, the estimated absorbed dose rates based on rock and soil radioactivity range from 9.49 to 62.51 nGy.h<sup>-1</sup> with a mean value and standard deviation of 19.41±10.35 nGy.h<sup>-1</sup>. Compared with the worldwide values, most of the results obtained in this current study fall within the expected range, with the average mean value of absorbed dose rate from all the samples being lower than the worldwide mean value.

The absorbed dose rate in air at 1 meter above the ground surface does not directly provide the radiological risk to which an individual is exposed [78,91]. The annual effective dose equivalent from outdoor terrestrial gamma radiation was estimated by taking into account the conversion coefficients from absorbed dose in air to effective dose and the outdoor occupancy factor. The effective dose for the different locations of rock and soil samples in this study varied from 0.012 to 0.10 mSv.y<sup>-1</sup>, with the arithmetic mean value and standard deviation of 0.028±0.014 mSv.y<sup>-1</sup>, which is comparable to the worldwide effective dose of 0.070 mSv.y<sup>-1</sup> [14].

The radiation hazard parameters in terms of the radium equivalent activity (Ra<sub>eq</sub>) and the external hazard index (H<sub>ex</sub>) were also evaluated. The Radium equivalent activity (Ra<sub>eq</sub>) is a single quantity which compares the activity concentrations of <sup>226</sup>Ra, <sup>232</sup>Th and <sup>40</sup>K in rock and soil samples in order to obtain a total activity concentration. The results for the calculated Ra<sub>eq</sub> from the current

work are summarized in Table 4.4. The values of  $Ra_{eq}$  range from 20.899 to 161.161  $Bq.kg^{-1}$  with an overall arithmetic mean and standard deviation of  $41.28 \pm 22.38 Bq.kg^{-1}$ . It can be seen that the  $Ra_{eq}$  values for all samples in the present study are lower than the accepted safety limit value of 370  $Bq.kg^{-1}$  as recommended by the Organization for Economic Cooperation and Development (OECD) [86,87,92]. According to Beretka and Mathew [81], Turhan and Ajayi [82], the use of these rock as raw materials for building does not constitute a health hazard of radiation [81,82,85].

The calculated values of the external hazard index for all soil samples studied vary from 0.057 to 0.44 and the average value was found to be  $0.114 \pm 0.061$ . The results show that the  $H_{ex}$  values for all rock soil samples are below the limit of unity, meaning that the radiation dose is below the permissible limit of 1  $mSv.y^{-1}$  recommended by ICRP 60 [14,82].

#### 4.4 Determine $^{222}Rn$ concentration and Assessment of Radiological Hazard

First, a reference measurement area was selected and the radon gas volume  $^{222}Rn$  was measured in a number of quarries equipped to take cement ore.  $^{222}Rn$  air concentration was measured using portable device Radon Scout Plus meters device GmbH which made by SARAD company in Germany.

The sensitivity of this device is 1.8 counts/ min  $\times$   $KBq/m^3$  (independent on the humidity) and response time 120 minutes to 95% of the final value [97]. High sensitivity with alpha spectrometry analysis, leads to a short response time even at low concentrations. According to the measuring instructions provided by SARAD company, for continuous measurement; more than 3 hours; the device should be placed in slow mode to increase the accuracy [98], Measurement of  $^{222}Rn$  concentration was done in five quarries of cement.

Due to the measurement of  $^{222}Rn$  concentration in indoor air guidelines, measuring was designed for 24 consecutive hours of each quarry (recommended by the EPA). After completion of the measurement of  $^{222}Rn$  concentration in indoor air, and outdoor air sites, also the concentration of  $^{222}Rn$  was carried out for 3 hours (background) near the entrance of quarries. In sum, the 50 measurements of  $^{222}Rn$  were done in indoor air of quarries.

Calculation effective dose and risk of lung cancer Estimation of annual effective dose by the indoor air  $^{222}Rn$  ( $ERn$ ) was conducted by UNSCEAR equation;

$$E_{Rn} (mSv / y) = C_{Rn} \times 0.4 \times 7000 \times 9 \times 10^{-6} E.q (4.1)$$

In this equation, geometric mean concentrations of indoor air  $^{222}\text{Rn}$  ( $\text{Bq}/\text{m}^3$ ), 0.4 is equilibrium factor of decay products of  $^{222}\text{Rn}$ , 7000 (h/y) is equal to 80% of the year (the settlement) and 9 is ( $\text{nSv}/\text{Bq}\cdot\text{m}^3\cdot\text{h}$ ) feed conversion ratio of  $^{222}\text{Rn}$  concentration to annual effective dose and  $10^{-6}$  conversion ratio of  $\text{nSv}/\text{mSv}$  [99]. To calculate the probability of lung cancer cases per million people (CPPP) by effective dose from  $^{222}\text{Rn}$ , equation (3.2) was used[100].

$$\text{CPPP} = E_{\text{Rn}} \times 18 \times 10^{-6} \text{ mSv}^{-1} \cdot \text{yE}\cdot\text{q} \quad (4.2)$$

The mean and the annual range of  $^{222}\text{Rn}$  concentration in indoor air of all cement quarries are ( $25.64 \pm 4.4$ )  $\text{Bq}/\text{m}^3$ . The range concentrations of background air of  $^{222}\text{Rn}$  are ( $12 \pm 2$ )  $\text{Bq}/\text{m}^3$ . The highest and lowest concentrations of  $^{222}\text{Rn}$  in the indoor air of all cement quarries are No.35 ( $9 \pm 1.5$ )  $\text{Bq}/\text{m}^3$  and No.49 ( $188 \pm 31$ )  $\text{Bq}/\text{m}^3$ , respectively shown in Table (4.6).

The mean concentration of  $^{222}\text{Rn}$  indoor air relative to WHO and EPA standards are 25.6% and 38.5%, respectively (Figure 4.6). Like the River Nile State area, the concentration of  $^{222}\text{Rn}$  indoor air of all cement quarries is less than the **WHO** guideline and **EPA** standard limits.

The annual mean effective dose of  $^{222}\text{Rn}$  in all cement quarries River Nile State are ( $0.66 \pm 0.11$ )  $\text{mS}\cdot\text{y}^{-1}$ . Effective dose by residents of River Nile State is less than standard **ICRP** ( $1\text{mSv}/\text{y}$ )[101,102].

**Table.4.7<sup>222</sup>Rn concentrations (Mean  $\pm$ SD)Bq/m<sup>3</sup>of indoor air samples of quarries cement factories River Nile State, Sudan :**

No	<sup>222</sup> Rn concentration (Bq/m <sup>3</sup> )		Effective dose (mSv/y)	Lung cancer risk	No	<sup>222</sup> Rn concentration (Bq/m <sup>3</sup> )		Effective dose (mSv/y)	Lung Cancer risk
1	28 $\pm$ 4.8	QS-1	0.70 $\pm$ 0.12	12.6 $\pm$ 2.2	26	35 $\pm$ 5.9	QA-3	0.88 $\pm$ 0.15	15.8 $\pm$ 2.7
2	20 $\pm$ 3.4	QS-1	0.50 $\pm$ 0.08	9 $\pm$ 1.4	27	59 $\pm$ 1.0	QA-3	1.49 $\pm$ 0.25	26.8 $\pm$ 4.5
3	15 $\pm$ 2.6	QS-1	0.38 $\pm$ 0.06	6.8 $\pm$ 1.1	28	18 $\pm$ 3.0	QA-4	0.45 $\pm$ 0.07	8.1 $\pm$ 1.3
4	23 $\pm$ 3.9	QS-1	0.58 $\pm$ 0.10	10.4 $\pm$ 1.8	29	37 $\pm$ 6.3	QA-4	0.93 $\pm$ 0.16	16.7 $\pm$ 2.9
5	18 $\pm$ 3.0	QS-2	0.45 $\pm$ 0.07	8.1 $\pm$ 1.3	30	21 $\pm$ 3.6	QA-4	0.53 $\pm$ 0.09	9.5 $\pm$ 1.6
6	21 $\pm$ 3.6	QS-2	0.53 $\pm$ 0.09	9.5 $\pm$ 1.6	31	26 $\pm$ 4.4	QA-5	0.66 $\pm$ 0.12	11.9 $\pm$ 2.2
7	24 $\pm$ 4.0	QS-2	0.60 $\pm$ 0.10	10.8 $\pm$ 1.8	32	21 $\pm$ 3.6	QA-5	0.53 $\pm$ 0.09	9.5 $\pm$ 1.6
8	15 $\pm$ 2.6	QS-3	0.38 $\pm$ 0.06	6.8 $\pm$ 1.1	33	26 $\pm$ 4.4	QA-5	0.66 $\pm$ 0.12	11.9 $\pm$ 2.2
9	20 $\pm$ 3.4	QS-3	0.50 $\pm$ 0.08	9 $\pm$ 1.4	34	23 $\pm$ 3.9	QA-5	0.58 $\pm$ 0.10	10.4 $\pm$ 1.8
10	12 $\pm$ 2.0	QS-3	0.30 $\pm$ 0.05	5.4 $\pm$ 0.9	35	9 $\pm$ 1.53	QT-1	0.23 $\pm$ 0.04	4.14 $\pm$ 0.72
11	12 $\pm$ 2.0	QS-3	0.30 $\pm$ 0.05	5.4 $\pm$ 0.9	36	20 $\pm$ 3.4	QT-1	0.50 $\pm$ 0.08	9 $\pm$ 1.4
12	21 $\pm$ 3.6	QS-4	0.53 $\pm$ 0.09	9.5 $\pm$ 1.6	37	29 $\pm$ 4.9	QT-1	0.73 $\pm$ 0.11	13. $\pm$ 2.0
13	28 $\pm$ 4.7	QS-4	0.70 $\pm$ 0.12	12.6 $\pm$ 2.2	38	20 $\pm$ 3.4	QT-1	0.50 $\pm$ 0.08	9 $\pm$ 1.4
14	36 $\pm$ 6.1	QS-4	0.91 $\pm$ 0.15	16.3 $\pm$ 2.7	39	23 $\pm$ 3.9	QT-2	0.58 $\pm$ 0.10	10. $\pm$ 1.8
15	29 $\pm$ 4.9	QS-5	0.73 $\pm$ 0.12	13.1 $\pm$ 2.2	40	15 $\pm$ 2.6	QT-2	0.38 $\pm$ 0.06	6.8 $\pm$ 1.1
16	38 $\pm$ 6.5	QS-5	0.96 $\pm$ 0.16	17.3 $\pm$ 2.9	41	18 $\pm$ 3.0	QT-2	0.45 $\pm$ 0.07	8.1 $\pm$ 1.3
17	18 $\pm$ 3.0	QS-5	0.45 $\pm$ 0.07	8.1 $\pm$ 1.3	42	26 $\pm$ 4.4	QT-2	0.66 $\pm$ 0.12	11.9 $\pm$ 2.2
18	15 $\pm$ 2.6	QA-1	0.38 $\pm$ 0.06	6.8 $\pm$ 1.1	43	38 $\pm$ 6.5	QT-3	0.96 $\pm$ 0.16	17.3 $\pm$ 2.9
19	32 $\pm$ 5.4	QA-1	0.81 $\pm$ 0.14	14.6 $\pm$ 2.5	44	15 $\pm$ 2.6	QT-3	0.38 $\pm$ 0.06	6.8 $\pm$ 1.1
20	32 $\pm$ 5.4	QA-1	0.81 $\pm$ 0.14	14.6 $\pm$ 2.5	45	12 $\pm$ 2.0	QT-3	0.30 $\pm$ 0.05	5.4 $\pm$ 0.9
21	20 $\pm$ 3.4	QA-1	0.50 $\pm$ 0.08	9 $\pm$ 1.4	46	15 $\pm$ 2.6	QT-3	0.38 $\pm$ 0.06	6.8 $\pm$ 1.1
22	12 $\pm$ 2.0	QA-2	0.30 $\pm$ 0.05	5.4 $\pm$ 0.9	47	15 $\pm$ 2.6	QT-4	0.38 $\pm$ 0.06	6.8 $\pm$ 1.1
23	29 $\pm$ 4.9	QA-2	0.73 $\pm$ 0.11	13.1 $\pm$ 2.0	48	26 $\pm$ 4.4	QT-4	0.66 $\pm$ 0.11	11.9 $\pm$ 2.2
24	26 $\pm$ 4.4	QA-2	0.66 $\pm$ 0.12	11.9 $\pm$ 2.2	49	188 $\pm$ 31.9	QT-4	4.74 $\pm$ 0.80	85.32 $\pm$ 14.4
25	26 $\pm$ 4.4	QA-3	0.66 $\pm$ 0.12	11.9 $\pm$ 2.2	50	12 $\pm$ 2.0	QT-4	0.30 $\pm$ 0.05	5.4 $\pm$ 0.9
					<b>Min</b>	<b>9 <math>\pm</math>1.53</b>		<b>0.23 <math>\pm</math>0.04</b>	<b>4.14 <math>\pm</math>0.72</b>
					<b>Max</b>	<b>188 <math>\pm</math>31.9</b>		<b>4.74 <math>\pm</math>0.80</b>	<b>85.32 <math>\pm</math>14.4</b>
					<b>Mean</b>	<b>25.64 <math>\pm</math> 4.4</b>		<b>0.66 <math>\pm</math>0.11</b>	<b>11.7 <math>\pm</math> 1.98</b>

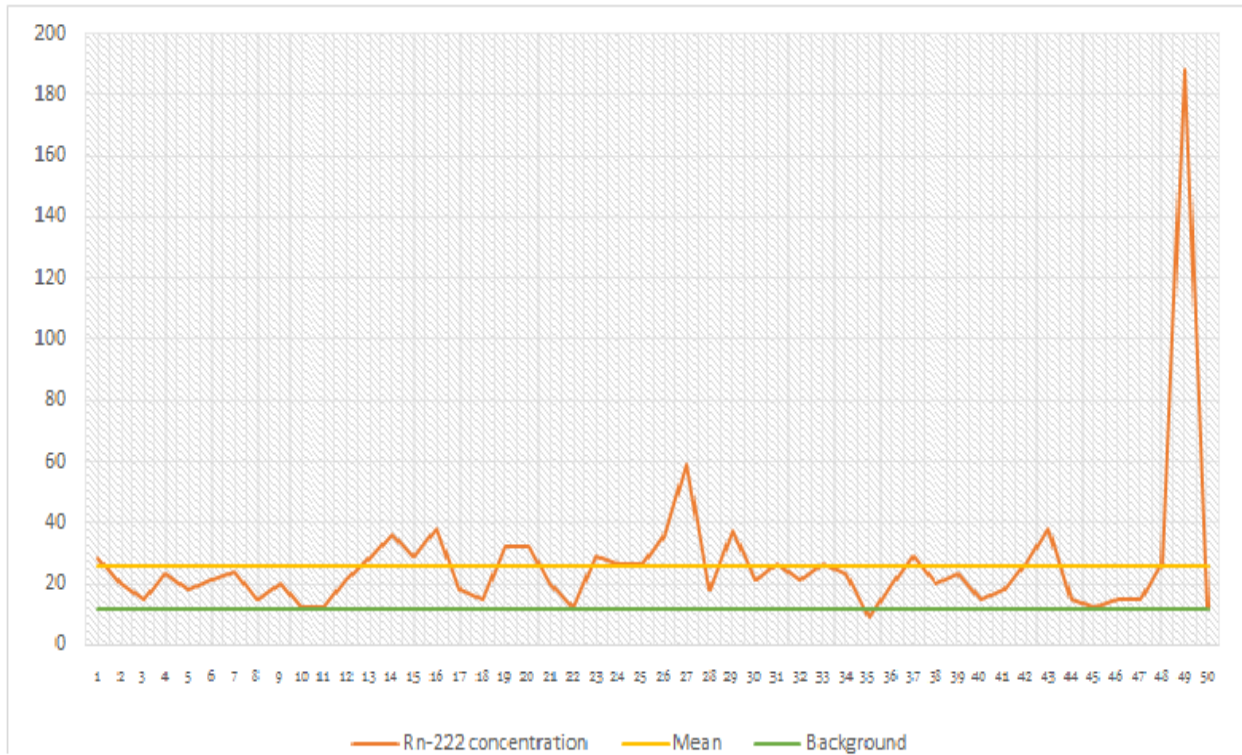


**Figure 4.6 Comparison of  $^{222}\text{Rn}$  indoor concentration in cement quarries, background and mean concentration**

The mean and annual ranges concentration of  $^{222}\text{Rn}$  indoor air of quarries cement factories is  $25.64 \pm 4.4\text{Bq/m}^3$ . Also, the mean and range of annual background air of  $^{222}\text{Rn}$  is  $12 \pm 2\text{Bq/m}^3$ . The highest and lowest concentrations of  $^{222}\text{Rn}$  indoor air of the No.49 are  $(188 \pm 31.9\text{Bq/m}^3)$  and 35 ( $9 \pm 1.53\text{Bq/m}^3$ ).

# **Chapter Five**

## **Conclusion and Recommendations**

# Chapter Five

## Conclusion and Recommendations

### 5.1 Conclusion

The level of natural radioactivity in cement factories Quarries, collected randomly from different locations in the River Nile state include several points of cement factories Quarries, Al-Salam cement, Atbara cement and Al Takamul cement factories and three (3) samples were taken from the additional materials used to manufacture cement has been evaluated using high resolution gamma-ray spectrometry. In this current study, the measurements showed that primordial radionuclides namely the  $^{238}\text{U}$  and  $^{232}\text{Th}$  decay chains and  $^{40}\text{K}$  are contained in all rock and soil samples. The measured activity concentrations of  $^{238}\text{U}$ ,  $^{232}\text{Th}$  and  $^{40}\text{K}$  across all of the rock and soil samples varied from 3.15 to 39.14, 7.42 to 60.59 and 38.29 to 612.59 Bq.kg<sup>-1</sup> with the average mean values of 8.32 , 13.76 and 172.63 Bq.kg<sup>-1</sup>, respectively. The obtained results of the activity concentrations of  $^{238}\text{U}$ ,  $^{232}\text{Th}$  and  $^{40}\text{K}$  were found to be higher than the upper range of the worldwide values identified by UNSCEAR (2000), 39.14, 60.59 and 612.59 Bq.kg<sup>-1</sup>, respectively, for soil sample no.66 which was obtained from the additional materials brought from outside the manufacturing area but the activity concentration of  $^{40}\text{K}$  measured from rock sample no.59 obtained at the location of AL Takamul Cement Factory Quarries.

The radiological hazard to humans due to the radioactivity arising from radionuclides contained in rock and soil collected from the areas studied was assessed. The estimated absorbed dose rates based on soil radioactivity range from 9.49 to 42.28 nGy.h<sup>-1</sup> with a mean value and standard deviation of  $19.41 \pm 10.35$  nGy.h<sup>-1</sup>. The effective dose for the different locations of rock and soil samples in this study varied from 0.012 to 0.10 mSv.y<sup>-1</sup>, with the arithmetic mean value and standard deviation of  $0.028 \pm 0.014$  mSv.y<sup>-1</sup>, which is comparable to the worldwide effective dose of 0.070 mSv.y<sup>-1</sup>. Total activity concentrations in term of the radium equivalent activity ( $R_{\text{a}_{\text{eq}}}$ ) range from 20.899 to 161.161 Bq.kg<sup>-1</sup> with an overall arithmetic mean and standard deviation of  $41.82 \pm 22.38$  Bq.kg<sup>-1</sup>, which are lower than the accepted safety limit value of 370 Bq.kg<sup>-1</sup> as recommended by the Organization for Economic Cooperation and Development (OECD). The calculated values of the external hazard index for all rock and soil samples studied vary from 0.057 to 0.44 and the average value was found to be  $0.114 \pm 0.061$ . The

results show that the  $H_{ex}$  values for all soil samples are below the limit of unity, meaning that the radiation dose is below the permissible limit of  $1 \text{ mSv.y}^{-1}$  recommended by ICRP 60. The values of the radiation hazard parameters from this current study are not extremely high compared to the world averages and the recommended values and therefore unlikely to cause additional radiological health risks to the people living in the areas studied.

Furthermore, hazards health of human exposure of radon-222 have been determined out of the statistical analysis didn't show any significant difference between the background concentrations of  $^{222}\text{Rn}$  of all cement quarries. Based on the **UNSCEAR** guidelines for annual doses of ionizing radiation by source, the recommended upper threshold effective dose of total radon and their progenies is  $1 \text{ mSv.y}^{-1}$ , with a typical range of observed doses up to  $0.66 \pm 0.11 \text{ mSv/y}$ . The mean risk of lung cancer in the cement quarries is  $11.7 \pm 1.98$  which is much lower than the standard ICRP (170-230 lung cancer).

## **5.2 Recommendations**

To overcome the problems encountered during this study, we recommend the following:

1. It seems necessary need to be carried out in order to allow comparison with other areas, which there Which can be quarries for the cement industry in Sudan, before its establishment.
2. More rock and soil samples from each sampling area need to be collected in order to obtain more accurate data.
3. Due to time limitations, the determination of activity concentration for each soil sample was measured only one time. Ideally, the measurements and estimations should to be repeated in order to obtain good statistical precision.
4. The results may be used as reference data for monitoring possible radioactivity pollution in future.
5. I would also recommend that the Radiation Protection institute be involved in future further radiological studies to implement any necessary professional steps for the good of the residents and the nation as a whole.

## Reference

- [1] R. Health and S. A. Council, “Naturally-Occurring Radioactive Material (NORM) in Australia : Issues for Discussion”, no. August, 2005.
- [2] Markkanen, M. Radiation Dose Assessments for Materials with Elevated Natural Radioactivity; Painatuskeskus Oy: Helsinki, Finland, 1995; p. 38.
- [3] Turhan, Ş. Assessment of the natural radioactivity and radiological hazards in Turkish cement and its raw materials. *J. Environ. Radioact.* 2008, 99, 404–414.
- [4] Righi, S.; Bruzzi, L. Natural radioactivity and radon exhalation in building materials used in Italian dwellings. *J. Environ. Radioact.* 2006, 88, 158–170.
- [5] Khan, K.; Khan, H.M. Natural gamma-emitting radionuclides in Pakistani Portland cement. *Appl. Radiat. Isotopes* 2001, 54, 861–865.
- [6] El-Taher, A.; Makhluף, S.; Nossair, A.; Abdel Halim, A.S. Assessment of natural radioactivity levels and radiation hazards due to cement industry. *Appl. Radiat. Isotopes* 2010, 68, 169–174.
- [7] Damla, D.; Cevik, U.; Kobya, A.I.; Celik, A.; Celik, N.; van Grieken, R. Radiation dose estimation and mass attenuation coefficients of cement samples used in Turkey. *J. Hazard. Mater.* 2010, 176, 644–649.
- [8] UNSCEAR, Report of the United Nations Scientific Committee on the Effects of Atomic Radiation 2010 - 2011.
- [9] Allisy, A. “Henri Becquerel: The discovery of radioactivity”, Becquerel’s Legacy: A Century of Radioactivity. Proceedings of a Conference, London: Nuclear Technology Publishing, 1996, pp.3-10.
- [10] Lilley, J. Nuclear Physics: Principles and Applications, Chichester: John Wiley & Sons, Ltd, 2001.
- [11] Eisenbud, M. and Gesell, T. Environmental Radioactivity from Natural, Industrial, and Military Sources (4th edition), London: Academic Press, 1997.
- [12] Klement, A.W. CRC Handbook of Environmental Radiation, Florida: CRC Press, Inc, 1982.
- [13] Watson, S.J., Jones, A.L., Oatway, W.B. and Hughes, J.S. “Ionising Radiation Exposure of the UK population”, Health Protection Agency, Centre for Radiation, Chemical and Environmental Hazards, Radiation Protection Division, Chilton, Didcot, Oxfordshire, OX11 0RQ, UK, 2005.
- [14] United Nations Scientific Committee on the Effects of Atomic Radiation, “Sources and Effects of Ionizing Radiation”, UNSCEAR Report Vol.1 to the

- General Assembly, with scientific annexes, United Nations Sales Publication, United Nations, New York, 2000.
- [15] National Council on Radiation Protection and Measurements, “Natural Background Radiation in the United States”, NCRP Report No.45. NCRP, Washington, D.C, 1975.
- [16] World Nuclear Association, “Radiation and Nuclear Energy”, <http://www.world-nuclear.org/info/inf30.html> [Updated August 2011]
- [17] International Atomic Energy Agency, “IAEA-TECDOC-1472”, Proceedings of an international Conference on Naturally Occurring Radioactive Materials (NORM IV), Poland: IAEA, Vienna, 2005.
- [18] Wilson, W. F, A Guide to Naturally Occurring Radioactive Material, Oklahoma: Pennwell Books, 1994.
- [19] International Atomic Energy Agency, “Extent of Environmental Contamination by Naturally Occurring Radioactive Material (NORM) and Technological Options for Mitigation”, Technical Reports Series No.419, IAEA, Vienna, 2003.
- [20] National Council on Radiation Protection and Measurements, “Environmental Radiation Measurement”, NCRP Report No.50. NCRP, Washington, D.C, 1977.
- [21] Zaki A. Mansoor, Takrid Muneam Nafae, Ali Kareem K. Jelaot. Assessment of Natural Radioactivity Levels and Radiological Hazards of Cement in Iraq. Nuclear Science. Vol. 3, No. 2, 2018, pp. 23-27.
- [22] Matiullah, A., Ur-Rehman, Sh., Ur-Rehman, A. and Faheem, M., “Measurement of Radioactivity in the Soil of Behawalpur Division, Pakistan”, Radiation Protection Dosimetry 112 (3), 2004, pp 443-447.
- [23] Tzotzis, M., Svoukis, E. and Tsertos, H., “A Comprehensive Study of Natural Gamma Radioactivity Levels and Associated Dose Rates from Surface Soils in Cyprus”, Radiation Protection Dosimetry 109 (3), 2004, pp 217-224.
- [24] Kurnaz, A., Kucukomeroglu, B., Keser, R., Okumusoglu, N.T., Kprkmaz, F., Karahan, G. and Cevik, U, “Determination of Radioactivity Levels and Hazards of Soil and Sediment Samples in Firtina Valley (Rize, turkey)”, Applied Radiation and Isotopes 65, 2007, pp 1281-1289.
- [25] S. P. Dunuweera and R. M. G. Rajapakse, “Cement types, composition, uses, environmental impact and possible solutions,” in Proceedings of the 28th International Symposium on Transport Phenomena, Peradeniya, Sri Lanka, September 2017.

- [26] T. C. Powers and T. L. Brownyard, "Studies of the physical properties of hardened Portland cement paste," *ACI Journal Proceedings*, vol. 43, no. 9, pp. 101–132, 1946.
- [27] F. Lea, *The Chemistry of Cement and Concrete*, February 2018, <https://ci.nii.ac.jp/naid/10003996296/>.
- [28] M. Schneider, M. Romer, M. Tschudin, and H. Bolio, "Sustainable cement production-present and future," *Cement and Concrete Research*, vol. 41, no. 7, 2011, pp. 642–650.
- [29] A. Elimbi, H. Tchakoute, and D. Njopwouo, "Effects of calcination temperature of kaolinite clays on the properties of geopolymer cements," *Construction and Building Materials*, vol. 25, no. 6, pp. 2805–2812, 2011.
- [30] M. Ali, R. Saidur, and M. Hossain, "A review on emission analysis in cement industries," *Renewable and Sustainable Energy Reviews*, vol. 15, no. 5, pp. 2252–2261, 2011.
- [31] M. Thiery, G. Villain, P. Dangla, and G. Platret, "Investigation of the carbonation front shape on cementitious materials: effects of the chemical kinetics," *Cement and Concrete Research*, vol. 37, no. 7, pp. 1047–1058, 2018.
- [32] *Portland Cement Clinker: The Bogue Calculation*, July 2017, <http://www.understanding-cement.com/bogue.html>.
- [33] IAEA, International Atomic Energy Agency "Collection and preparation of bottom rock samples for analysis of radionuclides and trace elements" Printed by the IAEA in Austria July 2003.
- [34] UNSCEAR-United Nations Scientific Committee on the Effects of Atomic Radiation. Report to General Assembly, Vol. I. New York: United Nations 1993.
- [35] Sam, A. K, Ahmed, "Radiochemical studies on environmental radioactivity in Sudan" PhD thesis, University of Khartoum, 1998.
- [36] Idris, A. M., "Investigation of some heavy metals and radionuclides in sediments from the Sudanese coast Red Sea" .M.Sc Thesis, University of Khartoum, 1999.
- [37] Gilmore, G.R., *Practical Gamma-ray Spectrometry*. 2nd ed., England: John Wiley & Sons Ltd, 2008.
- [38] "Sudan geography". Institute for Security Studies. 12 January 2005. Archived from the original on 13 May 2011.
- [39] "Geography of Sudan". Sudan Embassy in London. n.d. Archived from the

original on 30 September 2005.

- [40] Marble Occurrences in the Sudan <http://sdecoc.org/download/sudan1/Marble-in-the-Sudan.pdf>.
- [41] L'Annunziata, M. F, Radioactivity: Introduction and History, Amsterdam: Elsevier B.V, 2007.
- [42] National Council on Radiation Protection and Measurements, "A Handbook of Radioactivity Measurements Procedures (2nd edition)", NCRP Report No.58. NCRP, Maryland, 1985.
- [43] Choppin, G., Liljenzin, J. and Rydberg, J. Radiochemistry and Nuclear Chemistry (3rd edition), USA: Butterworth-Heinemann, 2002.
- [44] Gilmore, G.R, Practical Gamma-ray Spectrometry (2nd edition), Chichester: John Wiley & Sons Ltd, 2008.
- [45] Kaplan, I. Nuclear Physics (2nd edition), USA: Addison-Wesley Publishing Company, Inc, 1962.
- [46] Faires, R.A. and Boswell, G.G.J., Radioisotope Laboratory Techniques (4th edition), London: Butterworth & Co (Publishers) Ltd, 1981.
- [47] Krane, K. S., Introductory Nuclear Physics, Chichester: John Wiley & Sons Inc, 1988.
- [48] Burcham, W.E., Nuclear Physics: An Introduction (2nd edition), Harlow: Longman, 1983.
- [49] Knoll, G. F., Radiation Detection and Measurement (3rd edition), USA: John Wiley & Sons Inc, 2000.
- [50] Turner, J.E., Atoms, Radiation, and Radiation Protection (3rd edition), Weinheim: Wiley-VCH, 2007.
- [51] Lapp, R.E. and Andrews, H.L., Nuclear Radiation Physics (4th edition), London: Sir Isaac Pitman and Sons Ltd, 1972.
- [52] Cember, H. and Johnson, T.E., Introduction to Health Physics (4th edition), New York: McGraw-Hill Companies, Inc, 2009.
- [53] Curie, M., Debierne, A., Eve, A.S., Geiger, H., Hahn, O., Lind, S.C., Meyer, St., Rutherford, E. and Schweidler, E., "The Radioactive Constants as of 1930 Report of the International Radium-Standard Commission", Review of Modern Physics 3, 1931 pp 427- 445.
- [54] Harvey, B.G., Introduction to Nuclear Physics and Chemistry (2nd edition), New Jersey: Prentice-Hall Inc, 1969.

- [55] Adloff, J.-P. and Guillaumont, R., Fundamentals of Radiochemistry, London: CRC Press Inc, 1993.
- [56] Halliday, D., Introductory Nuclear Physics (2nd edition), New York: Johnson Wiley & Sons Inc, 1955.
- [57] Cetnar, J., “General Solution of Bateman Equations for Nuclear Transmutations”, Annals of Nuclear Energy, 2006, pp 33,640-645.
- [58] Prince, J.H., “Comments on Equilibrium, Transient Equilibrium, and Secular Equilibrium in Serial Radioactive Decay”, Journal of Nuclear Medicine, 1979, pp20, 162- 164.
- [59] Yu, K.N., Guan, Z.J., Stoks, M.J., Young, E.C., 1992. The assessment of natural radiation dose committed to the Hong Kong people. Journal of Environmental Radioactivity, 1992, pp17,31– 48.
- [60] Knoll, G. F, Radiation Detection and Measurement. 3rd ed. New York: John Wiley & Sons Ltd,2000.
- [61] Das, A. and Ferbel, T., Introduction to Nuclear and Particle Physics (2nd edition), London: World Scientific, 2003.
- [62] Kantele, J., Handbook of Nuclear Spectrometry, London: Academic Press Limited, 1995.
- [63] Duivenstijn, A.J. and Venverloo, L.A.J., Practical Gamma Spectrometry, Netherlands: N.V. Philips’Gloeilampenfabrieken, 1963.
- [64] Friedlander, G., Kennedy, J.W., Macias, E.S. and Miller, J.M., Nuclear and Radiochemistry (3rd edition), Chichester: John Wiley & Sons Inc, 1981.
- [65] Debertin, K. and Helmer, R.G., Gamma and X-Ray Spectrometry with Semiconductor Detectors, Amsterdam: Elsevier Science Publishers B.V, 1988.
- [66] Wahl, W., Radionuclide Handbook for Laboratory Workers in Spectrometry, Radiation Protection and Medicine, Germany: ISuS, 2007.
- [67] Noz, M. E. and Maguire Jr., G. Q., Radiation Protection in the Health Sciences, London: World Scientific Publishing Co. Pte. Ltd, 2007.
- [68] Martin, A. and Harbison, S., An Introduction to Radiation Protection (5th edition), London: Hodder Arnold, 2006.
- [69] International Commission on Radiological Protection., “Radiation Protection”, ICRP Publication 60. Elmsford, NY: Pergamon Press, Inc, 1991 .
- [70] United Nations Scientific Committee on the Effects of Atomic Radiation, “Sources and Effects of Ionizing Radiation”, UNSCEAR Report Vol.1 to

- the General Assembly, with scientific annexes, United Nations Sales Publication, United Nations, New York, 2008.
- [71] United Nations Scientific Committee on the Effects of Atomic Radiation, “Sources and Effects of Ionizing Radiation”, UNSCEAR Report Vol.1 to the General Assembly, with scientific annexes, United Nations Sales Publication, United Nations, New York, 2006.
- [72] E Joseph and R.Nasiru, “Correction in Efficiency of a Sodium Iodide Thallium Activated, Na(Tl) detector, Advances in Applied Science Research, vol 4 (1), 2013, pp 400-406.
- [73] IAEA, International Atomic Energy Agency “Collection and preparation of bottom sediment samples for analysis of radionuclides and trace elements” Printed by the IAEA in Austria July 2003.
- [74] Uosif, M.A.M “Gamma- ray spectroscopic analysis of selected samples from River Nile Sediments in Upper Egypt”. Radiation Protection Dosimetry, vol 123(2), 2007, pp 215-220.
- [75] Mohamed, A. Suliman, “Measurement of Natural Radioactivity in Ceramics Samples Imported from the Republic of China”. Master thesis Sudan Academy of Sciences, 2016.
- [76] Al-Hamarneh, I.F. and Awadallah, M.I., “Soil Radioactivity Levels and Radiation Hazard Assessment in the Highlands of Northern Jordan”, Radiation Measurements, 2009, pp 44, 102-110.
- [77] Ahmed, N.K. and El- Arabi, A.G.M., “Natural Radioactivity in Farm Soil and Phosphate Fertilizer and its Environmental Implications in Qena Governorate, Upper Egypt”, Journal of Environmental Radioactivity, 2005, pp 84, 51-64.
- [78] Jibiri, N.N., Farai, I.P. and Alausa, S.K., “Estimation of Annual Effective Dose due to Natural Radioactive Elements in Ingestion of Foodstuffs in Tin Mining Area of Jos-Plateau, Nigeria”, Journal of Environmental Radioactivity, 2007, pp 94, 31- 40.
- [79] Beck, H.L., “The physics of environmental radiation fields. Natural radiation environment II, CONF-720805 P2”, Proceedings of the Second International Symposium on the Natural Radiation Environment, 1972.
- [80] Chang, B.U., Koh, S.M., Kim, Y.J., Seo, J.S., Yoon, Y.Y., Row, J.W. and Lee, D.M., “Nationwide survey on the natural radionuclides in industrial raw minerals in South

- Korea”, *Journal of Environmental Radioactivity*, 2008, pp 99, 455- 460.
- [81] Beretka, J. and Mathew, P.J., “Natural Radioactivity of Australian Building Materials, Industrial Wastes and By-products”, *Health Physics*, 1985, 48,87-95.
- [82] Turhan, S. and Gundiz, L., “Determination of Specific Activity of  $^{226}\text{Ra}$ ,  $^{232}\text{Th}$  and  $^{40}\text{K}$  for Assessment of Radiation Hazards from Turkish Pumice Samples”, *Journal of Environmental Radioactivity*, 2008, pp 99,332-342.
- [83] Al-Kharouf, S. J., Al-Hamarneh, I. F. and Dababneh, M., “Natural Radioactivity, Dose Assessment and Uranium Uptake by Agricultural Crops at Khan Al- Zabeeb, Jordan”, *Journal of Environmental Radioactivity* vol 99 (7), 2008, pp 1192-1199, 2008.
- [84] Nada, A., Maksoud, T. M. A., Hosnia, M. A. El-Nagar, T. and Awad, S., “Distribution of Radionuclides in Soil Samples from a Petrified Wood Forest in El- Qattamia, Cairo, Egypt”, *Applied Radiation and Isotopes*, 2009, pp 67,643-649.
- [85] Ajayi, O. S., “Measurement of Activity Concentrations of  $^{40}\text{K}$ ,  $^{226}\text{Ra}$  and  $^{232}\text{Th}$  for Assessment of Radiation Hazards from Soils of the Southwestern Region of Nigeria”, *Radiation and Environmental Biophysics*, 2009, pp 48,323-332.
- [86] Belivermis, M., Kikic, O., Cotuk, Y. and Topcuoglu, S., “The Effect of Physicochemical Properties on Gamma Emitting Natural Radionuclide Levels in the Soil Profile of Istanbul”, *Environmental Monitoring and Assessment*, 2010, pp 163,15-26.
- [87] United Nations Scientific Committee on the Effects of Atomic Radiation., “Sources and Effects of Ionizing Radiation”, UNSCEAR Report Vol.1 to the General Assembly, with scientific annexes, United Nations Sales Publication, United Nations, New York, 1988.
- [88] Krieger, R., “Radioactivity of Construction Materials”, *Betonwerk Fertigteil Tech*, 1981, pp 47,468-473.
- [89] Dragovic, S. Jankovic, L. and Onjia, A., “Assessment of Gamma Dose Rate from Terrestrial Exposure in Serbia and Montenegro”, *Radiation Protection Dosimetry* Vol 121 (3),pp 297-302, 2006.
- [90] Baum, M., Knox, H. D. and Miller, T. R., *Nuclides and Isotopes: Chart of the Nuclides* (16th edition), Lockheed Martin Co, 2002.
- [91] Santawamaitre, T., Regan, P. H., Bradley, D. A., Matthews, M., Malain, D.

- and Al-Sulaiti, H. A., “An Evaluation of the Level of Naturally Occurring Radioactive Material in Soil Samples along the Chao Phraya River Basin”, *Nuclear Instruments and Methods in Physics Research A* 619(1-3), pp 453-456, 2010.
- [92] Organisation for Economic Cooperation and Development., “Exposure to Radiation from the Natural Radioactivity in Building Materials”, Report by a Group of Experts of OECD Nuclear Energy Agency. Paris, France: OECD, 1979.
- [93] Saad, H.R. and D. Al-Azmi, Radioactivity concentrations in sediments and their correlation to the coastal structure in Kuwait. *Applied Radiation and Isotopes*,. 56(6): pp. 991-997.43, 2002.
- [94] Goddard, C.C., Measurements of Outdoor Terrestrial Gamma Radiation in the Sultanate of Oman. *Health Phys.*, 2002. pp 82, No.6.
- [95] Al-Hamarneh, I.F. and M.I. Awadallah, Soil radioactivity levels and radiation hazard assessment in the highlands of northern Jordan. *Radiation Measurements*, 2009. 44(1): p.102-110.
- [96] UNSCEAR, Effects of Atomic Radiation to the General Assembly, in United Nations Scientific Committee on the Effect of Atomic Radiation. 2000, United Nations: New York.
- [97] [https://www.sarad.de/cms/media/docs/handbuch/Manual\\_Radon-Scout\\_EN](https://www.sarad.de/cms/media/docs/handbuch/Manual_Radon-Scout_EN), 2004, pp 24-03-17.pdf.
- [98] [https://www.sarad.de/cms/media/docs/handbuch/Manual\\_RadonVision6\\_EN\\_16-10-2015.pdf](https://www.sarad.de/cms/media/docs/handbuch/Manual_RadonVision6_EN_16-10-2015.pdf).
- [99] United Nations Scientific Committee on the Effects of Atomic Radiation (UNSCEAR),. Sources and Effects of Ionizing Radiation; United Nations Scientific Committee on the Effects of Atomic Radiation, USA, 2000.
- [100] Ismail, A.H., Jaafar, M.S., Indoor radon concentration and its health risks in selected locations in Iraqi Kurdistan using CR-39 NTDs, *Bioinformatics and Biomedical Engineering (iCBBE)*, 4th International Conference on. IEEE, 2010, PP. 1–8.
- [101] Protection, I.C.O.R., Age-dependent doses to members of the public from intake of radionuclides: part 2 ingestion dose coefficients: a report of a task group of Committee 2 the International commission on radiological protection. Elsevier Health Sciences, 1994.
- [102] ICRP, 1994. ICRP Publication 66: Human Respiratory Tract Model for

- Radiological Protection. Elsevier Health Sciences. Hassan, V., Arash, R., Mehdi, J., Ahmad, R., Ali, H.-B.A., Wali, Y.A., Ali, D., AbdulRasool, M., Abbas, P. 2011. Demonstration of malaria situation analysis, stratification, and planning in Minab District, southern Iran. *Asian Pacific J. Trop. Med.*, 1994, pp 4: 67–71.
- [103] Markus R. Zehring, *Gamma-Ray Spectrometry and the Investigation of Environmental and Food Samples*, May 24th 2017. *New Insights on Gamma Rays*, Ahmed M. Maghraby, Intech Open, DOI:10.5772/67099.
- [104] Sarad GmbH Radon Scout Monitor [https://www.sarad.de/cms/media/docs/handbuch/Manual\\_Radon-Scout\\_EN\\_24-03-17.pdf](https://www.sarad.de/cms/media/docs/handbuch/Manual_Radon-Scout_EN_24-03-17.pdf).
- [105] Salih, I., S., Eisa, S., Idriss, H. Radiation exposure of worker in storage areas for building materials.-*J. Taibah. Univ.Sci.*, 2010 8(4): 394-400

# Appendix

## List of Presentations & Publications

- Seminars and Presentations
  1. Title: Early warning and response mechanisms to radiological and nuclear emergencies in Sudan, Presented at the 1th A workshop on preparedness and response to radiological and nuclear emergencies 13September 2018, Khartoum, Sudan.
  2. Seminars title: Uses of radioactive sources in Sudan and previous accidents, Presented in the meeting hall of Sudan University of Science and Techology 10 March 2020, Khartoum, Sudan.
- Paper Publications
  1. Mohamed. A.H. Dahab, A.E. Elfaki, A.S. Alhag, Mohammed. H. Albashir “Determination of Radon-222 Levels and Hazards in Air Samples, Quarriers Cement Factories in River Nile State, Sudan” Journal of Scientific and Engineering Research Volume 7 Issue 4 2020 Page No. 85-90.
  2. Mohamed. A.H. Dahab, A.E. Elfaki, A.S. Alhag, Mohamed. A. Suliman “Verification of Components and Radioactivity Levels of Rock Samples, Quarries Atbara Cement factory in River Nile State, Sudan”Journal of Scientific and Engineering Research Volume 8 Issue 7 2021 Page No. 36-41.